STREAM TEMPERATURE DRIVERS AND MODELLING IN HEADWATER CATCHMENTS ON THE EASTERN SLOPES OF THE CANADIAN ROCKY MOUNTAINS

RYAN J. MACDONALD
M.Sc., University of Lethbridge, 2008

A Thesis
Submitted to the School of Graduate Studies
of the University of Lethbridge
in Partial Fulfilment of the
Requirements for the Degree

[DOCTOR OF PHILOSOPHY]

Department of Geography
University of Lethbridge
LETHBRIDGE, ALBERTA, CANADA

Dedication

This thesis is dedicated to my mother. Her continual support and guidance have led me here, I am forever indebted.

Abstract

This thesis quantified processes controlling stream temperature using a field study conducted in headwater catchments on the eastern slopes of the Canadian Rocky Mountains, Alberta. Hydrometeorological data from May-September of 2010 and 2011 were used to describe the drivers of inter-annual stream temperature variation in Star Creek. Inter-annual stream temperature variation was shown to be a function of catchment-scale moisture conditions, driven by seasonal differences in snow accumulation. This field study demonstrated that meteorological and hydrological processes must be considered simultaneously in order to understand stream temperature response to changing environmental conditions in mountain regions. A process-based modelling approach was developed to simulate stream temperature in Star Creek using hydrometeorological and geomorphological data collected during the field study. Modelling results suggest simulations of hydrometeorological variables needed for process-based stream temperature modelling are possible in data-sparse mountain regions using little input data. Model calibration was required because not all variables required for calculating the stream energy budget were measured. However, stream energy budget estimates did compare well with other estimates from field-based studies, providing confidence in the methods applied. A sensitivity analysis demonstrated that simulations were most sensitive to net radiation and parameterization/calibration of surface-subsurface interactions. Results from a climate change study presented in Chapter 4 suggest winter habitat for native salmonids may be reduced as a function of changes in the onset of spring snowmelt. Chapter 4 results suggest that bull trout (*Salvelinus confluentus*) populations are likely more sensitive to climate change than isolated

westslope cutthroat trout (*Oncorhynchus clarki lewisii*) populations. The climate change study was limited due to boundary conditions remaining constant for all simulations and modelling error. However, these results are supported by an inter-catchment comparison of air temperature, stream temperature, and stream discharge between Lynx, Lyons East and Star creeks. The inter-catchment comparison and climate change results present a conceptual framework of thermal response to climate change that has not been discussed in the literature. Overall, this thesis demonstrates that catchment- and regionally-specific conditions must be considered when assessing the potential impacts of environmental change on stream temperature and native salmonids.

Acknowledgements

I would like to first thank my family and friends for supporting me through this process. I give a special thank you to my mother, who has given me so much. Kelly and Eddie have always been there to help, thank you for giving me a foundation to lean on. My love for fish and the outdoors stems from my father, thank you for that dad. Thank you to Amy for putting up with me and for being such a strong support. Thank you to my supervisors Jim Byrne and Sarah Boon for having confidence in me; I can't express how much I appreciate all you have done. Thank you to Joe Rasmussen, Matt Letts, and Dan Johnson for support and constructive feedback. I would like to thank Steve Wondzell for his amazing contribution to this experience. I would like to say thank you to Uldis Silins for helping me so much in the field and with my project overall. I am forever grateful for my fellow grad students and field support who have helped me immensely. Thanks to Dez Tessler, Ashley Cox, Katie Burles, Reed Davis, Dave Dixon, Dave Lewis, Devin Cairns, Chris Williams, Mike Robinson, Mike Wagner, Kevin Bladon, Sarah Dalla Vicenza, Guy Duke, Kate Forbes, Tanya Byrne, Will Warnock, and the field crew from the Southern Rockies Watershed Project for their assistance. Thank you to Dan Moore for engaging in helpful discussions with me and to Jason Leach for being a fellow stream temperature nerd.

This research wouldn't have been possible without grants from Trout Unlimited Canada, the Natural Sciences and Engineering Research Council of Canada, the Prairie Adaptive Research Collaborative, the Alberta Conservation Association, Alberta Water Research Institute, Water and Environment Hub, and Alberta Sustainable Resources Development (Forest Management Division). Thank you to these great agencies.

Table of Contents

List of Figures

List of Tables

Chapter 1: Introduction

The study of thermal dynamics within streams has been the focus of many recent studies, motivated by threats from environmental change and the importance of stream temperature in governing aquatic ecosystem function (Webb *et al*. 2008). Native salmonid populations across mountain regions of western North America are currently threatened because they inhabit linear-dendritic habitat which is easily fragmented by disturbance and limited by the introduction of non-native species (Isaak and Reiman, 2013; Wenger *et al.* 2011a). Habitat for salmonids is projected to decrease by 47% over the next century in the western United States (Wenger *et al*. 2011b). On the eastern slopes of the Canadian Rocky Mountains native westslope cutthroat trout (*Oncorhynchus clarki lewisii*) and bull trout (*Salvelinus confluentus*) are currently threatened (ASRD, 2009; COSEWIC, 2009), and management activities such as the westslope cutthroat trout recovery program (EASRD, in prep) are being undertaken to help preserve these important species. Therefore, thermal response to natural and human-induced environmental change in headwater streams inhabited by these key species is important to both managers and researchers in Canada.

Quantifying thermal response to environmental change is inherently linked to our understanding of the factors controlling stream temperature and streamflow in headwater catchments. The relative contributions of stream water sourced from long- and short-catchment residence times are defined by internal geologic structure (McGuire *et al*. 2004), which ultimately determines the influence of streamflow on stream temperature (Johnson, 2004). Catchments with high proportions of streamflow contribution from sources with short residence times (shallow groundwater and soil water) are influenced

more strongly by atmospheric conditions. Streams with high proportions of source water with long residence times (deeper groundwater) are more likely to be in disequilibrium with the atmosphere (Tague *et al*. 2007). Recent research in British Columbia and Antarctica has in fact demonstrated that surface-subsurface interactions substantially influence stream temperature, with hyporheic exchange flow significantly influencing the stream heat budget (Story *et al*. 2003; Moore *et al*. 2005; Cozzetto *et al*. 2006; Leach and Moore 2011). The role of hyporheic exchange flow in governing stream temperature is likely greatest when the proportion of hyporheic exchange flow to total streamflow is high (Wondzell, 2011), and when source water residence times are relatively long. Hyporheic interactions that involve water traveling through shorter or faster flow paths likely have a smaller influence stream temperature because the relative differences between stream and hyporheic water temperature are reduced (Wondzell, 2012).

Stream-streambed interactions also control stream temperature through conduction and friction. Streambed conduction varies with substrate type and can provide a nighttime (daytime) heat source (sink) that varies by season (Evans *et al*. 1998; Johnson, 2004; Moore *et al.* 2005; Brown *et al.* 2006; Hannah *et al*. 2008). Friction is a relatively small component of the stream heat budget, and acts as a heat source (Theurer *et al*. 1984) (Fig. 1.1).

The effects of catchment-scale hydrologic, geomorphic, and hydrogeologic controls on stream temperature are confounded by complex stream-atmosphere interactions that change substantially over space and time. The stream energy budget is largely controlled by the amount of solar radiation received at the water surface (Brown, 1969), which is moderated by riparian vegetation (Johnson, 2004). Incoming shortwave

radiation increases stream temperature, while longwave radiation to (from) the stream surface acts to increase (decrease) stream temperature. Latent and sensible heat exchange at the air-water interface also contribute to the stream energy budget (Leach and Moore, 2010; Hannah *et al*. 2008; Garner *et al*. 2012). Negative (positive) sensible heat fluxes influence heat diverging from (converging onto) the stream surface. Negative (positive) latent heat fluxes affect stream temperature through evaporation (condensation) from (to) the stream surface. The effect of the atmosphere on stream temperature is influenced by stream exposure time, governed by the width, depth, and velocity of water traveling through the stream channel (Webb and Zhang, 1997) (Fig. 1.1).

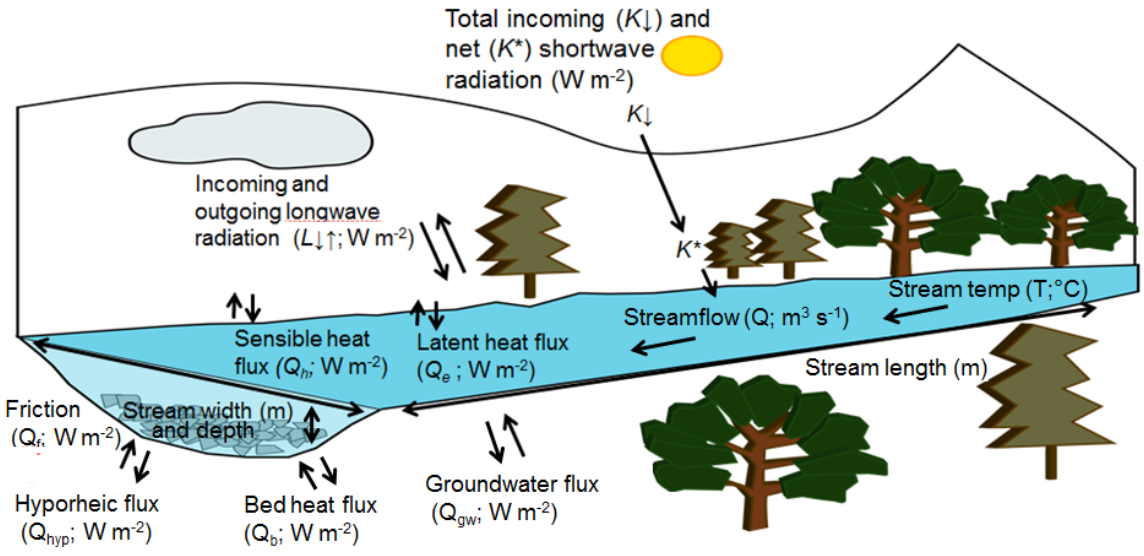

Figure 1.1: Diagram representing the stream and riparian zone, and heat budget terms that influence stream temperature.

Field-based studies have defined the important stream energy budget. Therefore, these types of studies provide key insight into getting the "right answers for the right reasons" (Kirchner, 2006) by improving our process understanding (Sidle, 2006). Unfortunately, field-based studies are not often feasible and there is a strong reliance on

models to quantify the effects of environmental change on stream temperature. Statistical models have been developed using geospatial data to represent important parameters controlling stream temperature and to assess thermal response to climate change (e.g., Isaak *et al*. 2010; Mantua *et al*. 2010; Jones *et al*. 2013). While statistical models are useful for directing management strategies, they may be limited given that there is discrepancy between correlation and causation in describing processes controlling stream temperature (Johnson, 2004). Process-based models enable more physically robust analysis of factors influencing thermal regimes. However, they are not always transferable across catchments and they require large amounts of input data which are not frequently collected (Benyahya *et al*. 2010).

"Getting the right answers for the right reasons" is a challenge, particularly since modelling errors may not be random in nature and rather stem from a lack of process knowledge (Beven, 2012). Recent discrepancy in observed stream temperature trends as a result of climate warming (Arismendi *et al*. 2012) argues that errors in assessing thermal regime responses to environmental change are epistemic in nature. Coupled process-based modelling and field-based studies provide an opportunity to improve process representation and verify model assumptions, improving our overall ability to adequately adapt to future challenges in preserving habitat for native salmonid populations.

The eastern slopes of the Canadian Rocky Mountains are experiencing rapid environmental change through altered landuse, natural disturbance, and climate (Silins *et al*. 2009; Schindler and Donahue, 2006; St. Jacques *et al*. 2010; MacDonald *et al*. 2012). These changes threaten aquatic ecosystems by altering natural thermal regimes (Poole and Berman, 2001). There has been no research to-date assessing the processes

controlling stream temperature in headwater catchments on the eastern slopes of the Canadian Rocky Mountains. In fact, most studies of thermal response to environmental change have been conducted in catchments with relatively strong Pacific climate influence (Tung *et al*. 2006; Isaak *et al*. 2011; Diabat *et al*. 2012; Jones *et al*. 2013). Catchments with Continental climates like those on the eastern slopes of the Rocky Mountains may have fundamentally different thermal and hydrological responses to factors such as climate change. This research has three objectives to help better understand potentially important factors controlling stream temperature response to environmental change in this region:

1. Define key atmospheric and hydrologic variables controlling stream temperature at the reach-scale through a detailed field study;

2. Incorporate the reach-scale stream water and energy balance into a watershed-scale hydrometeorological model using both existing algorithms and field measurements; and,

3. Use the resulting model to assess how environmental change (climate change) may affect stream temperature, hydrology, and native salmonids in headwater streams.

1.1. **Thesis structure**

Each of the three research objectives is presented as an individual chapter in this thesis. Chapter 2 describes a field study conducted on the eastern slopes of the Canadian Rocky Mountains that quantifies stream energy and water budgets. Data from the field study were used to compare processes controlling inter-annual variation in summer stream temperature. Chapter 3 presents the development of a modelling approach for data sparse mountain regions using data from the field-based study. A sensitivity analysis is

used to assess how stream temperature may respond to future climate scenarios in a subsurface and snowmelt dominated catchment in Chapter 4. The simulated responses are compared to observations of inter-catchment hydrological and thermal characteristics. Potential changes in native salmonid life-history as a function of changes in the timing of spring runoff and altered thermal regimes are assessed. The conclusion is presented in Chapter 5, summarizing the major findings of this work and identifying needs for future research in this field of study.

Chapter 2: A comparison of surface and subsurface influences on summer temperature in a headwater stream

2.1. **Introduction**

Stream temperature governs aquatic ecosystem function by directly influencing water quality, ecosystem productivity, and the physiological functioning of aquatic organisms (Allen, 1995; Caissie, 2006; Webb *et al*. 2008). Maintaining cold-water habitat during the summer is critical for the survival of native salmonids (Rieman *et al*. 2007; Isaak *et al*. 2010). Natural and anthropogenic disturbances such as drought, wildfire, insect infestation, and industrial development affect catchments across North America. These disturbances can significantly alter stream temperature regimes (Poole and Berman, 2001; Morrison *et al.* 2002; Mohseni *et al.* 2003; Dunham *et al.* 2007), and changes in thermal regime resulting in habitat loss and increased hybridization with non-native species pose a substantial threat to native salmonids in headwater systems (Muhlfeld *et al.* 2009; Isaak *et al.* 2011).

Stream temperature is governed by changes in the energy budget of the stream, with solar radiation constituting the dominant non-advective source of heat input during the summer. Solar radiation is supplemented by latent and sensible heat exchanges at the air-water interface, which have a smaller contribution to the stream energy budget in small forested streams (Brown 1969; Brown and Krygier, 1970; Webb and Zhang 1997; Johnson and Jones 2000; Hannah *et al.* 2008; Leach and Moore, 2010). Factors such as riparian shading, local topography, streambed conduction, friction, substrate type, and surface-subsurface interactions can also contribute to stream temperature regimes (Theurer, 1984; Webb and Zhang, 1997; Story *et al.* 2003; Hannah *et al.* 2004; Johnson,

2004; Moore *et al.* 2005; Brown *et al.* 2006; Hannah *et al.* 2008; Leach and Moore, 2010; Leach and Moore, 2011; Guenther *et al.* 2012).

Field studies assessing stream temperature controls continually improve our understanding of thermal regimes, and are currently lacking in many regions (e.g., Garner *et al.* 2012). Process-based field studies have shown that the inter-annual variation in stream temperature can be a function of changes in meteorological conditions and riparian cover (Groom *et al.* 2011; Garner *et al.* 2012). However, it is also important to consider factors such as hydrology (Hannah *et al.* 2008), particularly at longer temporal scales, as hydrological conditions can vary considerably (Zhang *et al.* 2001; Coulibaly and Burn, 2004).

Interactions between a stream and its surroundings are fundamentally controlled by catchment-scale geomorphic characteristics (Tague *et al*. 2007). Catchment-scale controls on source water residence time are important given that hyporheic exchange flow can act as a significant thermal buffer in small streams and alter stream temperature patterns (Pool and Berman, 2001; Arismendi *et al*. 2008). These controls are also important because water originating from deep groundwater sources with long residence times typically cools streams during summer and warms them in winter, providing salmonids with thermal refugia and habitat for rearing, determines the selection of spawning locations, and affects stream water quality (Ward, 1994; Power *et al.* 1999). Streams with high proportions of deep groundwater are critical to the survival of salmonids because many populations at-risk are currently limited to headwater streams where historically they inhabited much larger ranges (Behnke, 2002).

This study was focused in the Star Creek catchment, southwestern Alberta, which is representative of habitat of two cold water adapted species; native westslope cutthroat trout (*Oncorhynchus clarki lewisii*) and bull trout (*Salvelinus confluentus*), listed as threatened and species of special concern, respectively (ASRD, 2009; COSEWIC, 2009). To-date there have been no process-based stream temperature studies conducted on the eastern slopes of the Canadian Rocky Mountains, a region with extensive recreation, industrial, agricultural, and municipal use. Therefore, this field study was conducted to assess the inter-annual variation of summer stream temperature in a headwater stream by: (1) quantifying the dominant variables governing stream temperature; and (2) quantifying how these factors change between two hydro-climatically different years.

2.2. **Study Area**

Star Creek is a 1059 ha tributary of the Crowsnest River in the Oldman River catchment, southwestern Alberta (Fig. 2.1a). The Star Creek catchment ranges in elevation from 1475 m to 2631 m, and is dominated by east and west aspects. The catchment has a mean slope of 44% (Dixon, 2011). The surficial geology is characterized by glacial till and colluviums below 1900 m above sea level (asl), and talus, cirque tills, and exposed bedrock above 1900 m (Bayrock and Reimchen, 2007). At elevations below 1700 m the montane vegetative cover is dominated by lodgepole pine (*Pinus contorta*) and Engelmann spruce (*Picea engelmannii*) with small stands of trembling aspen (*Populus tremuloides*) at lower elevations. Between 1700 and 1900 m, the subalpine vegetative cover is comprised of subalpine fir (*Abies lasiocarpa*), Engelmann spruce and white spruce (*Picea glauca*). The high elevation alpine portion of the catchment (above

1900 m) is characterized by alpine meadows consisting of low grasses and coniferous shrubs, as well as talus slopes and bare rock (Silins *et al.* 2009).

The region receives 31% of its 576.5 mm normal (1971-2000) annual precipitation as snow. The highest precipitation occurs in June (64.1 mm) and the lowest precipitation occurs in March (36.2 mm). Normal (1971-2000) mean annual air temperature for the region is 3.5°C with the highest mean air temperature occurring in July (14.5°C) and the lowest mean occurring in January (-7.8°C; Environment Canada, 2012a).

This study incorporates a detailed study site used to measure hydrometeorological conditions within a 1200 m study reach characterized as an intermediate between step-pool and pool-riffle channel types (following Montgomery and Buffington, 1997). The study site is located at Star Main (Fig. 2.1c), in the middle of Star Creek catchment, ranges in elevation from 1502-1507 m asl. The entire study reach is from the confluence of Star West-fork, Star East-fork, and Star McLaren to Star Main (Fig. 2.1b) and has an elevation range of 1502-1532 m asl. At the study site, the mean channel slope is 5.0 %, with a 3 m plunge pool at the upstream end that flows into a 20 m rapid followed by a 9 m sheet, with a 71 m riffle at the downstream end of the site. The mean bankfull channel width is 3.3 m with a mean bankfull depth of 0.36 m. The mean channel slope is 4.3%; the mean bankfull channel width is 3.8 m with a mean bankfull depth of 0.34 m at the reach scale. The dominant substrate is cobble, with sub-dominant substrate composed of boulders and gravel. Riparian cover is dominated by lodgepole pine, with 37% canopy closure.

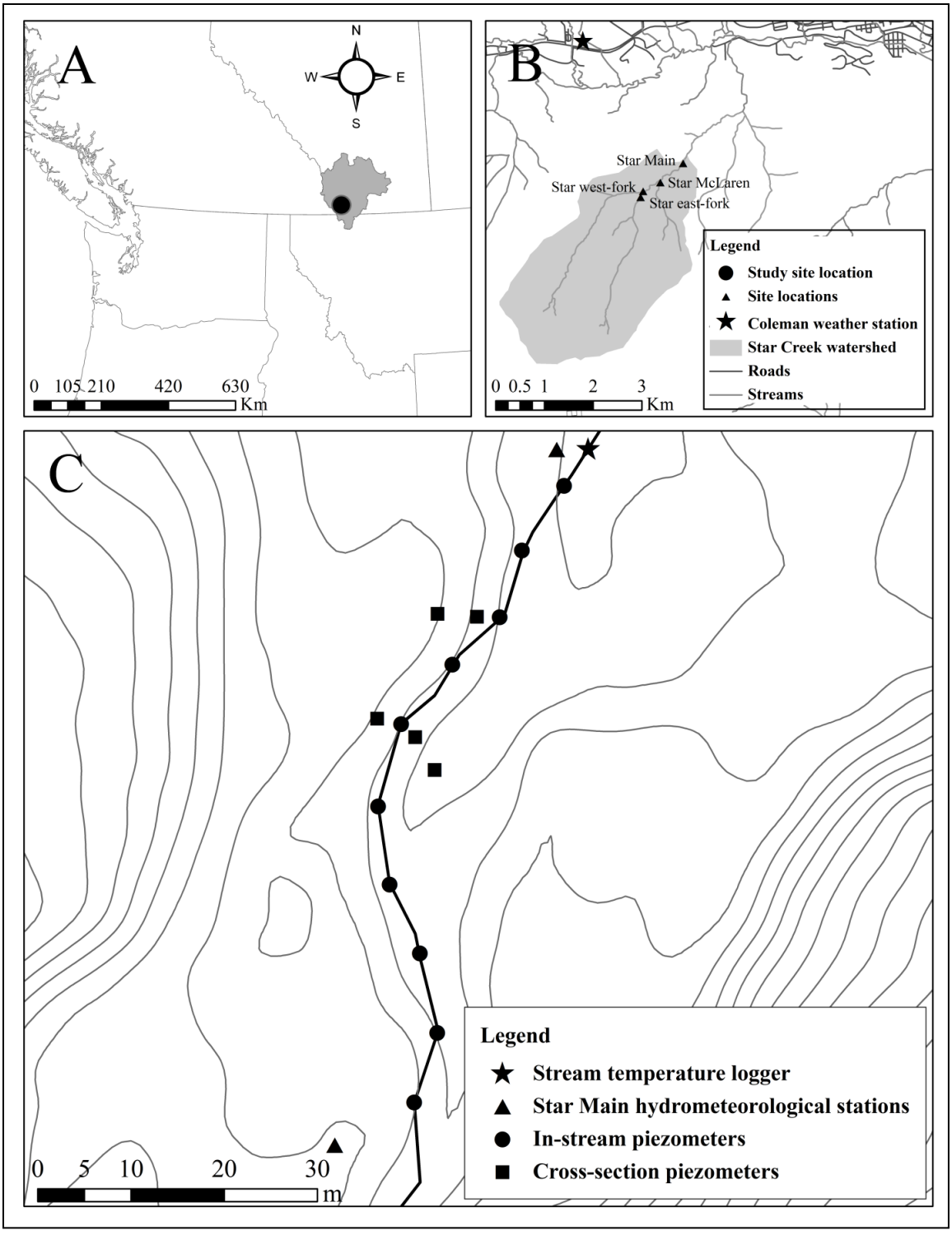

Figure 2.1: The study location in the Oldman River Watershed (A); study reach in the Star Creek Watershed (B); and the detailed study site located at Star Main (C).

2.3. **Methods**

2.3.1. Stream morphology and riparian cover

Stream surveys were conducted using a Leica Geosystems level and stadia rod to determine the channel slope and cross-section characteristics. Measurements of bankfull width (characterized using the lower limit of perennial vegetation), depth, and substrate type (Gordon *et al.* 2004) were taken every 10 m of stream length. Measurements of stream depth and substrate length (along the longest axis) were taken at 20 equal intervals dependant on stream width across each cross-section. Sub-reach classification was used to categorize channel units into nine categories: fall, cascade, chute, rapid, riffle, sheet, run, scour pool or plunge pool (Hawkins *et al.* 1993). All stream morphology data were combined to classify Star Creek into one of: colluvial, dune-ripple, pool-riffle, plan-bed, step-pool, cascade, or bedrock (Montgomery and Buffington, 1997). This potentially enables the results of our study to be applied in other catchments of similar morphology.

Hemispherical photographs were taken at the center of the stream at 10 m length intervals to characterize riparian cover. A Canon EOS 5D digital SLR camera with a full-frame sensor and a Sigma 180° true fisheye lens attached to a levelled tripod at 1.4 m above the stream surface was used. Images were processed using Gap Light Analyzer v2.0 (GLA) (Frazer *et al.* 1999) to derive percent canopy cover (page 10).

2.3.2. Stream energy balance data

A meteorological station was installed at the downstream end of the study site in May 2010 1 m from the stream bank at an elevation of 1502 m asl in order to quantify the surface energy balance of the stream. Hourly and daily averages of 10 second (s) readings of air temperature (T_a; °C), relative humidity (*RH*; %), wind direction and speed (u; m s^{-1})

were recorded at 2 m above the stream bankfull depth. Net radiation (Q^*; W m^{-2}) was recorded (Table 2.1) at 1 m above bankfull depth, directly above the stream surface. All data were recorded on a Campbell Scientific (CSC) CR1000 data logger. Hourly precipitation (mm) measurements were collected using a Jarek PVC tipping bucket rain gauge in an opening surrounded by an open lodgepole pine canopy approximately 10 m from the stream bank at the upstream end of the detailed study site (Fig. 2.1c).

A HOBO UA-004-64 pendant temperature sensor located at the downstream end of the detailed study site was used to collect hourly averages of 1 minute readings of stream temperature (T_s; °C). Enclosures built from white PVC (3.8 cm diameter) were used to prevent damage to the sensors and to minimize the effects of heating from shortwave radiation. Comparison of T_s values between open and closed enclosures showed a 10 minute time lag between enclosure types during peak daily T_s, with the open enclosures responding more quickly. However, the average difference in T_s between open and closed enclosures was within the range of error of the sensor.

2.3.3. Stream mass balance data

To quantify the reach-scale stream mass balance, discharge (Q; m^3 s^{-1}) was estimated using stage-discharge relationships at Star East-fork, Star West-fork, and Star Main gauging stations, and at Star McLaren using a compound weir (120^oV-notch below a rectangular throat). Stage (mm) was measured in the stilling pond of the Star McLaren weir, Star East-fork and Star West-fork inside of stilling-wells constructed from 7.6 cm PVC tubing with holes drilled vertically along the tubing at 5 cm intervals. Measurements were taken using HOBO U20 pressure transducers in the stilling-wells; while a dry gas bubbler system (Waterlog models H-350 LITE and H355) with a CSC CR-10X data

logger was used to measure and record stage at the Star Main gauging site. Stream discharge was measured weekly at all gauging sites during periods of high, low, and median *Q* using a FlowTracker® acoustic doppler velocimeter (SonTek-YSI). Stage-discharge relationships were used to calculate continuous stream discharge at all gauging sites except Star McLaren, where a weir-specific rating equation was used. Periodic current metering and slug injection salt dilution gauging (Moore, 2005) using a YSI Pro 30 logging electrical conductivity meter were used to verify discharge measurements from the McLaren weir. *Q* estimates were then used to calculate the difference in discharge (ΔQ) between the upstream tributaries (Star East-fork, Star West-fork, and Star McLaren) and the downstream gauging site (Star Main).

Table 2.1: Description of instruments used in the study and their accuracy.

Variable	Instrument used	Accuracy
T_a **and** ***RH***	HMP45C212 (Vaisala Inc.)	+/- 0.01°C; +/-2% RH (0-90%); +/- 3% RH (>90%)
u	05103-10A Wind Monitor (RM Young Company)	+/- 0.3 m s^{-1}
Q*	NR-Lite Net Radiometer (Kipp & Zonen)	+/- 10%; 0.3 – 30 µm
stage	HOBO U-20-001-01 (Onset Corporation); H-355 and 350-Lite Gas Purge Bubblers (Design Analysis Assoc. Inc.)	+/- 0.05% ; +/- 0.61 mm
T_s	HOBO UA-004-64 Pendant Loggers (Onset Corporation)	+/- 0.54°C

Two cross-sections located 30 m apart were to measure water table levels in the stream banks. The cross-sections were selected based on the ease of piezometer installation, as the alluvial material was difficult to penetrate. Solinst 30 cm PVC piezometers were installed 1.5 m below the ground surface at approximately 45° to the stream bank at each cross-section, similar to Woessner (2000). Piezometers were located 1 m from the stream bank and at 5 m intervals out from the stream bank (Fig. 2.1c).

Given the difficulty with installation, only three piezometers were installed in the upstream cross-section and two in the downstream cross-section. Ten in-stream steel drive-point piezometers (15 cm in length) were installed at 10 m intervals along the stream centreline to a depth of 25 cm into the substrate to characterize hyporheic exchange flow (C. Westbrook, pers. comm.; Baxter *et al.* 2003).

Morning water level measurements were collected between 900 and 1100 hrs weekly during the high flow period (May to June) and bi-weekly during the baseflow period (July to September) to determine up- and downwelling within the streambed, and the depth to the water table adjacent to the stream. Measurements were taken using a Heron Instruments manual water level tape. A removable stilling well built from 7.6 cm diameter PVC tubing with holes drilled at 5 cm intervals was placed over the piezometer to ensure measurement accuracy of stream water levels beside each in-stream piezometer. Water level measurements from the in-stream piezometers were used to calculate the vertical hydraulic gradient (*VHG*) at each piezometer (Baxter *et al.* 2003):

$$VHG = \frac{\Delta h}{\Delta l} \qquad (2.1)$$

where, Δh is the difference in head between the water level inside the piezometer and the level of the stream surface (cm), and Δl is the depth from the streambed surface to the first hole in the piezometer sidewall (cm) (Baxter *et al.* 2003). Summer mean *VHG* and depths to water table were derived from July and August measurements in both years, allowing for direct comparison between years during the baseflow period.

Snow water equivalent (*SWE*) data were collected during the winters of 2010 and 2011 (February to April) at eight permanent 500 m long snow survey transects (Dixon,

2011). Transects were oriented perpendicular to the stream channel and captured the local variation in topography and vegetative cover. At each transect snow depth measurements were taken at 10 m intervals and surveys were conducted on approximately the same dates between years (Dixon, 2011).

2.3.4. Baseflow separation

Automated baseflow separation was applied to determine the approximate proportions of source water contribution to Star Creek in 2010 and 2011. The baseflow separation analysis was used to identify:

1. Quickflow – flow through soils and shallow groundwater (interflow) with short residence times; and,
2. Baseflow – flow through deeper groundwater with long residence times.

A recursive filtering technique described by Arnold *et al*. (1995) was used. While empirical hydrograph separation techniques do not have a physical basis, they do provide an objective and repeatable approach to estimate the comparative fast (quickflow) and slow (baseflow) components comprising stream hydrograph response in the absence of tracer or isotope data. They are used here to provide an approximation of the proportion of hydrograph response driven by baseflow contributions. The high frequency signal (quickflow) is filtered from the low frequency signal (baseflow) using three successive low pass filters (forward, backward, and forward) to identify the proportion of the hydrograph derived from baseflow (Arnold *et al.* 1995 and Arnold and Allen 1999). Each pass of the filter results in a lower baseflow as a percentage of total streamflow. A mean of pass 1 and 2 was used as an estimate of baseflow for both study periods, as this has

previously been shown to provide reasonable baseflow estimates (Arnold and Allen, 1999).

2.3.5. Stream energy and mass balance calculations

We assume, for the purpose of this study, that hydrometeorological and T_s measurements collected at the detailed study site are representative of the entire study reach. We acknowledge that this is not realistic; however, given that the objective is to compare inter-annual differences in T_s and processes controlling T_s, this assumption is reasonable. We could not calculate all heat inputs and outputs to the stream because we lacked data for bed and hyporheic temperature. Therefore, in order to assess the processes controlling T_s over the study reach we compared surface energy fluxes which consisted of: measured net radiation (Q^*; W m^{-2}), and calculated sensible (Q_h) and latent (Q_e) heat (W m^{-2}). Calculations were conducted at an hourly time-step for each day during the study period.

$$Q_e = 285.9(0.132 + 0.143 * u)(e_a - e_w) \quad (2.2)$$

where, e_a and e_w are the vapour pressures of air and water respectively (Moore *et al.* 2005b).

$$Q_h = \beta * Q_e \quad (2.3)$$

where, β is the Bowen ratio (Leach and Moore, 2010).

We also compared Q, ΔQ, depth of water (*depth*; m) and wetted width (*WW*; m) between years. The *depth* of water was determined as a linear relationship between Q and

measured *depth* during all manual *Q* measurements collected at Star Main (n = 22, R^2 = 0.78), the same relationship was applied to both years.

2.3.6. Data analysis

Given that all continuous hydrometeorological data and calculated fluxes used in this study are temporally autocorrelated, comparisons were conducted on a weekly basis using paired t-tests to assess differences. Correlations were assessed between weekly mean, maximum, minimum and range in T_s and *Q* values using a combined sample of both years of data. *VHG* data can be problematic, resulting in inaccurate descriptions of surface-subsurface exchange due to the possibility of *VHG* patterns representing variations in subsurface flow or hydraulic conductivities of the stream bed (Krause *et al.* 2012). Therefore, we used a mean *VHG* value of all ten piezometers for each day of measurement for comparison between years. To compare means of distance to water table, the non-parametric Mann-Whitney U test was used. Precipitation was analyzed by assessing daily total amounts and the frequency of events, no statistical comparisons were made. *SWE* data were compared by Dixon (2011). Significance for all statistical tests presented in the results is at the 95% confidence level.

2.4. **Results**

Mean, maximum, minimum, and the range in weekly T_s were significantly different between years (Fig. 2.2; Table 2.3). T_s was generally lower in 2011, with the greatest inter-annual difference in mean, maximum, minimum, and range in weekly T_s during July, while the least difference in mean, maximum, and range in weekly T_s occurred in August. The least difference in minimum weekly T_s occurred in May and

August (Fig. 2.2). A reversal occurred in September 2010, where mean, maximum, minimum, and the range in weekly T_s were lower than 2011 (Fig. 2.2).

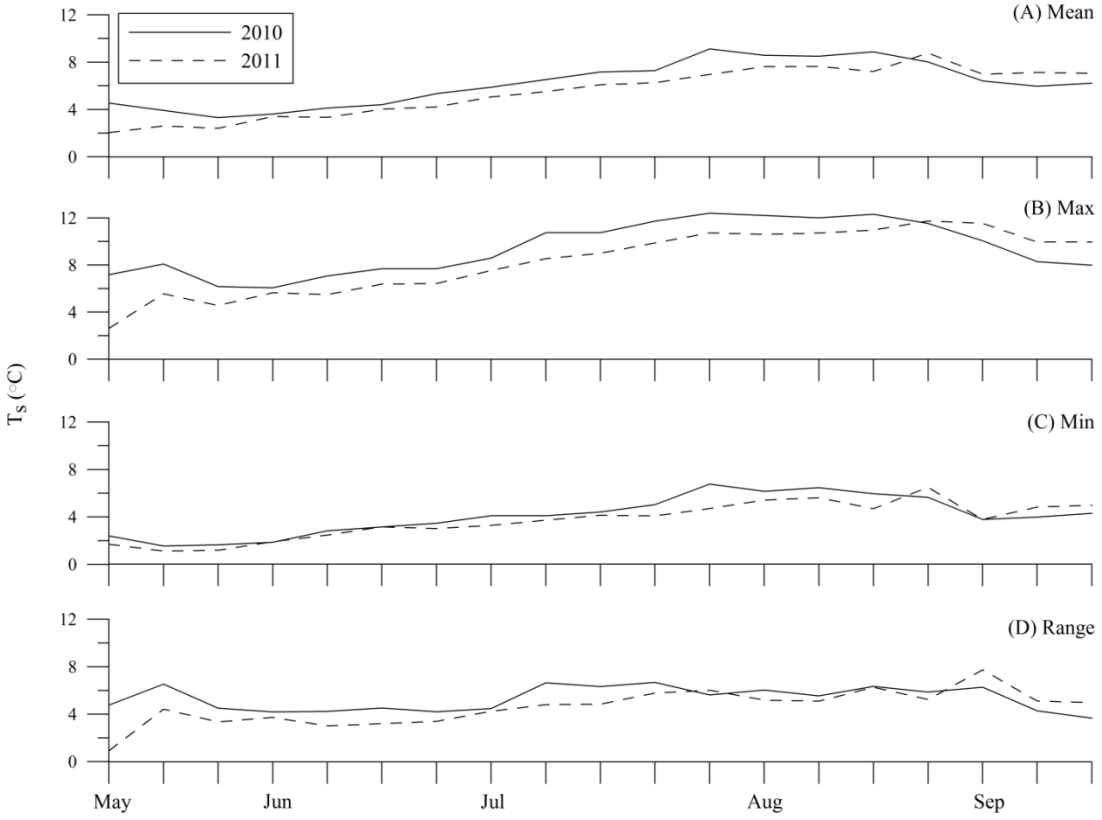

Figure 2.2: Mean (A), maximum (B), minimum (C), and range (D) in weekly T_s at Star Main for the study period from May 15 to September 15, 2010 and 2011.

Mean weekly Q^* values were not significantly different between years, with 2011 having a higher overall mean (Table 2.2; Fig. 2.3a). Given that hemispherical photos were only taken in 2011, difference in canopy closure could not be quantified. However, field observations did not suggest a change in riparian vegetation cover between years. Estimated mean weekly Q_e values were also not significantly different between years; however, lower (more negative) values occurred in August and September 2011 and May 2010 (Table 2.3; Fig. 2.3b). There was also no significant difference in estimated mean weekly Q_h, with higher (more positive) values in 2011 for a larger proportion of the study

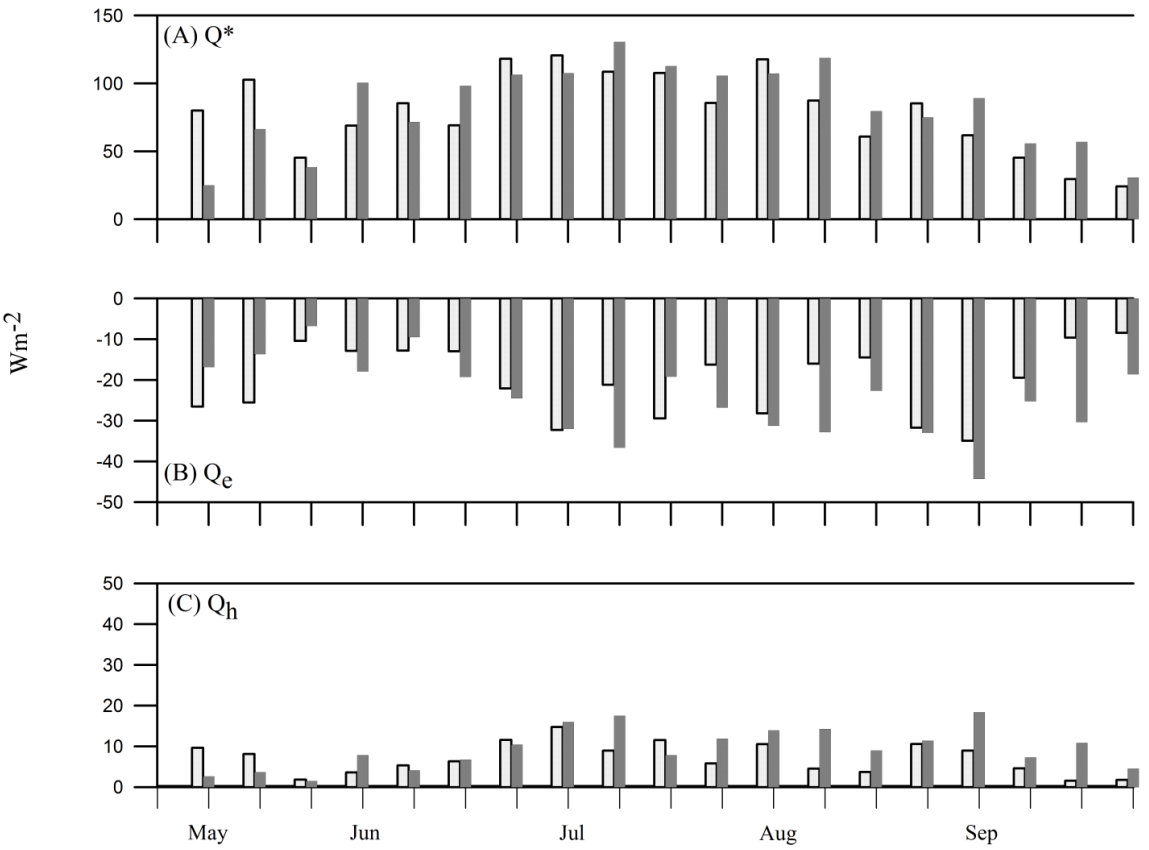

Figure 2.3: A comparison of mean weekly Q^* (A), Q_e (B), and Q_h (C) at Star Main for 2010 and 2011.

period (Table 2.2; Fig. 2.3c). There were significant differences in mean weekly Q between years (Table 2.2). Generally, 2011 had higher Q; however, in September 2010 Q was higher than in 2011 (Fig. 2.4). Peak Q was two times greater in 2011 relative to 2010 and the hydrograph was more variable (Fig. 2.4). Weekly mean Q was inversely correlated with mean, maximum, minimum, and range in weekly T_s. The highest correlation was between Q and mean weekly T_s ($r = -0.65$, $n = 38$, $p < 0.0001$), with maximum weekly T_s being secondary ($r = -0.64$, $n = 38$, $p < 0.0001$). The correlation between Q and range in weekly T_s ($r = -0.57$, $n = 38$, $p = 0.0002$) was higher than with minimum weekly T_s ($r = -0.55$, $n = 38$, $p = 0.0004$).

Table 2.2: Summary of variable means over the study period and p-values for paired t-test. Bolded values are significant differences.

Variable (units)	Mean value over the study period (2010/2011)	p values (df = 18)
T_s *max (°C)*	**9.40/8.30**	**0.006**
T_s *min (°C)*	**4.09/3.71**	**0.03**
T_s *mean (°C)*	**6.20/5.50**	**0.001**
T_s *range (°C)*	**5.30/4.60**	**0.02**
Q^* *(W m^{-2})*	79.17/82.96	0.50
Q_e *(W m^{-2})*	-20.27/-24.26	0.07
Q_h *(W m^{-2})*	7.04/9.47	0.05
Q (m^3 s^{-1})	**0.22/0.31**	**0.005**
ΔQ (m^3 s-1)	**0.03/0.11**	**0.009**
Depth (m)	**0.13/0.15**	**0.004**

Observed precipitation values over the study period differed substantially between years: 2010 had higher precipitation than 2011 (Fig. 2.4). However, the most dramatic differences were in August and September with 270% and 1966% more precipitation, respectively, occurring in 2010. During the study period 2010 had 59 precipitation events > 0.25 mm (the detection limit of the gauge), while in 2011 there were only 15 events >0.25 mm. Catchment-scale mean annual *SWE* derived from manual snow course measurements was 6.23 ± 4.97 cm in 2010, and 23.56 ± 7.27 cm in 2011, a difference of 116% (Dixon, 2011).

The estimated mean proportion of baseflow contribution to total *Q* over the study period was 74% in 2010 and 68% in 2011. However, 2011 had a higher peak estimated baseflow contribution to streamflow (Table 2.3; Fig. 2.5). Reach-scale mean weekly *ΔQ* was also significantly different between 2010 and 2011 during the study period (Table 2.3; Fig. 2.5). Peaking during the ascending limb of the hydrograph, *ΔQ* was higher in

2011 during May, June, July and lower in September, similar to estimated subsurface contribution to total *Q* (Fig. 2.5). During the end of May and the end of June (before and after peak *Q*) 2010 had negative ΔQ values. In 2011 during the same periods ΔQ remained positive, with the exception of two days in May.

Mean *WW* values over the study period of 3.54 and 3.61 m in 2010 and 2011 respectively, were not significantly different (df = 9, p = 0.29). Estimated mean weekly *depth* values were significantly different for the study period, with 2011 having greater mean weekly *depths* than 2010 except in September, when 2010 had a higher mean weekly *depth* (Table 2.2).

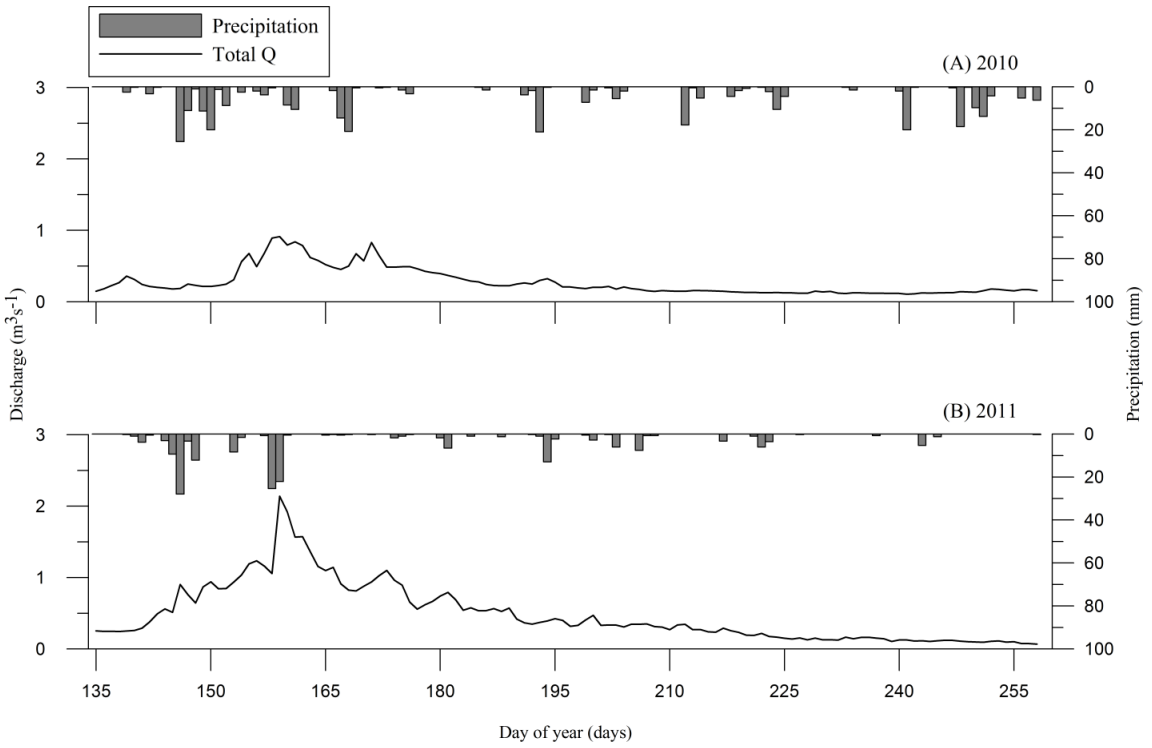

Figure 2.4: Daily total precipitation and mean daily *Q* for the study period from May 15 to September 15, 2010 (A) and 2011 (B).

Mean distance to water table was substantially lower in mid July 2011, while no significant difference was found between years in mid to late August (df = 13, p = 0.82;

Table 4). Mean *VHGs* were not significant different between years (df = 3, p = 0.59), with negative and positive values during late spring shifting towards positive and negative values during late summer in 2010 and 2011, respectively (Table 2.3).

Table 2.3: Mean distance to the water table calculated using measurements in all five cross-section piezometers for three dates in 2010 and 2011. Mean *VHG* using measurements of all 10 in-stream piezometers on four dates in 2010 and 2011.

	Mean distance to water table (cm)		**Mean VHG**	
Date (2010, 2011)	***2010***	***2011***	***2010***	***2011***
July 2, June 27	N/A	N/A	-0.07	0.37
July 16, July 14	117.4	88.4	0.04	0.08
July 30, July 29	115.3	111.7	0.07	-0.05
August 20, August 18	114.0	114.0	0.06	0.00

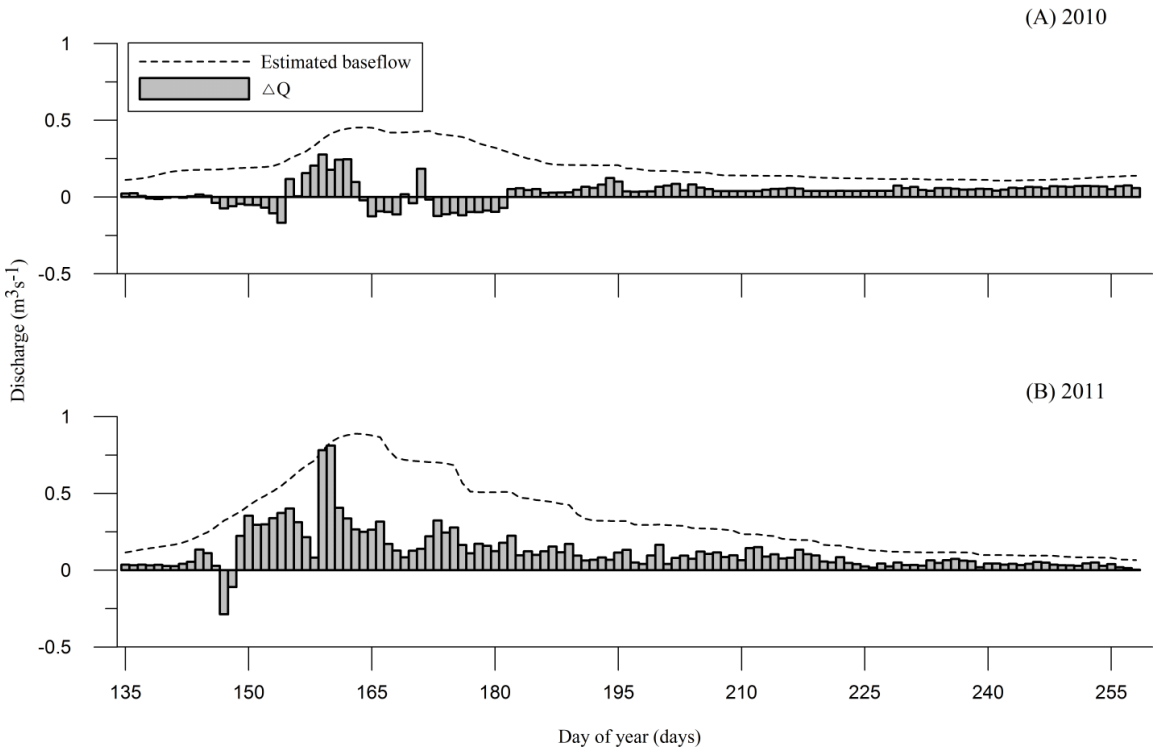

Figure 2.5: Estimated baseflow contribution to total *Q* and daily *ΔQ* downstream of the study reach for the study period from May 15 to September 15 in 2010 and 2011.

2.5. **Discussion**

This study demonstrates that inter-annual differences in T_s in Star Creek during 2010 and 2011 were primarily driven by hydrological conditions. By assessing the processes governing T_s, this study demonstrates that surface atmospheric processes, well understood to drive T_s in some small streams, do not fully explain inter-annual differences in summer T_s in Star Creek. This is supported by the findings that mean weekly Q^*, which dominates the energy budget of small streams (Brown, 1969; Brown and Krygier, 1970; Sinokrot and Stefan, 1993; Webb and Zhang, 1997; Johnson, 2004; Hannah *et al.* 2008; Leach and Moore, 2010), did not differ significantly between 2010 and 2011. In addition, mean weekly Q^* was generally higher in July 2011 which is when T_s differences were greatest between years, suggesting the effect of Q^* on T_s was outweighed by other factors.

Although no significant difference was found, lower (more negative) mean weekly Q_e values in 2011 were likely driven by higher T_a and u, and lower RH in 2011. Higher (more positive) mean Q_h values in 2011 were also likely a function of higher T_a. Based on their opposite signs, the effects of Q_e and Q_h on T_s acted against each other and given that turbulent fluxes have been shown to play a relatively minor role in governing summer T_s in small forested streams (Johnson, 2004; Hannah *et al.* 2008; Leach and Moore, 2010), Q_e and Q_h do not explain the consistent inter-annual T_s differences observed in Star Creek. These results suggest there are underlying mechanisms other atmospheric controls which are governing inter-annual differences of T_s in Star Creek.

Continuous hydrometeorological data enabled us to quantify differences in hydrological conditions, shown to be a confounding factor when assessing T_s patterns with relation to heat budgets (Hannah *et al.* 2008). In 2010, lower Q throughout most of the study period resulted in higher T_s, with the exception of September, where 2011 had lower Q and subsequently higher T_s. The inverse relationship between T_s and Q, also shown by Moore *et al.* (2005), is a function of a greater heat storage capacity in larger volumes of water (greater *depth*) which decreases the water column response surface to energy changes (Webb, 1996).

These results demonstrate that in order to advance our understanding of the potential impacts of environmental change on T_s, it is important to characterize the mechanisms governing inter-annual variation in hydrological conditions. Moisture conditions, the source of streamflow, and catchment characteristics can all play a substantial role in governing a streams thermal regime (Ward, 1994; Brown and Hannah, 2007). Consistently lower T_s and higher Q values during the most of the study period in 2011 were most likely a function of differences in catchment-scale moisture conditions - indicated by higher ΔQ, estimated baseflow contributions to Q, and distance to water table. This was contrasted in September, where higher Q, ΔQ, and estimated baseflow contribution to Q in 2010 indicated moisture conditions were wetter due to greater precipitation, resulting in lower T_s relative to 2011. Lower Q^* and Q_h in 2010 also likely contributed to lower T_s in September, demonstrating that meteorological and hydrological characteristics should be considered simultaneously.

The effect of catchment-scale moisture conditions on Q is related to inter-seasonal differences in the relationship between the stream and subsurface, evidenced through

negative ΔQ values corresponding with negative *VHG* in early July 2010 being contrasted by positive *VHG* and ΔQ in July of 2011. Peak ΔQ occurring in both years prior to peak *Q* and a more variable hydrograph in 2011 in the absence of higher summer precipitation demonstrate that snowmelt provides a key source of shallow and deep groundwater recharge, and subsequent discharge in this catchment. Snowmelt can provide 40 to 70% of groundwater recharge in catchments that receive 25-50% of annual precipitation as snow (Earman *et al.* 2006). Therefore, we suggest that higher SWE in 2011 would have resulted in higher groundwater recharge and subsequent discharge to the stream relative to 2010.

The relationship between catchment-scale moisture conditions and subsurface contributions to *Q* is important for Star Creek where the channel type is an intermediate between step-pool and pool-riffle, and thus conducive to surface-subsurface exchange (Kasahara and Wondzell, 2003; Buffington and Tonina, 2009). Our results (ΔQ, estimated baseflow contribution to *Q*) suggest that a primary source of *Q* in Star Creek is contributed from water sources with long residence times. Therefore, inter-seasonal changes in surface-subsurface exchange, driven by the relationship between stream stage and subsurface hydraulic gradients (Woessner, 2000), likely played a key role in governing T_s differences among years. Similar hydrologic controls on T_s have been observed at smaller temporal scales (Brown and Hannah, 2007). Seasonal variation of stream-subsurface hydraulic gradients in response to hydrologic events (Sophocleous, 2002; Lautz, 2012) suggests these interactions have the potential to strongly influence the temporal variation in T_s. Indeed, the effect of surface-subsurface exchange has been the focus of recent studies demonstrating these exchanges are as important as atmospheric

fluxes in governing T_s patterns (Leach and Moore, 2011). These complex surface-subsurface interactions and moisture conditions should be considered when assessing temporal T_s patterns in snowmelt dominated systems because shifts in snowmelt timing can alter the timing of groundwater discharge to streams, reducing late season Q (Huntington and Niswonger, 2012).

Changes in snowmelt timing (Stewart, 2009; MacDonald *et al.* 2011) and reductions in late-season Q (St. Jacques *et al.* 2010) as a result of atmospheric warming pose a substantial challenge for managing streams inhabited by native salmonid species. Although maximum T_s approached 12°C in July and August of 2010 and 2011, respectively, this temperature is well within the thermal tolerance of native westslope cutthroat trout (19.9°C; Bear, 2007) which inhabit an isolated portion of Star Creek. However, mean summer T_s values of approximately 7.3 °C were suggested by Rasmussen *et al*. (2010) to play a role in limiting hybridization between westslope cutthroat trout and non-native rainbow trout (*Oncorhynchus mykiss*). Given that rainbow trout occupy much of the Oldman River basin (M. Coombs pers. Comm.), the T_s conditions present during 2010 and 2011 suggest the upper portion of Star Creek studied here provides important habitat for the preservation of native westslope cutthroat trout in this region.

2.6. **Conclusion**

This work demonstrated that changes in hydrological conditions can play a substantial role in governing T_s in snowmelt and groundwater-dominated systems. Snowmelt and rainfall contributions to catchment-scale moisture conditions resulting in increased Q had a persistent cooling effect on summer T_s in Star Creek. Star Creek is

representative of many streams in mountain regions across western North America, and the T_s response of these systems to environmental change is likely to be governed by changes in both atmospheric and hydrologic conditions. Further research assessing the spatial and temporal variation in processes governing the interaction between surface and subsurface water sources in mountain catchments would enable a greater understanding of T_s dynamics in these systems.

The preservation of thermal habitat for salmonids depends on the maintenance of cold summer and warm winter T_s, both affected by groundwater contributions to streams (Power *et al*. 1999). It is expected that snow accumulation will decline in the future; therefore, future work should be directed towards understanding the role of snowmelt in determining shallow and deep groundwater recharge, and the subsequent effects on T_s.

Chapter 3: A process-based stream temperature modelling approach for mountain regions

3.1. **Introduction**

Stream temperature has been the focus of much recent research, primarily because temperature is a critical variable for aquatic ecosystem function (Buisson *et al*. 2008; Durance and Ormerod, 2009). The interaction between the surface (atmospheric) and subsurface (stream bed, hyporheic exchange, and groundwater flow) processes determining the thermal characteristics of streams is complex. Reach-scale studies continue to demonstrate that net radiation dominates the heat budget of most small streams (Brown 1969; Brown and Krygier, 1970; Sinokrot and Stefan, 1993; Webb and Zhang 1997; Johnson and Jones 2000; Hannah *et al.* 2008; Leach and Moore, 2010; Hebert *et al.* 2011; Garner *et al*. 2012). Latent and sensible heat fluxes act as secondary atmospheric controls, accounting for a relatively small proportion of the heat budget (Webb and Zhang, 1997; Johnson 2004; Leach and Moore, 2010). Hyporheic exchange flow can act to buffer stream temperature patterns (Poole and Berman, 2001; Story *et al*. 2003; Arrigoni *et al.* 2008; Leach and Moore, 2011). Collectively, reach-scale field studies have demonstrated that substantial spatial and temporal variation exists in both surface and subsurface processes controlling stream temperature (Webb *et al.* 2008). However, representing these processes in regions with limited data, and at scales applicable to environmental management-related questions presents a significant challenge.

Previous studies have applied statistical modelling methods, making use of correlations between stream temperature and variables such as stream discharge, air

temperature, and physical catchment characteristics to quantify stream temperature response to environmental change at relatively large spatial scales (Mohseni *et al.* 2003; Isaak *et al.* 2010; Jones *et al*. 2013). While statistical models are useful due to their relatively low input data requirements and spatial applicability, it is important to recognize the difference between correlation and causation when assessing processes controlling stream temperature (Johnson 2003). This distinction is important because getting the "right answers for the right reasons" (Kirchner, 2006) or "wrong answers for the right reasons" provides insight to further develop our conceptual understanding of how inter-related processes affect stream temperature. Therefore, modelling frameworks that incorporate the representation of key processes controlling stream temperature are necessary for understanding thermal response to environmental change (Norton and Bradford, 2009).

There are a number of process-based models available such as WET-Temp (Cox and Bolte, 2007) and SNTEMP (Theurer *et al.* 1984), later built upon to develop Heat Source (Boyd and Kasper, 2003) or models like SHADE-HSPF (Chen *et al.* 1998) and CEQUEAU (St-Hilaire *et al.* 2000) which integrate stream temperature and catchment-scale hydrological modelling. These models and others are useful for assessing causal relationships because they represent key processes controlling stream temperature. However, a limitation of process-based models is they often have high input data requirements and can be difficult to apply in data-sparse regions (Benyahya *et al.* 2007).

To-date, the application of process-based stream temperature models in complex mountain catchments is limited, presenting a challenge for fully understanding the effects of anthropogenic and natural environmental disturbance on stream temperature. Most

mountain regions lack the hydrometeorological and physiographic data required to simulate the stream energy and mass budget in process-based models. To help fill this gap, we developed a modelling approach that uses readily available hydrometeorological and physiographic data as spatial inputs to a process-based stream temperature model. This chapter describes the application of the Generate Earth Systems Science input (GENESYS) hydrometeorological model (MacDonald *et al*. 2009) with spatial and temporal downscaling routines developed in a Geographical Information System (GIS) to simulate energy and mass budget variables important for process-based stream temperature modelling.

3.2. **Study area**

Data for model development and testing were collected in Star Creek, described in Chapter 2. The three sites used for model development in this study are Star West upper Star East, and Star Main, located at elevations of 1691, 1597 and 1502 m asl, respectively (Fig. 3.1). Canopy closure, estimated using hemispherical photographs processed in Gap Light Analyzer v2.0 (GLA; Frazer *et al.* 1999), is 41%, 46% and 37% at Star West upper, Star East, and Star Main respectively. Over the entire stream, the mean bankfull channel width is 3.0 m with a mean wetted width of 2.6 m, a mean bankfull depth of 0.34 m and mean wetted depth of 0.21 m during a stream survey in August.

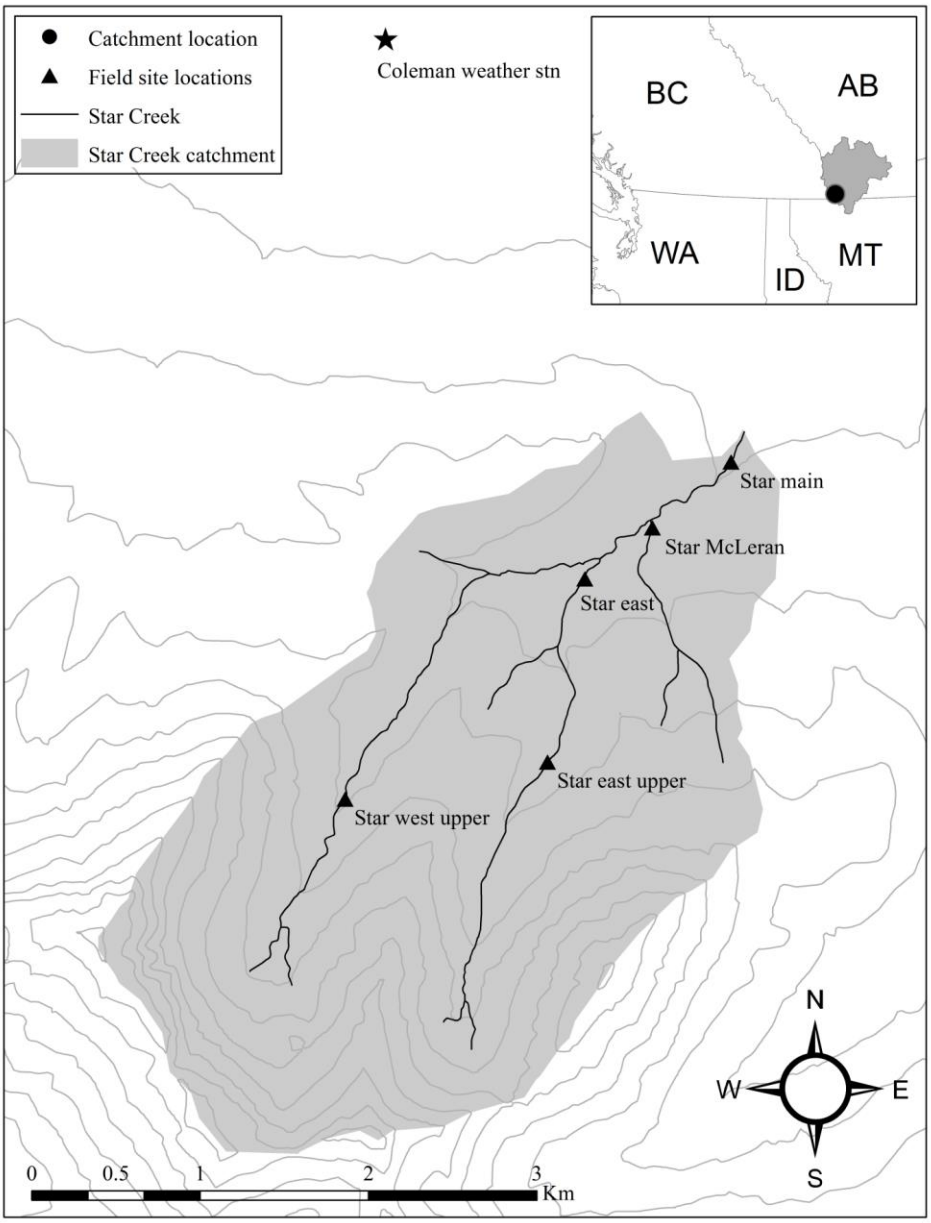

Figure 3.1: The Star Creek catchment, in the headwaters of the Oldman River, Alberta.

3.3. **Methods**

3.3.1. Stream morphology and riparian cover

The model parameterization used stream morphology data for Star Creek collected during stream surveys at the sub-reach (fall, cascade, chute, rapid, riffle, sheet, run, scour pool or plunge pool; Hawkins *et al.* 1993) and reach (colluvial, dune-ripple,

pool-riffle, plan-bed, step-pool, cascade, or bedrock; Montgomery and Buffington, 1997) scales. An advantage to using stream classification is that as stream morphology data become available through sources like provincial governments (e.g., BC-MOE, 2012), classification systems can be used to define a set of model parameters that can be applied over a range of catchments. A Lidar Digital Elevation Model (DEM) with a 1 m cell size (ASRD, 2008) was used to calculate channel slope and aspect along the entire stream.

Canopy closure values were assigned for each of the riparian cover types (mixed pine-spruce, lodgepole pine (*Pinus contorta*), and trembling aspen (*Populus tremuloides*) in Star Creek based on the Alberta Vegetation Inventory (AVI) spatial vegetation polygon data (ASRD, 2010). The AVI data were also used to describe landcover types for the entire catchment, which consisted of lodgepole pine, Engelmann spruce (*Picea engelmannii*), trembling aspen, subalpine fir (*Abies lasiocarpa*), white spruce (*Picea glauca*), alpine meadow, and talus. Soil characteristics were determined for each of the landcover types based on AVI polygon data. A total of 12 soil pits were dug (two per landcover type) to a depth of 1.5 m. Soil horizon depths and textures were measured *in situ* for each of the horizons (A, B, and C) identified in the pits (see Klute, 1986). Field capacity values were defined for each pit and landcover type based on texture as per Saxton and Rawls (2006).

3.3.2. Stream energy and mass balance data

Energy balance, mass balance, and stream temperature data used for this study were collected for the period between May 15 and December 31, 2010. Hydrometeorological stations located at Star West upper and Star Main (Fig. 3.1) were used to quantify the surface energy balance of the stream and to verify the model's ability

to accurately represent stream temperature conditions (T_s; °C). At each station hourly and daily mean air temperature (T_a; °C), relative humidity (RH; %), and wind speed (u; m s^{-1}) were calculated from 10 second measurements taken 2 m above the stream bankfull depth. Hourly mean net radiation (Q^*; W m^{-2}) was calculated from 10 second measurements taken directly over the stream surface at 1 m above bankfull depth. Hourly total precipitation (mm) was measured approximately 10 m from the stream bank at the Star Main site. Hourly mean T_s was calculated from 1 minute measurements at the Star West upper, Star East upper, Star East, Star McLaren, and Star Main sites (Fig. 3.1).

Hourly mean stream discharge (Q; m^3 s^{-1}) was estimated using stage (cm) - discharge relationships at the Star Main, Star East, and Star West upper gauging stations, and at Star McLaren using a compound weir. Hourly mean stream stage was calculated from 10 second measurements taken in-stream at each site. Manual Q measurements were collected once per week over the study period at each site. Manual Q measurements were also collected once per month during June, July, August, and September at ten locations spaced approximately 100 m apart along Star Creek from Star Main to immediately upstream from the confluence of Star West and Star East (Fig. 3.1).

3.3.3. Hydrometeorological model

We used output from the GENESYS model to provide hydrometeorological inputs to a process-based stream temperature model. The advantage of using this modelling approach is that GENESYS uses readily available meteorological data to extrapolate hydrometeorological conditions over mountainous terrain (MacDonald *et al*. 2009). Daily maximum T_a, minimum T_a, average u, and total precipitation from the Star

Main station were used as input to the GENESYS model for the period from January 1 to December 31, 2010.

The GENESYS model has been primarily used to simulate snow water equivalent (*SWE*) (Lapp *et al.* 2005; MacDonald *et al.* 2009; MacDonald *et al.* 2011; MacDonald *et al.* 2012) by integrating a GIS and a series of physical subroutines to estimate hydrometeorological variables for individual hydrological response units (HRUs). Using a combination of landcover from the AVI (ASRD, 2010), 100 m elevation bands, and relative radiation derived using the Lidar DEM, 90 HRU's were developed for the Star Creek catchment.

For each HRU, daily maximum and minimum T_a were estimated using regional monthly lapse rates derived from the Parameter-elevation Regressions on Independent Slopes Model (PRISM) monthly normal (1971-2000) data (Daly *et al.* 2008). Daily precipitation estimates were also made for each HRU using regional monthly lapse rates derived from PRISM. Daily maximum and minimum T_a outputs from the GENESYS model were used to estimate hourly mean T_a with a method developed by Parton and Logan (1981), where hourly T_a for daytime hours is calculated as:

$$T_{a(i)} = (T_{\max} - T_{min}) - \sin\left(\frac{\pi * m}{Y + 2\alpha}\right) + T_{min} \qquad (3.1)$$

where, $T_{a(i)}$ is air temperature (°C) for the i^{th} hour, T_{max} is maximum daily T_a (°C), T_{min} is minimum daily T_a (°C), m is the number of hours between minimum daily T_a and sunset, Y is day length (hours), and $\boldsymbol{\alpha}$ is a lag coefficient for $T_{max.}$(1.8). For night time hours T_a is calculated as:

$$T_{a(i)} = T_{min} + (T_{sunset} - T_{min}) * \exp\left(-\frac{b * n}{z}\right) \quad (3.2)$$

where, T_{sunset} is the air temperature at sunset (°C), estimated as a function of daylight hours, b is a night time temperature coefficient (2.2), n is the number of hours from sunset to the time of T_{min}, and z is the night length (hours). Day and night hours were determined using the day of year and latitude (Parton and Logan, 1981).

Hourly T_a estimates were used to calculate vapour pressure gradients and *RH* (Glassy and Running, 1994):

$$RH = \frac{es}{esd} * 100 \quad (3.3)$$

where, *es* is vapour pressure at dew point (kPa) and *esd* is vapour pressure at T_a (kPa). Dew point temperature (T_d; °C) was estimated as a function of T_a (T_d = 0.6 * T_a – 5.5) derived by Dalla Viccenza (2012). Atmospheric transmissivity (*TRANS*; %) was also calculated for each day (Bristow and Campbell, 1984):

$$TRANS = A[1 - \exp(-Bcoeff * \Delta T^{Ccoeff})] \quad (3.4)$$

where, *A* is the maximum atmospheric transmittance expected based on elevation of the HRU, *Bcoeff*, and *Ccoeff* are coefficients set to 0.003 and 2.4 respectively (Sheppard, 1996); and ΔT (°C) is the daily range in T_a.

A daily hydrological balance was calculated during the snow-covered period for each HRU using:

$$SWE_{(t)} = SWE_{(t-1)} + Precip_{(t)} - Int_{(t)} - Subl_{(t)} - IF_{(t)} \quad (3.5)$$

where, *SWE* is the snow water equivalent (mm), *Precip* is simulated daily total rain or snow (mm), *Int* is canopy interception (mm), *Subl* is sublimation (mm), *IF* is infiltration

(mm), and *t* is the time step (days). Soil moisture conditions (*SM;* mm) were simulated from snowmelt onset throughout the snow-free period using:

$$SM_{(t)} = SM_{(t-1)} + IF_{(t)} + Precip_{(t)} - ET_{(t)} - Recharge_{(t)} - Run_{(t)} \quad (3.6)$$

where, *ET* is evapotranspiration (mm) *Run* is runoff (mm), and recharge is groundwater recharge (mm) contributing to catchment groundwater storage.

For all water balance components the model applies a sloped area under-estimation factor (*SAUEF*) developed by Kienzle (2010) to correct for the sloped area of the catchment:

$$SAUEF = 1 + SAUE/100 \quad (3.7)$$

where, SAUE is the sloped area under-estimation, calculated as:

$$SAUE = (100/COS(Slope_{degrees} * \pi/180)) - 100 \quad (3.8)$$

Precipitation phase (rain or snow) is determined by applying an algorithm developed by Kienzle (2008) which uses mean daily and threshold T_a to determine the proportions of rain and snow:

$$\Pr = 5\left(\frac{T_{am} - T_t}{1.4T_r}\right)^2 + 6.76\left(\frac{T_{am} - T_t}{1.4T_r}\right)^2 + 3.19\left(\frac{T_{am} - T_t}{1.4T_r}\right) + 0.5 \quad (3.9)$$

where, Pr is the proportion of precipitation that falls as rain, T_{am} is the mean daily air temperature (°C), T_t is the threshold mean daily temperature (3.7°C), and T_r is the range of air temperatures where both rain and snow can occur (16°C).

Snow *Int* is calculated using a method developed by Hedstrom and Pomeroy (1998):

$$Int = I * 0.678 \quad (3.10)$$

where, *I* is the intercepted snow load at the start of unloading from the canopy (mm) and 0.678 is an unloading coefficient (Hedstrom and Pomeroy, 1998). Rain *Int* is calculated using an empirical formula developed by Von Hoyningen-Huene (1983):

$$Int = 0.30 + 0.27Rain + 0.13LAI - 0.013Rain^2 + 0.0285RainLAI * LAI - 0.007LAI^2 \quad (3.11)$$

where, *LAI* is leaf area index derived from the AVI dataset. *Subl* (kg m^{-1} s^{-1}) is estimated with a method developed by Déry *et al.* (1998) for both open and forested areas:

$$Subl = \frac{d_m}{d_t} \mathrm{N}_{(z)} \quad (3.12)$$

where, $\frac{d_m}{d_t}$ is the change in mass of a blowing snow particle from sublimation per second and $N_{(z)}$ is the number of blowing snow particles per unit volume (assumed to be 9.09 x 107 m^{-3}; Déry *et al.* 1998). In forested areas of the catchment, *Subl* estimates are only made for snow retained in the canopy. *ET* is calculated using a modified Penmann-Monteith method (Valiantzas, 2006):

$$ET = 0.038\, Q^* \sqrt{T_a} + 9.5 - 2.4\left(\frac{Q^*}{R_a}\right)^2 + 0.075(T_a + 20) * \left(1 - \frac{RH}{100}\right) \quad (3.13)$$

where, R_a is extraterrestrial radiation (W m^{-2}) calculated in the GIS.

Snowmelt (mm) is estimated with a temperature-index routine developed by Quick and Pipes (1977):

$$Snowmelt = \mathrm{PTM}[T_{max}(TCEADJ * T_{min})] \quad (3.14)$$

where, T_{max} is maximum daily air temperature (°C), T_{min} is minimum daily air temperature (°C), *TCEADJ* is an energy partitioning multiplier (Wyman, 1995), and PTM is the melt factor (mm; $°C^{-1}$). A variable melt factor is applied to represent changes in landcover and the time of year (Dewalle *et al.* 2002). A routine using the Soil Conservation Service curve number (SCS-CN) approach (USDA SCS, 1985) was added to the GENESYS model and applied to estimate *Run* and water contributing to *IF*:

$$Run = \frac{(Input - \lambda S_{max})}{Input + (1 - \lambda)S_{max}} \tag{3.15}$$

where, *Input* is daily total precipitation and snowmelt (mm), λ is a constant set to 0.2 (Beven, 2001), and S_{max} is a maximum volume of water retention (mm^3), calculated as:

$$S_{max} = 2.54\left(\frac{1000}{CN} - 10\right) \tag{3.16}$$

Curve number (*CN*) values depend on soil type (defined for each HRU from field measurements) and antecedent moisture conditions, with a range between 50 (high soil moisture storage potential) and 80 (low soil moisture storage potential).

The current version of the GENESYS model assumes groundwater recharge is an exponential function of *SM*, where higher *SM* has a higher contribution to recharge and lower *SM* has a lower contribution to recharge. This method is not physically-based; however, given the complexity in quantifying groundwater recharge in mountain catchments (Magruder *et al*. 2009), this approach provides an approximation of recharge that is similar to methods used in other studies (Yoo, 2012).

A runoff routing routine was added to the GENESYS model which applies the Muskingum method:

$$O2 = C1I1 + C2I2 + C3O1 \quad (3.17)$$

where, *O1*and *O2* are inflow and outflow discharges, respectively (m^3 s^{-1}); C1, C2, and C3 are dimensionless parameters; and *I1* and *I2* are inflow discharges at time 1 and time 2, respectively (m^3 s^{-1}).

An exponential storage-discharge curve was applied to estimate the baseflow contribution to *Q* in the GENESYS model as a function of *Recharge*. The storage-discharge curve in GENESYS was calibrated using estimated baseflow contribution to *Q* at Star Main derived with the recursive filtering technique described in Chapter 2 (Arnold *et al*. 1995; Arnold and Allen 1999). Baseflow contribution to *Q* estimates from GENESYS and total stream length were used to estimate lateral groundwater inflow (Q_{in}; m^3 s^{-1} m^{-1}) in Equation 3.33 (Herb and Stefan, 2011).

3.3.4. The Mountain Stream Temperature model

Outputs from the GENESYS model used as input to the Mountain Stream Temperature (MST) model included hourly mean T_a and *RH*, daily mean *Q*, subsurface contribution to *Q*, and *TRANS*. A *u* model was not developed; therefore, hourly mean observed *u* calculated from 10 second readings at the Star Main meteorological station was used in this study (Fig. 3.2).

The MST model applies temperature response units (TRUs) to spatially represent processes affecting T_s. TRUs are based on the same logic as HRUs, in that the physiographic characteristics of a stream are represented with spatial data. Three spatial datasets were used to derive TRU's for Star Creek. A stream shapefile was used to derive stream order, the Lidar DEM was used to determine stream slope and aspect, and the AVI

land cover data were used to describe dominant riparian vegetation types (lodgepole pine, Engelmann spruce, and trembling aspen). An overlay analysis of stream order, slope, aspect, and riparian vegetation type was used to identify homogeneous regions along the stream. Confluences of tributaries were used also to define starting points of TRUs. The result of this analysis identified 11 TRUs for Star Creek, ranging in length from 382 to 593 m. TRUs were contiguous; each TRU represents the upstream boundary for the subsequent downstream TRU. For each TRU, mean bank full width (m), channel slope (m m^{-1}), substrate type (gravel, cobble, boulder), upper and lower contributing catchment area (m^2), and the riparian vegetation type representing the majority of the TRU area were used in model parameterization.

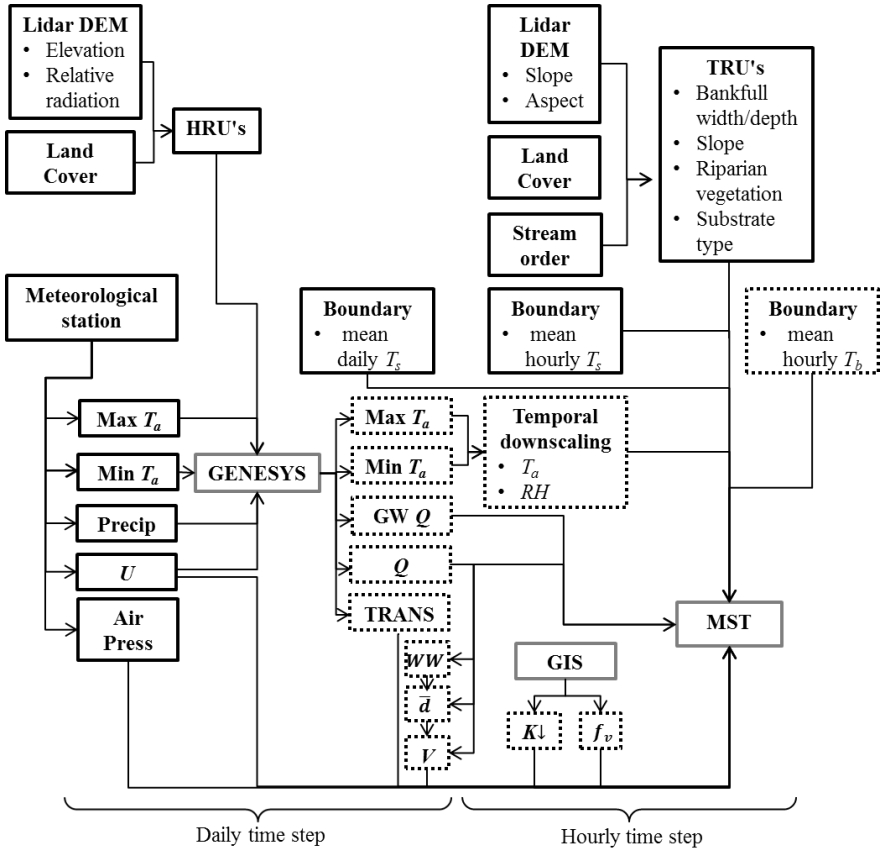

Figure 3.2: Flow diagram of the modelling process going from meteorological and GIS data to the GENESYS and MST models. Boxes with black outlines indicate model inputs, grey outlines indicate modelling steps, and dashed outlines indicate simulated variables used as input to the MST model.

An automated area-weighting program was developed in a GIS to provide hydrometeorological and channel morphology inputs to the MST model for each TRU. This program can be applied using any source of spatial data and enables the model to be easily transferable between catchments. Spatial hydrometeorological outputs from the GENESYS model, GIS-based radiation estimates, and spatial landcover classes were weighted by their proportional representation of a TRU (Fig. 3.3).

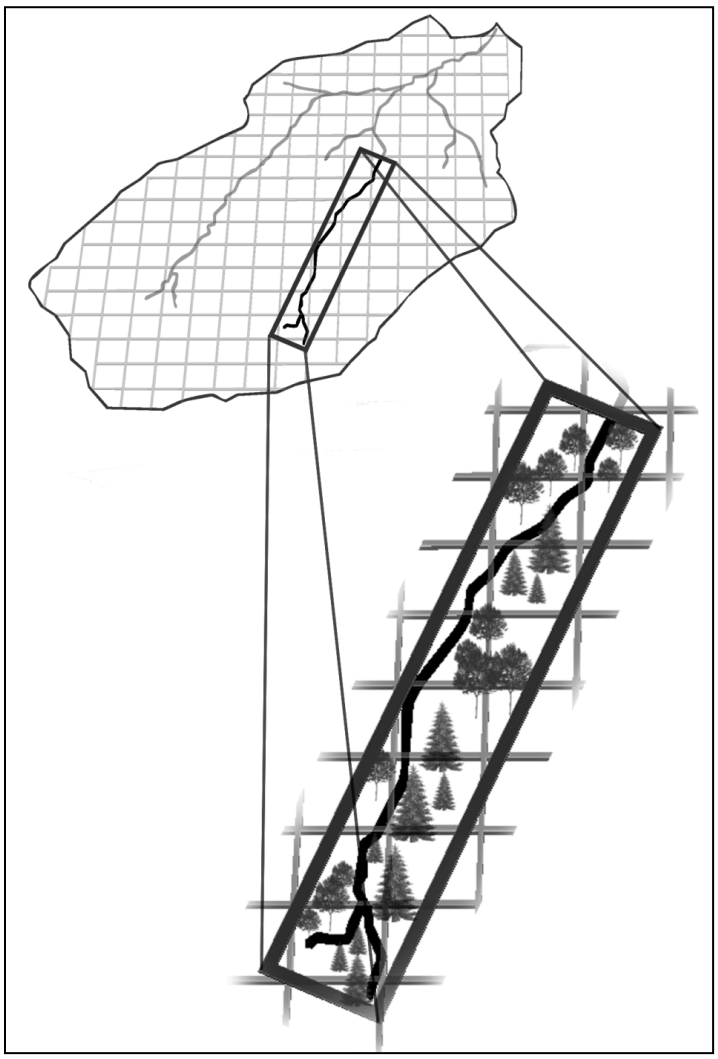

Figure 3.3: Conceptual diagram of coupling the GENESYS and MST models. The dark box represents a TRU in the MST model, while the light grid squares represent HRUs from the GENESYS model.

The MST model applies approaches developed by Leach and Moore (2010, 2011) and Boyd and Kasper (2003). Like most process-based T_s models, the MST model requires an upstream T_s measurement to provide boundary conditions, where a parcel of water is "released" from the upstream measurement location at an hourly time step. Measured hourly mean T_s from Star West upper and Star East upper were used in this simulation. The relationship between T_a, Q and T_s derived using measured data from Star East upper (R^2 = 0.76, *RMSE* = 0.74, n = 3145) was used to provide initial values of T_s for Star McLaren. One dimensional advection and heat transfer inputs to the stream are estimated for each TRU using (Boyd and Kasper 2003):

$$\frac{dT_s}{dt} = -V\frac{dT_s}{dx} + \frac{(Q^* + Q_h + Q_e + Q_b + + Q_{gw} + Q_f)}{C * \rho * \bar{d}} \quad (3.18)$$

where, $\frac{dT_s}{dt}$ is the difference in T_s per unit of time (s). Velocity (V; m s^{-1}) is estimated as a function of Q, wetted width (WW; m), and wetted depth ($\bar{d}$; m). Continuous daily estimates of $\bar{d}$ were derived using multiple linear regression with WW and Q as predictive variables (R^2 = 0.64, *RMSE* = 0.01, n = 40). Continuous daily WW estimates were derived with linear regression with Q as the predictive variable (R^2 = 0.48, *RMSE* = 0.47, n = 40). All WW, Q, and $\bar{d}$ data were collected during manual measurements on Star Creek. Q^* is net radiation (W m^{-2}), Q_h is sensible heat flux (W m^{-2}), Q_e is latent heat flux (W m^{-2}), Q_b is the bed heat flux (W m^{-2}), Q_{gw} is the heat flux from groundwater (W m^{-2}), and Q_f is the heat flux from friction (W m^{-2}). C is the specific heat of water (4182 J (kg °C)$^{-1}$), and ρ is the density of water (998.2 kg m^{-3}) in each TRU.

3.3.5. Net Radiation estimates

Hourly estimates of net short- (K^*; W m^{-2}) and longwave (L*; W m^{-2}) radiation were used to estimate Q^*. The MST model applies the solar radiation tool in Arc GIS 10.0 to the 1 m Lidar DEM to spatially estimate hourly top of canopy maximum incoming shortwave radiation ($K\downarrow$; W m^{-2}) (assuming clear sky conditions) for each point along the stream. The area-weighted mean of hourly $K\downarrow$ was calculated automatically in the GIS for each TRU. Shading coefficients (*VegCoeff*) were derived for lodgepole pine, trembling aspen, and Engelmann spruce to account for the shading effect of riparian vegetation throughout the day (Herb and Stefan 2011). The *VegCoeff* values at Star West upper (Engelmann spruce) and Star Main (lodgepole pine/trembling aspen) were calibrated to minimize root mean square error (*RMSE*) between simulated and observed Q^* at each site. *TRANS* output from GENESYS and *VegCoeff* were used as input to the MST model on a daily basis to adjust K^* as a function of atmospheric transmissivity:

$$K^* = TRANS * K\downarrow * VegCoeff \quad (3.19)$$

The longwave radiation model was adapted from Leach and Moore (2010), described here in detail given assumptions and modifications to model inputs were made. Hourly mean longwave radiation from surrounding riparian vegetation, topography, and the atmosphere ($L\downarrow$; W m^{-2}) was estimated using the sky view factor (f_v), calculated in a GIS (Cimmery, 2010) with the Lidar DEM, emissivity of the atmosphere (ε_a), emissivity of the terrain and vegetation (ε_{tv}), the Stefan-Boltzmann constant (σ; 5.67 x 10^{-8} W m^{-2} K^{-4}), and T_a for each TRU:

$$L\downarrow = [f_v\varepsilon_a + (1 - f_v)\varepsilon_{tv}]\sigma(T_a + 273.2)^4 \quad (3.20)$$

where, ε_{tv} was assumed to be 0.96 (Link and Marks, 1999). The method used by Leach and Moore (2010) was applied to calculate ε_a:

$$\varepsilon_a = (1 + kcf)\varepsilon_o \quad (3.21)$$

where, *cf* is the cloud fraction and *k* is a constant that is dependent on cloud type. The *cf* value was estimated based on the ratio between K^* and $K\downarrow$ for K^*:$K\downarrow$< 0.2, *cf* = 1.0, and for K^*:$K\downarrow$ > 0.2, *cf* values decreased linearly to zero. Leach and Moore (2010) applied a *k* value of 0.26, which is the mean value of altostratus, altocumulus, stratocumulus, stratus, and cumulus cloud types based on Braithwaite and Olesen (1990). Given that the study area receives similar cloud types and uses a similar modelling approach to Leach and Moore (2010), the same value was applied. In addition, ε_a was applied to all days in the simulation given that cloud data were not available and qualitative field observations show that the region typically experiences cloud cover on a daily basis from orographic effects. For night time ε_a we applied the mean of daytime values from the previous day.

Clear-sky atmospheric emissivity (ε_o) as calculated using the Prata (1996) equation:

$$\varepsilon_o = 1 - (1 + w)exp[-(1.2 + 3.0pw)^{0.5}] \quad (3.22)$$

For this equation, precipitable water content (*pw*; cm) was estimated using (Leach and Moore, 2010):

$$pw = 465\left[\frac{e_a}{(T_a + 273.2)}\right] \quad (3.23)$$

Longwave radiation emitted from the stream water surface ($L\uparrow$; W m^{-2}) was estimated using:

$$L\uparrow = 0.95\sigma(T_s + 273.2)^4 \quad (3.24)$$

where, 0.95 is the emissivity of the stream, assumed to remain constant for the entire simulation. L^* was then estimated using:

$$L^* = 0.95L\downarrow - L\uparrow \quad (3.25)$$

Hourly Q^* estimates for each TRU were then calculated using:

$$Q^* = K^* + L^* \quad (3.26)$$

3.3.6. Latent and sensible heat fluxes

Latent and sensible heat flux calculations also follow Leach and Moore (2010), provided here in detail. Latent heat flux (Q_e) was calculated using an empirical equation (Webb and Zhang 1997) adapted by Moore *et al*. (2005):

$$Q_e = 285.9(0.132 + 0.143 * U)(e_a - e_w) \quad (3.27)$$

where, e_a is the vapour pressure of air (kPa) and e_w is the vapour pressure at the water surface (kPa), which is assumed to equal saturation vapour pressure (e_{sat}) calculated as a function of T_s (Leach and Moore, 2010).

$$e_{sat}(T) = e_0 * \exp\left[\frac{L_v}{\Re_v} * \left(\frac{1}{T_o} - \frac{1}{T}\right)\right] \quad (3.28)$$

where, e_o is 0.611 kPa, T_o is 273.2 K, T is the temperature of the air or water (K), L_v is the latent heat of vaporization (2.5 x 10^6 J kg^{-1}), and $\Re v$ is the gas constant of water vapour (461.5 J K^{-1} kg^{-1}). Estimates of e_a as a function of *RH* and e_{sat} were then calculated with:

$$e_a = \left(\frac{RH}{100}\right) e_{sat} \tag{3.29}$$

Sensible heat flux (Q_h) was estimated using:

$$Q_h = \beta * Q_e \tag{3.30}$$

where, β is the Bowen Ratio which was estimated with:

$$\beta = 0.66 * \left(\frac{Press}{1000}\right) * [(T_s - T_a)/(e_w - e_a)] \tag{3.31}$$

where, *Press* is air pressure (kPa) at the Coleman weather station (Fig. 3.1; Environment Canada, 2012b).

3.3.7. Bed, groundwater, and friction heat fluxes

The bed heat flux was determined using Moore *et al*. (2005):

$$Q_b = K_c(T_b - T_s)/(0.05\ \text{m}) \tag{3.32}$$

where, K_c is the substrate thermal conductivity (W m^{-1} °C^{-1}), assumed to equal 2.6 which is the same value applied by Moore *et al.* (2005), assuming a substrate porosity of 0.3 (Boyd and Kasper, 2003). Bed temperature (T_b; °C) at 0.05 m was derived using a similar method to hourly T_a estimates. Maximum and minimum daily T_b values were calibrated as 80% and 120% of maximum and minimum daily T_s, respectively (e.g., maximum T_s = 5.0 and maximum T_b = 4.0; minimum T_s = 2.0 and minimum T_b = 2.4) to minimize *RMSE*

between observed and simulated hourly mean T_s values at Star Main. The calibrated daily maximum and minimum T_b values were used as T_{max} and T_{min} in Equations 3.1 and 3.2 to derive estimates of hourly T_b. The diurnal cycles of T_a and T_s were similar; therefore, constants in Equations 3.1 and 3.2 were maintained for T_b estimates.

The ground water heat flux was determined using Moore *et al.* (2005):

$$Q_{gw} = \rho C Q_{in}(T_{gw} - T_s)/WW \tag{3.33}$$

where, T_{gw} is groundwater temperature (5.20°C), considered equivalent to mean annual T_a (Meisner *et al*. 1988).

Heat from friction (Q_f; W m^{-2}) was estimated using Theurer *et al*. (1984):

$$Q_f = 9805 * \left(\frac{Q}{WW}\right) * Slope \tag{3.34}$$

3.3.8. Surface and subsurface flows

Q values for each TRU were calculated as a proportion of basin area contributing to the upstream and downstream ends of the TRU. The change in *Q* increased linearly between upstream and downstream ends of each TRU and accounted for inflows from tributaries.

Hyporheic exchange flow (Q_{hyp}; m^3 s^{-1}) was calculated using Darcy's law (Domeninco and Shwartz, 1990):

$$Q_{hyp} = A_s * K_s * \frac{dh_d}{dx} \tag{3.35}$$

where, $\frac{dh_d}{dx}$ is the change in hydraulic head (m) over the length of each TRU (m), A_s is the cross-sectional area of the seepage face (m^2), and K_s is the substrate hydraulic conductivity (m s^{-1}). $\frac{dh_d}{dx}$ values were parameterized for each TRU, and ranged between 0.05 (farthest downstream TRU) and 0.15 (farthest upstream TRU) in this version of the model. The $\frac{dh_d}{dx}$ parameterization was based on maintaining Q_{hyp} values that agreed with the relationship between Q and Q_{hyp} derived by Wondzell (2012) using Q data and calculated Q_{hyp} at Star Main and Star West upper. A K_s value of 1.36 x 10^{-4} m s^{-1} was assumed for all TRU's, which is similar to the upper range found by Hatch *et al*. (2010) and within the range of values reported by Wondzell (2011). A_s values were determined using:

$$A_s = h_s * P_w \tag{3.36}$$

where, h_s is the seepage face thickness (m), calculated as a function of TRU length and slope (m). The wetted perimeter (P_w; m) was calculated using:

$$P_w = W_b + 2 * \bar{d} * \sqrt{1 + Z^2} \tag{3.37}$$

where, W_b is stream bottom width (m), estimated as a function of bankfull width (W_{bf}; m), bankfull depth (D_{bf}; m), and Z. W_{bf} and D_{bf} data were collected during stream surveys on Star Creek and Z is the dimensionless stream channel side slope ratio.

3.3.9. Spatial stream temperature modelling

T_s was calculated for each TRU and each hourly time step with Euler's method, similar to Leach and Moore (2011):

$$T_{s_{i+1,t+1}} = T_{s_{i,t}} + \Delta t * \frac{dT_s}{dt} \quad (3.38)$$

Exposure time (Δt) was determined as a function of V and TRU length (m), while i is the TRU end point and t is the time step.

A mixing model was used to account for mixing of tributaries and Q_{hyp} with stream water:

$$T_{s_{i,t}} = \frac{T_{s_{i,t}} Q_{i,t} + T_{in_{i,t}} Q_{in_{i,t}}}{Q_{i,t} + Q_{in_{i,t}}} \quad (3.39)$$

where, T_{in} (°C) and Q_{in} (m^3 s^{-1}) are the temperature and Q values from a tributary or hyporheic exchange flow (Leach and Moore, 2011; Boyd and Kasper, 2003). The temperature of hyporheic exchange flow (T_{hyp}; °C) was assumed to equal mean daily T_s in each TRU, interpolated linearly between Star West upper and Star Main, and between Star East upper and Star East. The use of mean daily T_s was based on the assumption that there is a high proportion of water with relatively long residence times within the hyporheic zone and that mean daily T_{hyp} can be similar to that of the water column (Arrigoni *et al.* 2008; Wondzell 2012).

3.3.10. Model performance assessment

Model performance was assessed by comparing simulated hydrometeorological variables with observations at Star West upper and Star Main. Simulated T_s was compared with observations at Star Main. The assessment criteria were *RMSE*, Nash Sutcliffe coefficient (*NS*; Nash and Sutcliffe, 1970), and the coefficient of determination (R^2). *NS* was used to assess Q simulations, whereas R^2 was used to assess T_a, *RH*, and Q*.

3.3.11. Sensitivity Analysis

A sensitivity analysis was conducted in order to assess the MST model's sensitivity to parameterization and calibration. Variables selected for this analysis were: T_{hyp}, T_b, *WW*, $\bar{d}$, Q^* and Q. Each variable was increased and decreased by 10% then used individually as input to all TRU's in the MST model (i.e. only one variable was altered at a time). The 10% changes were used to enable comparisons while also maintaining a physically meaningful range of values for all variables. The percent difference in mean daily T_s and range in daily T_s were then compared with the initial base model run, demonstrating the relative influence of each variable on T_s simulations.

3.4. **Results**

3.4.1. MST input simulations

Simulated hourly T_a compared well temporally with observed T_a at Star West upper, indicated by a high R^2 value. However, hourly T_a simulations did have a relatively high *RMSE*. Mean hourly *RH* was not simulated as well, indicated by a low R^2 value and high *RMSE*. Errors in hourly mean Q^* simulations were similar between Star Main and Star West upper, with high R^2 (Table 3.1).

Simulated daily mean Q for the period from May 15 to December 31, 2010 compared well with observed mean daily Q at Star Main as indicated by a high *NS* value (Fig. 3.4; Table 3.1). However, the model did not simulate Q well during the early winter period. Q_{hyp} was estimated to account for a maximum of 3.4% of total Q during baseflow periods and a minimum of 0.4% of total Q during the high flow period of 2010 (Fig. 3.4).

Table 3.1: Summary of root mean square error (*RMSE*), Nash-Sutcliffe (*NS*) and the coefficient of determination (R^2) statistics for simulated hydrometeorological variables from May 15 to Dec 31, 2010. *NS* was not assessed (N/A) for atmospheric variables.* indicates Star Main and ** indicates Star West upper.

Variable	*RMSE*	*NS*	R^2
****Mean hourly T_a**	3.55	N/A	0.87
****Mean hourly *RH***	8.77	N/A	0.55
Mean hourly *Q*	58.50	N/A	0.73
****Mean hourly *Q****	55.48	N/A	0.68
Mean daily *Q	0.04	0.85	N/A
***Mean hourly T_s**	0.77	0.79	N/A
Mean hourly ΔT_s	0.74	0.67	N/A

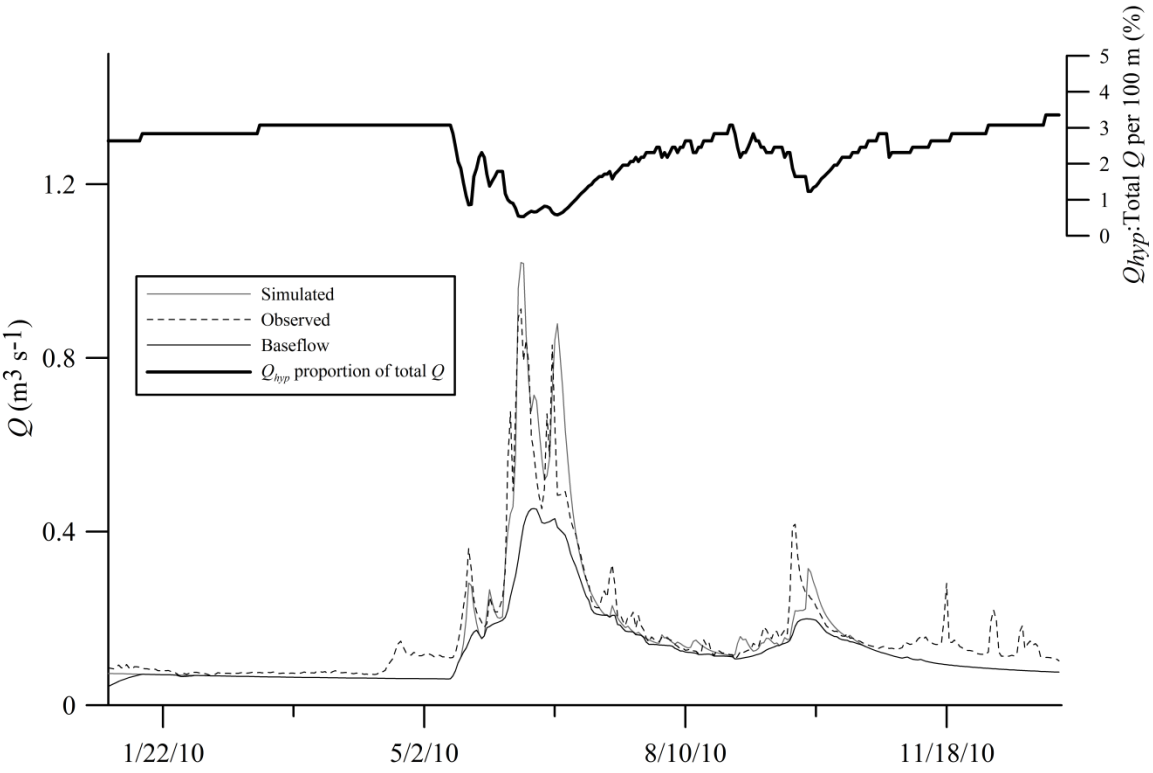

Figure 3.4: Simulated and observed daily *Q* at Star Main for the period from January 1 to December 31, 2010 is shown on the bottom plot and corresponds with the y-axis on the left. The top plot corresponds with the y-axis on the right and is the simulated proportion of Q_{hyp} to total *Q* per 100 m stream length over the same time period.

3.4.2. Energy budget and stream temperature simulations

Simulated Q^* was the dominant source of heat, with a higher magnitude during the summer period. The diurnal influence of Q^* was positive (negative) during the daytime (nighttime) (Fig. 3.5a). Simulated Q_h was a relatively small heat source (Fig. 3.5b) and Q_e was a net heat sink during the entire period (Fig. 3.5c). Q_b was primarily a heat sink (source) during the daytime (nighttime), with a higher magnitude during the summer (Fig. 3.5d). Simulated Q_f accounted for a relatively small proportion of the energy budget; it was highest during the peak Q period and consistently positive (Fig. 3.5e). Q_{gw} was estimated to be a relatively small component of the simulated energy budget, and was primarily negative (positive) during the summer (spring, fall and winter) (Fig. 3.5f).

Hourly mean T_s at Star Main was well simulated over the period from May 15 to December 31, 2010, indicated by a high *NS* and low *RMSE* (Table 3.1). The change in mean hourly T_s from Star West upper to Star Main (ΔT_s; °C) was not simulated as well as hourly T_s (Table 3.1), with lower *NS* and higher *RMSE*. Maximum, minimum, and mean daily T_s were over simulated during the warm summer period (Fig. 3.6a, 3.6b, and 3.6c). The range in daily T_s at Star Main was primarily under simulated for the summer period (Fig. 3.6d).

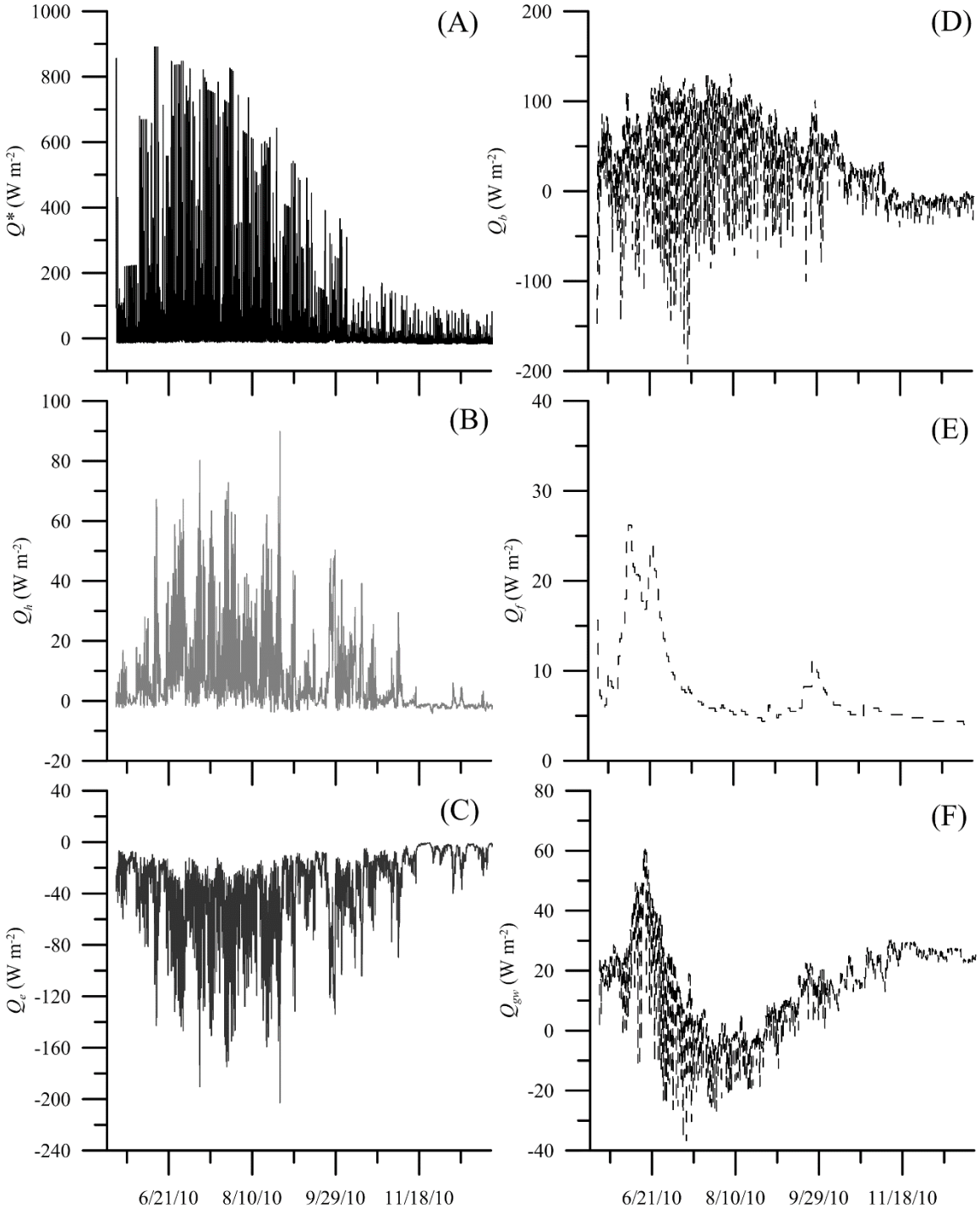

Figure 3.5: Simulated hourly mean Q^* (A), Q_h (B), Q_e (C), Q_b (D), Q_f (E), and Q_{gw} (F) for the TRU representing Star Main for the period from May 15 to December 31, 2010.

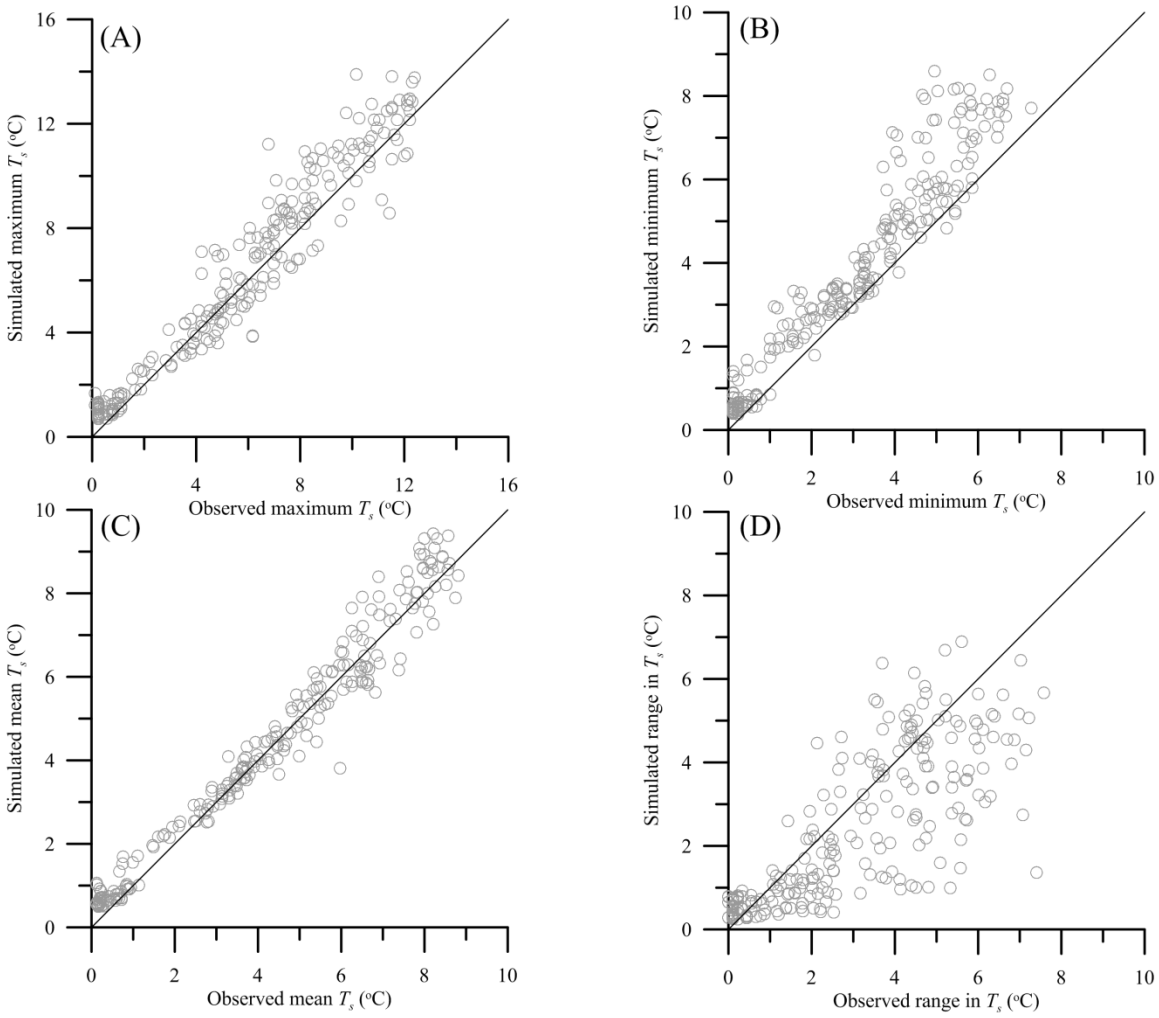

Figure 3.6: Observed and simulated daily T_s maximum (A), minimum (B), mean (C), and range (D) at Star Main for the period from May 15 to December 31, 2010. The line is 1:1.

3.4.3. Sensitivity Analysis

Overall, the simulated range in daily T_s was more sensitive to model parameterization than the mean daily T_s. The effect of changes in T_{hyp} on the daily T_s range was relatively small, and did not affect daily mean T_s. Daily mean T_s was most influenced by changes in T_b and daily T_s range was most affected by Q^*. MST model outputs were also relatively sensitive to changes in $\bar{d}$. The model outputs had higher

sensitivity to decreased than increased *WW*, and were more sensitive to increases than decreases in *Q* (Table 3.2).

Table 3.2: Sensitivity analysis results with increases and decreases of 10% in T_{hyp}, T_b, *WW*, *d*, *Q**, and *Q*. Values shown are percent differences relative to the base model run over the period from May 15 to December 31, 2010.

	Differences in daily T_s mean (%)		**Differences in daily T_s range (%)**	
Variable	***Increase 10%***	***Decrease 10%***	***Increase 10%***	***Decrease 10%***
T_{hyp}	2%	-2%	0%	0%
T_b	3%	-4%	1%	-1%
WW	0%	0%	1%	-3%
$\bar{d}$	0%	0%	-6%	5%
Q^*	0%	0%	8%	-9%
Q	-1%	0%	-2%	0%

3.5. **Discussion**

This study demonstrated that techniques used to couple the GENESYS and MST models can provide spatial estimates of hourly hydrometeorological conditions in the Star Creek catchment. Given that the GENESYS model is designed to use inputs of only T_a, precipitation, and catchment physiographic data, this method is particularly useful in remote regions where hydrometeorological observations are a primary limiting factor in process-based T_s modelling (Benyahya *et al.* 2007). The modelling approach accounted for catchment-scale variation in meteorological conditions at the hourly time step, which are important for process-based modelling because local meteorological variation can affect model performance (Benyahya *et al.* 2010). Therefore, this approach to T_s modelling is more transferable than models which are unable to quantify meteorological conditions spatially.

While this study aimed to quantify all key processes controlling $T_{s,}$ calibration of the MST model was necessary given that data were not available to calculate each term in the energy and mass balance equations. Other studies have applied similar methods where model fits are optimized by calibrating terms like shading coefficients, Q_{gw}, and channel characteristics (Cox and Bolte 2007; Herb and Stefan 2011), demonstrating this approach is reasonable. *RMSE* was minimized between simulated and observed hourly mean T_s at Star Main through model calibration and results are comparable to other T_s modelling studies where *RMSE* values range between 0.1 and 1.6 (Caissie *et al*. 2007; Cox and Bolte 2007; Herb and Stefan 2011). However, given that the MST model was calibrated, it is important to consider how each term in the stream heat budget compares with previous studies to determine whether or not the calibration causing T_s to be simulated well is reasonable.

Results of this study indicate that Q^* is the dominant energy budget term influencing T_s, which is consistent with numerous previous studies (Brown 1969; Brown and Krygier, 1970; Sinokrot and Stefan, 1993; Webb and Zhang 1997; Johnson and Jones 2000; Hannah *et al.* 2008; Leach and Moore, 2010; Hebert *et al.* 2011). GIS-based methods presented here to efficiently estimate $K\downarrow$ in a mountain catchment have promise due to increasing availability of high-resolution DEMs. Unfortunately, the resolution of the AVI data used in model parameterization of riparian cover did not resolve the complexities in spatial changes of riparian vegetation critical for understanding Q^* (Hannah *et al.* 2008; Leach and Moore, 2010). Uncertainty in canopy closure estimates likely had a substantial effect on T_s simulations given that the MST model was most

sensitive to changes in Q^*. Therefore, over-simulated Q^* was likely one of the primary drivers of T_s over-simulations.

Q_e was the primary heat sink and Q_h was a relatively small heat source, similar to results found by Hannah *et al.* (2008) and Leach and Moore (2010). It is likely that the Q_h flux was slightly underestimated, while both under- and over-simulations of the Q_e flux are likely given errors in T_a and *RH* estimates. However, as previous work has shown, Q_e and Q_h fluxes can offset each other (Leach and Moore, 2010), thus, errors in these atmospheric fluxes likely do not result in substantial T_s simulation errors.

MST model sensitivity to T_b demonstrates that accounting for the temporal T_b variability in headwater streams is important (Constanz and Thomas, 1997; Story *et al.* 2003; Johnson, 2004; Guenter *et al.* 2012), and suggests that Q_b can play a role in shifting mean daily T_s. This is due to the fact that simulated Q_b was a heat sink (source) during the day (night) (Evans *et al.* 1998; Hannah *et al*. 2008), dominating the nighttime summer simulated stream energy budget.

Results suggest Q_f represents a small heat source that should be considered in Star Creek and other high-gradient streams (Theurer *et al.* 1984). Similarly, Q_{gw} was estimated as a relatively small component of the heat budget with a magnitude similar to that simulated by Moore *et al.* (2005). This small heat flux; however, does provide some damping of atmospheric effects on T_s (Tague *et al*. 2007); therefore, important in headwater catchments. Improving Q_{gw} simulations and understanding the role of this flux still requires better spatial and temporal characterization of both positive and negative

groundwater fluxes at the reach scale (Payn *et al*. 2009), as Leach and Moore (2011) showed that concurrent gains and losses can significantly affect T_s simulations.

Q_{hyp} is an important buffer of T_s patterns, particularly during baseflow periods (Poole and Berman 2001). The estimated proportion of Q_{hyp} to total Q is reasonable based on the high stream gradient and small size of Star Creek (Buffington and Tonina, 2009; Kasahara and Wondzell, 2003; Wondzell, 2011). The T_{hyp} parameterization in this iteration of the MST model was based on the assumption that a high proportion of Q_{hyp} flow was from source water with long residence times. The T_{hyp} sensitivity analysis suggests that increased (decreased) T_{hyp} can increase (decrease) mean daily T_s in Star Creek. Similar results were found by Arrigoni *et al*. (2008) who demonstrated that Q_{hyp} discharge zones with long flow paths can decrease daily mean T_s during the summer in the Umatilla River, Oregon.

The primary advantage to applying a process-based modelling approach is that it enables further investigation into potential sources of modelling error. Errors in T_s simulations are likely a function of the combined effects of modelling techniques, Q and Q^* estimates, and lack of process representation in the MST model. The Euler method applied is sensitive to estimates of exposure time, which were derived using estimated V. Over- or under-estimates would alter T_s simulations given that V largely determines channel-water residence time. The sensitivity analysis demonstrates that $\bar{d}$ and WW can also have a large effect on T_s, as in-stream heat storage is inversely proportional to volume of water (Webb and Zhang 1997). The sensitivity analysis also demonstrated that increased Q results in decreased T_s, thus over-simulations of T_s in early spring were most likely a function of under-simulated Q. The compound effects on T_s simulations of errors

in $\bar{d}$, *WW*, and *Q* were as important as *Q** in the stream energy budget given that these terms are not independent of one another. Overall, these results demonstrate that models should aim to quantify meteorological, hydrological, and geomorphological controls in order to accurately simulate T_s.

This study suggests further investigation into processes controlling T_s will improve T_s modelling. It is likely that some of the errors in simulated T_s are epistemic in nature given that the MST model aimed to describe all important energy and mass balance components of Star Creek. For example, in-stream ice-cover and snow melt into the stream likely played a key role in the heat budget of Star Creek during the winter and spring periods. The effects of ice and snow were not accounted for in the MST model. Ice cover during the winter period likely played a large role in decreasing T_s from Star West upper to Star Main and T_s was not simulated well during the spring period. The finding of poor simulations in the spring period is similar to previous work where authors suggest that not accounting for snowmelt likely resulted in T_s simulation errors (Caissie *et al*. 2007). Incoming solar radiation during the spring was high and the fact that *Q** also dominates the energy budget of snowmelt in the study region (Burles and Boon, 2011) suggests melting snow into streams should be considered as an important heat flux governing T_s. Further work should be focused on resolving this process and knowledge may be gained from snow and ice melt studies conducted in lakes, where the effects of ice and snow melt on water temperature are better understood (e.g., Williams, 1969; Liston and Hall, 1995).

3.6. **Conclusion**

Applying process-based stream temperature models with limited input data is a substantial challenge, particularly in diverse mountain catchments. This study demonstrates that coupled hydrometeorological and T_s models provide a useful framework for simulating stream temperature at scales relevant to management decision making. Methods presented here can be applied in a range of catchments using readily available meteorological and physiographic data. However, results do suggest that process understanding and representation within the model can be improved. The sensitivity analysis demonstrates that calibrated variables and model parameterization can have a large effect on T_s simulations. It is, therefore, imperative that field-based studies are used to guide model development by quantifying processes controlling T_s at a range of spatial and temporal scales.

Chapter 4: Potential future climate effects on mountain hydrology, stream temperature, and native salmonid life history

4.1. **Introduction**

Native salmonids appear to have a competitive advantage over non-native species only within specific thermal and nutrient regimes (Rasmussen *et al*. 2010; Warnock and Rasmussen, 2013). Therefore, changes in thermal conditions within a stream can result in physiological or behavioral responses in aquatic organisms and reduced habitat availability for native species (Poole and Berman, 2001; Wenger *et al.* 2011a). Native westslope cutthroat trout (WCT; *Oncorhynchus clarkii lewisi*) and bull trout (BT; *Salvelinus confluentus*) are restricted in their current spatial distribution relative to their historical range due to the introduction of non-native species and environmental degradation (Rasmussen *et al*. 2010; Wenger *et al.* 2011b; Warnock *et al*. 2013). The majority of the current range of WCT and BT is restricted to mountain catchments (Behnke, 2002). Therefore, high elevation mountain streams provide critical refugia for these species (Paul and Post, 2001) given that these streams exhibit thermal and nutrient regimes best-suited to native salmonids.

Previous work has shown that human-induced atmospheric warming will alter hydro-climatic regimes in mountain regions across western North America (Barnett *et al*. 2008). Expected changes include earlier spring snowmelt (Mote *et al*. 2005; Stewart *et al*. 2009; MacDonald *et al*. 2011), reductions in late season streamflow (St. Jaques *et al*. 2010), increased drought (Pederson *et al*., 2010; Sauchyn and Bonsal, 2013), and subsequently increased human demand on water resources (Schindler and Donahue, 2006). Stream thermal regimes are likely to respond to changes in hydro-climatic regimes

(Cristea and Burges, 2010) because the capacity for streams to store heat is inversely proportional to volume (Poole and Berman, 2001; Webb *et al*. 2003). Degradation of thermal habitat as a result of anthropogenic and natural disturbance, coupled with competition from introduced species, will likely further reduce habitat availability for native salmonids in the Rocky Mountains (Meyer *et al*. 1999; Isaak *et al.* 2012a; Isaak *et al.* 2012b; Jones *et al*. 2013). Therefore, it is important to understand how hydrologic and thermal regimes of mountain streams will respond to climate change.

Predicting climate change effects on stream temperature is complicated by numerous interactions between a stream and its surrounding environment. For example, recent work describing the stream temperature contributions of surface-subsurface exchange (Leach and Moore, 2011), bed temperature (Guenther *et al*. 2012), riparian cover (Groom *et al*. 2011), and catchment-scale moisture conditions (MacDonald *et al*. 2013) demonstrate the challenge in quantifying their response to changing environmental conditions. These interactions are also difficult to quantify at spatial and temporal scales relevant to management decision making. Therefore, studies often use correlations between air temperature, stream temperature, and sometimes streamflow for stream temperature predictions rather than solving complex heat budgets (Mohseni *et al*. 2003; van Vliet *et al*. 2011). Although predictions using air-stream temperature correlations are useful, they do not describe the influence of key stream temperature drivers (Johnson, 2003). Furthermore, decreasing stream temperature trends over recent decades suggest stream thermal response to climate change may be poorly understood (Arismendi *et al*. 2012).

Process-based modelling can provide key insights into the mechanisms affecting stream temperature, and into subsequent salmonid life-history response to future climatic conditions (Johnson, 2003). We used a field study coupled with a process-based modelling approach to evaluate the hydrological and thermal sensitivity of a headwater stream to future climate scenarios. We also assessed potential WCT and BT incubation period changes, as this is life-history stage is highly sensitive to thermal and hydrological regimes (Beacham and Murray 1990; Baxter and McPhail, 1999). Our objectives were to: (1) define which seasons were most sensitive to a range of future climate scenarios, where the criteria for sensitivity were changes in streamflow and stream temperature; and (2) determine the response of WCT and BT incubation periods and the timing of fry emergence.

4.2. **Study area**

This study primarily uses data collected at Star Creek, a headwater tributary of the Crowsnest River, Alberta (Fig. 4.1) which is typical habitat for native WCT and is representative of BT habitat. Star Creek has an estimated groundwater contribution to total streamflow of 68% (Silins *et al*. 2009), flowing from a step-pool channel to an intermediate pool-riffe/step-pool channel type (Montgomery and Buffington, 1997). The Star Creek catchment ranges in elevation from 1475 to 2631 m. The mean channel slope in Star Creek is 5% with dominantly cobble and gravel substrate. The mean bankfull channel width is 3.0 m, with a mean wetted width of 2.6 m. Riparian cover is dominated by lodgepole pine (*Pinus contorta*), with willow (*Salix* spp) and alder (*Alnus* spp) comprising the sub canopy.

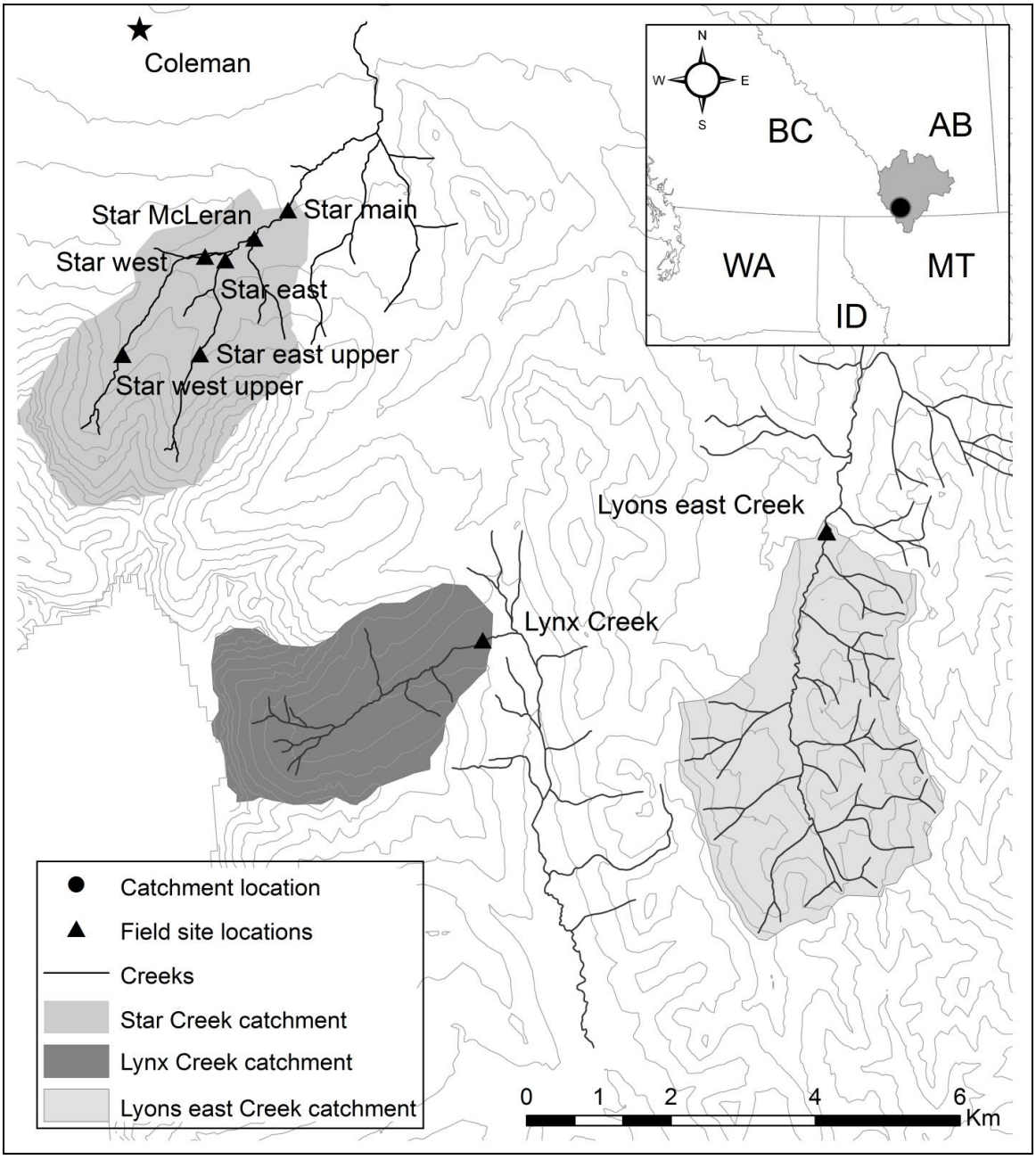

Figure 4.1: Star, Lynx, and Lyons east catchments, in the headwaters of the Oldman River, Alberta.

Data were also collected from study sites at Lyons East and Lynx Creeks (Fig. 4.1) to conduct an inter-catchment comparison of stream temperature (T_s; °C), air temperature (T_a; °C), and total stream discharge (Q; $m^3\ s^{-1}$) patterns. Although surface-subsurface interactions can be controlled by catchment-scale geomorphology (Baxter and

Hauer, 2000), the T_s, T_a, and Q comparisons between Star, Lynx, and Lyons East Creeks provide context for potential salmonid habitat response as a result hydro-climatic change. Lyons East Creek has high streamflow contribution from shallow subsurface water sources, with an estimated 43% of total streamflow from deeper groundwater (Silins *et al*. 2009). It is inhabited primarily by introduced rainbow trout (RT; *Oncorhynchus mykiss*) and is classified as a pool-riffle channel type based on Montgomery and Buffington (1997). The Lyons East catchment ranges in elevation from 1632 to 2639 m, with a mean stream channel slope of 3%, and the streamed is cobble and gravel substrate. The mean bankfull channel width is 5.4 m, with a mean wetted width of 2.8 m.

Lynx Creek has an estimated 63% of total streamflow contribution from deeper groundwater (Silins *et al*. 2009) and is habitat for a genetically pure population of WCT (AESRD, in prep). The Lynx Creek catchment has an elevation range of 1441 to 2027 m, with a mean stream channel slope of 6%, and is classified as an intermediate pool-riffle/step-pool channel type (Montgomery and Buffington, 1997). The dominant substrate is cobble, with sub-dominant gravels. The mean bankfull channel width is 4.7 m and the mean wetted width is 3.5 m. Both Lyons East and Lynx Creeks have burned lodgepole pine riparian cover, with willow, alder, and grass sub-canopies.

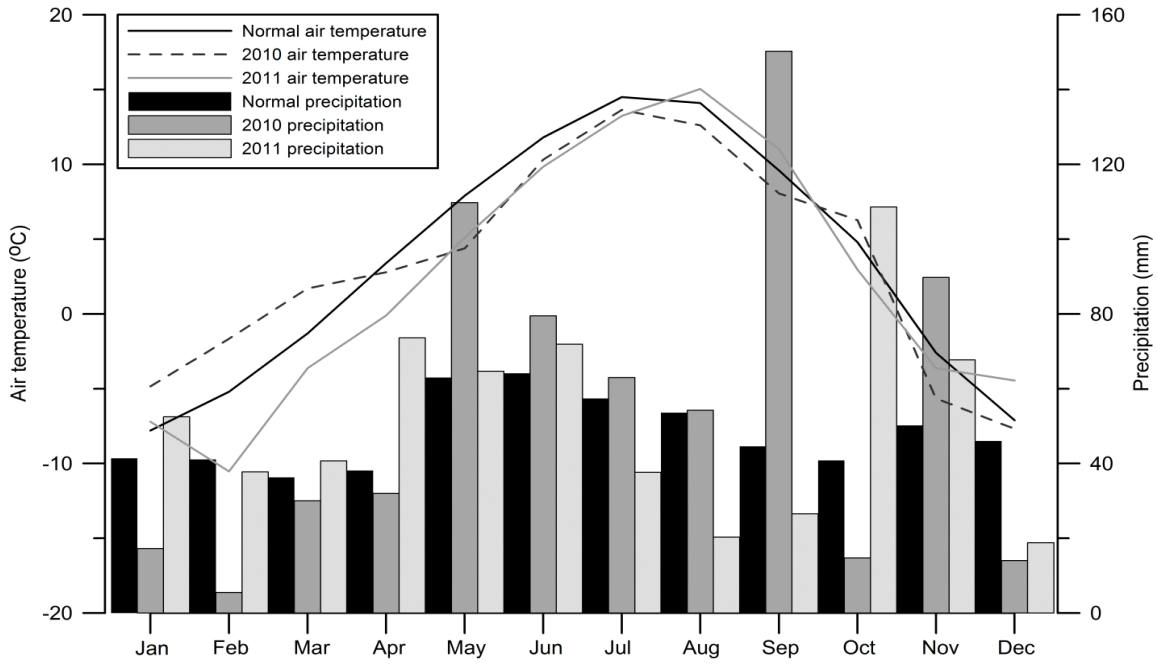

Figure 4.2: Air temperature and precipitation at Star Creek during the study period (2010-2011) compared to normal (1971-2000) air temperature and precipitation at Coleman.

The Crowsnest Pass region is characterized by a continental climatic regime, and receives an average of 576.5 mm total precipitation annually (31% snow), with peak precipitation occurring in June (64.1 mm). Normal (1971-2000) mean annual air temperature for the region is 3.5°C; the warmest month is July (14.5°C) and coldest month is January (-7.8°C; Fig. 4.2) (Environment Canada, 2012a). Air temperatures for all months during the study period were within the normal range of values. The 2010 to 2011 period represented a range of precipitation conditions, with 2010 having relatively low fall-winter precipitation and high summer precipitation, while 2011 had primarily above average precipitation during the period from fall to spring, but below average summer precipitation (Fig. 4.2; Environment Canada, 2012a).

4.3. **Methods**

4.3.1. Data collection

Hydrometeorological stations were installed at two locations within the Star Creek watershed: Star Main and Star West upper (Fig. 4.1), and measured hourly mean T_a, relative humidity (*RH*; %), and wind speed (u; m s^{-1}) at 2 m above the stream bankfull depth. Hourly mean net radiation (Q^*; W m^{-2}) was recorded directly over the stream surface at 1 m above bankfull depth. Hourly total precipitation (mm) was measured approximately 10 m from the stream bank at the Star Main site. All hourly means and totals for meteorological data were derived from 10 second readings. Hourly mean T_s was derived from 1 minute readings at five sites within the Star Creek watershed: Star West upper, Star East upper, Star East, Star McLaren, and Star Main (Fig. 4.1). Hourly mean Q was estimated using stage (cm) - discharge relationships derived from 10 second stage readings at all sites except Star McLaren, where Q was estimated using a compound weir. Manual Q measurements were collected weekly at all stations during periods of high, low, and median Q from May 15, 2010 to September 15, 2011.

Hourly mean T_a, and stream stage values were derived from 10 second readings at Lyons and Lynx Creeks (Fig. 4.1). Hourly mean Q was estimated from stage-discharge relationships for the period from January 1, 2011 to December 31, 2011, while T_a and T_s were measured from June 1, 2011 to December 31, 2011. Hourly mean T_s values were calculated from 1 minute readings.

4.3.2. Hydrometeorological model

We applied a coupled approach using the Generate Earth Systems Science input (GENESYS) and Mountain Stream Temperature (MST) models (MacDonald *et al*. 2009;

MacDonald *et al*. in review). The GENESYS model has been used in numerous studies to investigate the impacts of climate change on snowpack in mountain catchments (Lapp *et al*. 2005; Larson *et al*. 2011; MacDonald *et al*. 2011; MacDonald *et al*. 2012). Daily simulations of hydrometeorological variables were generated using hydrologic response units (HRUs) and a series of process-based modelling routines.

Daily maximum and minimum T_a were estimated for each HRU using regional T_a lapse rates derived for each month from Parameter-elevation Regressions on Independent Slopes Model (PRISM) normal (1971-2000) data (Daly *et al.* 2008). Daily precipitation estimates were derived for each HRU using regional monthly precipitation lapse rates which were also derived from the PRISM normal dataset.

A daily hydrological balance was calculated for each HRU during the snow-covered period using:

$$SWE_{(t)} = SWE_{(t-1)} + Precip_{(t)} - Int_{(t)} - Subl_{(t)} - IF_{(t)} \quad (1)$$

where, *SWE* is the snow water equivalent (mm), Precip is simulated daily total rain or snow (mm), *Int* is canopy interception (mm), *Subl* is sublimation (mm), *IF* is infiltration (mm) and *t* is the time step (days). Soil moisture conditions (*SM;* mm) were simulated from the onset of snowmelt using:

$$SM_{(t)} = SM_{(t-1)} + IF_{(t)} + Precip_{(t)} - ET_{(t)} - Recharge_{(t)} - Run_{(t)} \quad (2)$$

where, *ET* is evapotranspiration (mm), *Run* is runoff (mm), and recharge is groundwater recharge (mm) contributing to catchment groundwater storage. The GENESYS model routes *Run* using the Muskingum routing method to simulate *Q*. To estimate the groundwater contribution to total *Q* (baseflow) an exponential storage-discharge curve was applied (Chapter 3).

4.3.3. Stream temperature model

Outputs from the GENESYS model used as input to the MST model include: T_a, *RH*, *Q*, and atmospheric transmissivity (*TRANS*; %). Simulated daily maximum and minimum T_a was used to estimate hourly T_a with a method developed by Parton and Logan (1981). Hourly T_a estimates were then used to calculate hourly *RH* values (Glassy and Running, 1994). *TRANS* was estimated using Bristow and Campbell (1984).

The MST model applies previously developed process-based methods (Boyd and Kasper, 2003; Leach and Moore, 2010; Leach and Moore, 2011). T_s values were simulated using temperature response units (TRUs), which apply the same logic as HRUs but represent the physiographic characteristics of a stream. We used hourly mean T_s from Star West upper, Star East upper, and Star McLaren in this simulation to provide the boundary conditions for the model. For each TRU, advective and heat inputs to the stream were estimated (Boyd and Kasper 2003) as:

$$\frac{dT_s}{dt} = -V\frac{dT_s}{dx} + \frac{(Q^* + Q_h + Q_e + Q_b + + Q_{gw} + Q_f)}{C * \rho * \bar{d}} \quad (3)$$

where, $\frac{dT_s}{dt}$ is the difference in T_s per unit of time (s). Velocity (*V*; m s^{-1}) is estimated as a function of *Q*, wetted width (*WW*; m) and wetted depth ($\bar{d}$; m). *WW*, *Q*, and $\bar{d}$ data collected from manual *Q* measurements on Star Creek were used to derive continuous estimates of $\bar{d}$ for each TRU by applying multiple linear regression with *WW* and *Q* as predictive variables (R^2 = 0.64, *RMSE* = 0.01, *n* = 40). Continuous *WW* estimates were also derived for each TRU with linear regression, where the predictive variable was *Q* (R^2 = 0.48, *RMSE* = 0.47, n = 40). *C* is the specific heat of water (4182 J kg °C^{-1}), ρ is the

density of water (998.2 kg m^{-3}), and $\bar{d}$ is the mean wetted depth (m) in each TRU. Q^* is net radiation (W m^{-2}), estimated using Arc GIS 10.0 and Leach and Moore (2010). Q_e is latent heat flux (W m^{-2}), estimated using a method described in Moore *et al*. (2005) and Q_h is sensible heat flux (W m^{-2}) which was determined using Leach and Moore (2010). The bed heat (Q_b; W m^{-2}), and groundwater (Q_{gw}; W m^{-2}) fluxes were estimated using Moore *et al*. (2005) and the heat flux from friction (Q_f; W m^{-2}) was estimated using Theurer *et al*. (1984).

T_s was estimated for each TRU and each hourly time step with Euler's method, similar to Leach and Moore (2011):

$$T_{s_{i+1,t+1}} = T_{s_{i,t}} + \Delta t * \frac{dT_s}{dt} \quad (4)$$

The exposure time (Δt) was determined as the product of stream velocity (V; m s^{-1}) and TRU length (m), i is the TRU end point and t is the time step.

To account for mixing of both surface and subsurface water a mixing model was used:

$$T_{s_{i,t}} = \frac{T_{s_{i,t}} Q_{i,t} + T_{in_{i,t}} Q_{in_{i,t}}}{Q_{i,t} + Q_{in_{i,t}}} \quad (5)$$

where, T_{in} (°C) and Q_{in} (m^3 s^{-1}) are the temperature and Q values from a tributary or hyporheic exchange flow (Leach and Moore, 2011; Boyd and Kasper, 2003). Q values for each TRU were assumed to be proportional to the basin area contributing to the upstream and downstream ends of the TRU, accounting for inflows from tributaries. Hyporheic exchange flow (Q_{hyp}; m^3 s^{-1}) was calculated using Darcy's Law (Domeninco and Shwartz,

1990). Calculated Q_{hyp} ranged between 0.4% and 4.7% of total Q per 100 m of stream, which is consistent with other estimates for steep headwater catchments (Wondzell, 2011). The temperature of Q_{hyp} was parameterized as mean daily T_s in each TRU based on the assumption that mean daily T_{hyp} can be similar to mean daily T_s of the water column (Arrigoni *et al.* 2008) and that Star Creek has a high proportion of streamflow contribution from source water with long residence times.

The model verification presented here is for the time period from May 15, 2010 to September 15, 2011 as this is the period when Q* data were available. T_s, T_a, and Q verifications were also conducted for this time period for standardization of results. The Nash-Sutcliffe (*NS*) efficiency coefficient, the correlation coefficient (R^2), and root mean square error (*RMSE*) were used as measures of model performance.

4.3.4. Sensitivity analysis

This study used the "delta" method which applies absolute mean monthly T_a changes to the observed time series using future T_a predictions (Diabat *et al.* 2012; Hay *et al.* 2000). We applied a constant T_a change to the GENESYS model daily time series input for 2010 and 2011. Daily T_a output from the GENESYS model was then downscaled to hourly T_a using Parton and Logan (1981) and used as input to the MST model. Groundwater temperature (°C) used to calculate Q_{gw} (Moore *et al*. 2005) was adjusted by the same magnitude as T_a; this is based on the assumption that groundwater temperature closely approximates mean annual T_a (Miesner *et al*. 1988).

We used future T_a estimates from General Circulation Model (GCM)-derived climate change scenarios for the periods from 2039 to 2069 (2050s) and 2070 to 2099

(2080s) for this analysis. These scenarios are from the IPCC Fourth Assessment report (AR4), and are available via the Pacific Climate Impacts Consortium (PCIC). Spatially downscaled T_a predictions were obtained from the Climate WNA high resolution climate data tool version 4.7 (Wang *et al*. 2012). Climate WNA provides climate output (T_a, precipitation) from climate change scenarios for any point in western North America, enabling elevation-adjusted estimates of future climatic conditions. The mean and standard deviation of monthly change in maximum and minimum T_a for all 20 climate change scenarios available from Climate WNA were used to derive three scenarios for both the 2050s and 2080s. Using the mean and standard deviation of all 20 scenarios captures the representative variation in plausible future T_a conditions. Scenarios 1, 2, and 3 represent the mean, +1 standard deviation, and -1 standard deviation, respectively (Table 4.1). We did not apply precipitation changes given that the 2010 to 2011 precipitation at Star Creek represents a range of conditions relative to the 1971-2000 normal at Coleman (Fig. 4.2), and there is often considerable variation in GCM simulations of future precipitation (Barrow and Yu, 2005).

Changes in the simulated ratio of snow to total seasonal precipitation relative to 2010 and 2011 were quantified for all three scenarios to evaluate the hydrometeorological response to future climate scenarios. Absolute changes in simulated mean daily Q and baseflow, as well as mean, maximum, and minimum daily T_s relative to 2010 and 2011, were calculated for all three scenarios to quantify the hydrological and thermal response to future climate scenarios. Changes in seasonal mean T_s were calculated relative to 2010 and 2011 to quantify inter-seasonal differences in seasonal T_s response. Absolute WCT and BT incubation period changes were quantified with the cumulative thermal unit

(CTU) method, which assumes egg hatching requires a constant number of accumulated thermal units, defined as the mean daily temperature above 0°C (Beacham and Murray, 1990).

Table 4.1: Seasonal change in maximum ($\Delta Max\ T_a$) and minimum ($\Delta Min\ T_a$) air temperature relative to the 2010-2011 period for all three future climate scenarios derived using Climate WNA.

	Spring		**Summer**		**Fall**		**Winter**	
Scenario	***ΔMax*** T_a (°C)	***ΔMin*** T_a (°C)	***ΔMax*** T_a (°C)	***ΔMin*** T_a (°C)	***ΔMax*** T_a (°C)	***ΔMin*** T_a (°C)	***ΔMax*** T_a (°C)	***ΔMin*** T_a (°C)
1 (2050)	1.72	2.05	3.20	3.63	1.81	1.61	-0.54	-0.16
2 (2050)	2.63	3.01	4.52	4.92	2.83	2.67	0.51	1.01
3 (2050)	2.83	3.20	4.23	4.68	2.78	2.56	0.59	1.12
1 (2080)	0.62	0.91	2.16	2.58	0.84	0.66	1.68	1.43
2 (2080)	4.11	4.47	6.09	6.43	4.23	3.97	1.89	2.57
3 (2080)	1.16	1.56	2.96	3.42	1.44	1.38	-0.86	-0.55

The incubation period for WCT was assumed to start at peak spring *Q* due to the complexity in determining the timing of WCT spawning, which is related to both *Q* and T_s (Brown and Mackay, 1995). The date of WCT emergence was estimated based on WCT eggs requiring 300 CTUs post-peak *Q* to hatch (Drinan, 2010). The initiation of BT spawning is related to T_s and photoperiod (McPhail and Baxter, 1996). Given that the exact mechanisms for the initiation of BT spawning are not fully understood, we used a standardized date of September 21 because spawning activity in south-eastern Alberta typically peaks in late September (Hurkett *et al.* 2011) and this date provides a reasonable surrogate to account for photoperiod. The date of emergence for BT was estimated based on the assumption that 350 CTU are required post-peak *Q* to hatch (Gould, 1987). CTU values of 300 and 350 for WCT and BT respectively were used to estimate date of

emergence for 2010-2011 as well as all three future climate scenarios in both the 2050 and 2080 periods.

4.4. **Results**

4.4.1. Model verification

Atmospheric variable simulations were assessed at an hourly time step as this was the temporal resolution required for the MST model. Simulated mean hourly Q^* compared well with observed values at Star Main for the period from May, 15 2010 to September 15, 2011 (R^2 = 0.73, *RMSE* = 58.5, n = 11736). Mean hourly T_a simulations compared well with observed values at Star Main for the same period (R^2 = 0.75, *RMSE* = 5.5, n = 11736).

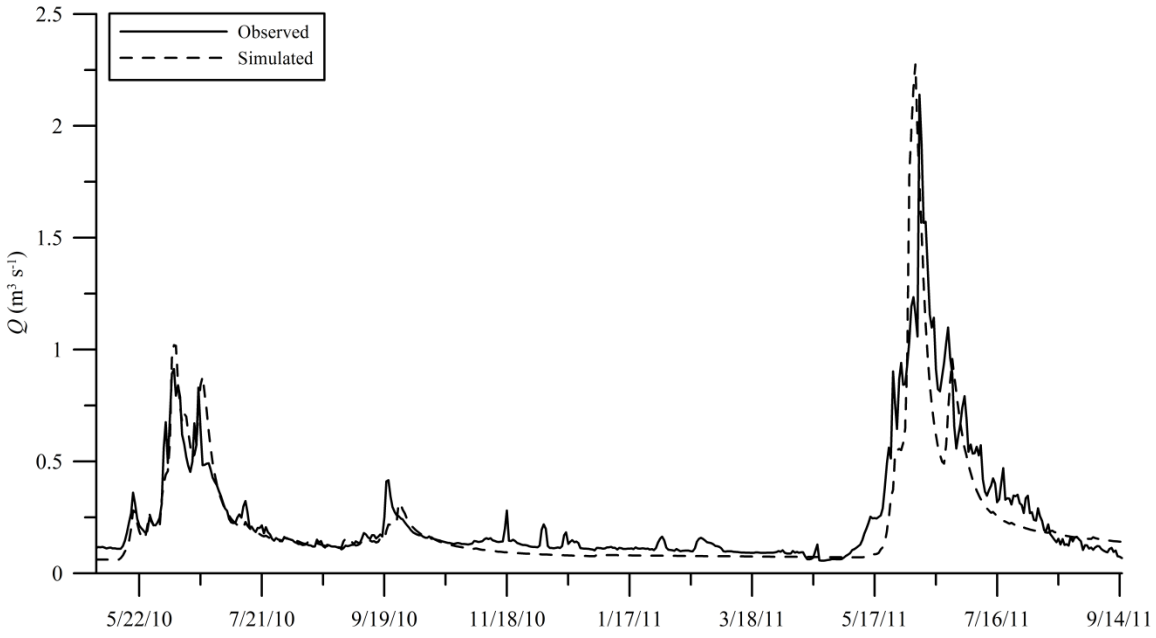

Figure 4.3: Observed and simulated daily mean *Q* for Star Creek from May 15, 2010 to September 15, 2011.

Simulated mean daily *Q* compared well with observed mean daily *Q* for the period from May, 15 2010 to September 15, 2011 (*NS* = 0.76, *RMSE* = 0.13, n = 489).

The simulated timing of peak *Q* for both years was within two days of observed, with a higher peak *Q* in 2011. The recession towards baseflow was simulated better in 2010 than 2011. In 2011 the GENESYS model was not responsive to precipitation events during late summer and early fall. Winter *Q* events were not simulated as well. However, baseflow was simulated well, with a small negative bias (Fig. 4.3).

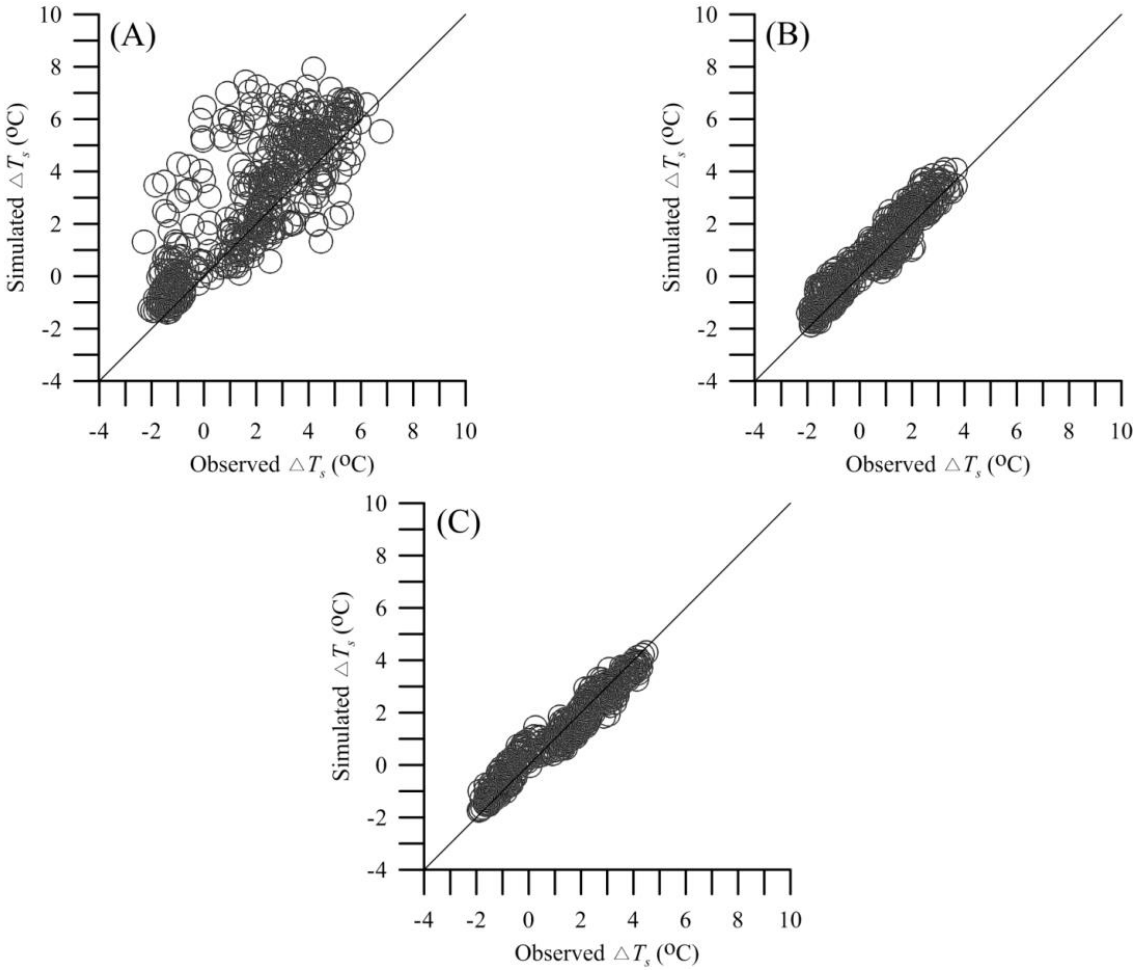

Figure 4.4: Scatter plots of observed and simulated maximum (A), minimum (B) and mean (C) daily ΔT_s from Star West Upper to Star Main for the period from May 15, 2010 to September 15, 2011. The line is 1:1.

The daily mean, maximum and minimum of hourly change in T_s from Star West upper to Star Main (ΔT_s; °C) were used to assess model performance for the period from May 15, 2010 to September 15, 2011. The daily mean ΔT_s was simulated well (Fig. 4.4a,

NS = 0.92, *RMSE* = 0.31, n = 489). The daily maximum ΔT_s was not simulated as well (Fig. 4.4b, *NS* = 0.69, *RMSE* = 1.43, n = 489); however, daily minimum ΔT_s was simulated well (Fig. 4.4c, *NS* = 0.93, *RMSE* = 0.41, n = 489). Over the entire study period, mean daily T_s simulations compared well with observed mean daily T_s (Fig. 4.5, *NS* = 0.96, *RMSE* = 0.30, n = 489). However, simulated mean daily T_s did not compare well with observed T_s during the early spring, where simulated values were consistently positively biased. Simulations were consistently negatively biased during the freshet period from mid-May to mid-June (Fig. 4.5).

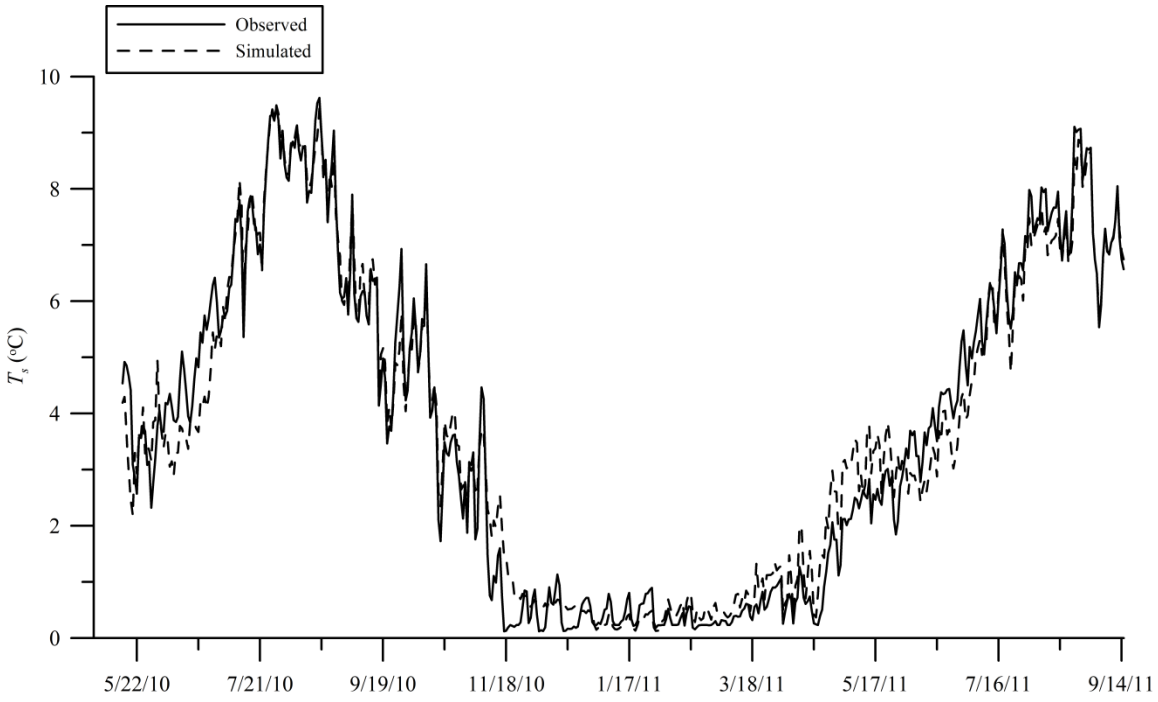

Figure 4.5: Observed and simulated mean daily T_s for Star Main from May 15, 2010 to September 15, 2011.

4.4.2. Limitations

- Given that the relationship between T_s and T_a is nonlinear, and inapplicable in cold winter periods where ice is present (Mohseni and Stefan, 1999), and that T_a

plays a relatively small role in the stream heat budget (Johnson, 2004), we assumed that the boundary T_s, hyporheic exchange flow temperature, and stream bed temperature conditions remained constant. Since boundary T_s conditions weren't shifted to account for long-term shift in mean T_s expected under atmospheric warming (Jones *et al*. 2013), there is likely a conservative negative bias in T_s predictions during warm summer periods.

- Winter high Q events were not well simulated. This is important because winter T_s is dependent on Q (Power, 1999). It is difficult to determine if winter Q events were actually driven by increased Q or if these events are artifacts in the data resulting from increased stream stage from ice formation.
- Consistent errors in historical T_s simulations occur just before and during spring freshet. These errors are likely result from: 1) the processes representing the effects of snow and ice on T_s were explicitly not accounted for in the MST model and; 2) simulated historical Q is lower than observed during the early spring, and higher than observed during freshet. These errors in simulated Q likely resulted in over and under T_s estimates of 1°C during the early spring and freshet periods, respectively.
- Boundary u conditions remained constant. Increases or decreases in u affect Q_e in the MST model. Therefore, changes in u would have affected T_s simulations.
- The MST model also did not account for changes in riparian cover as a function of climate warming. It is likely that this would have a significant impact given that T_s is highly influenced by incoming shortwave radiation (Johnson, 2004).

4.4.3. Sensitivity analysis

The ratio of snow to total monthly precipitation decreased in all three scenarios, and in both 2050 and 2080 periods relative to the historical record. The simulated percent change in the ratio of snow to total monthly precipitation was greatest for spring, with a maximum 42% decrease in Scenario 2 for the 2080 period. Winter was projected to experience the least amount of change in precipitation phase, with a 6% decrease in Scenario 2 for the 2080 period (Fig. 4.6).

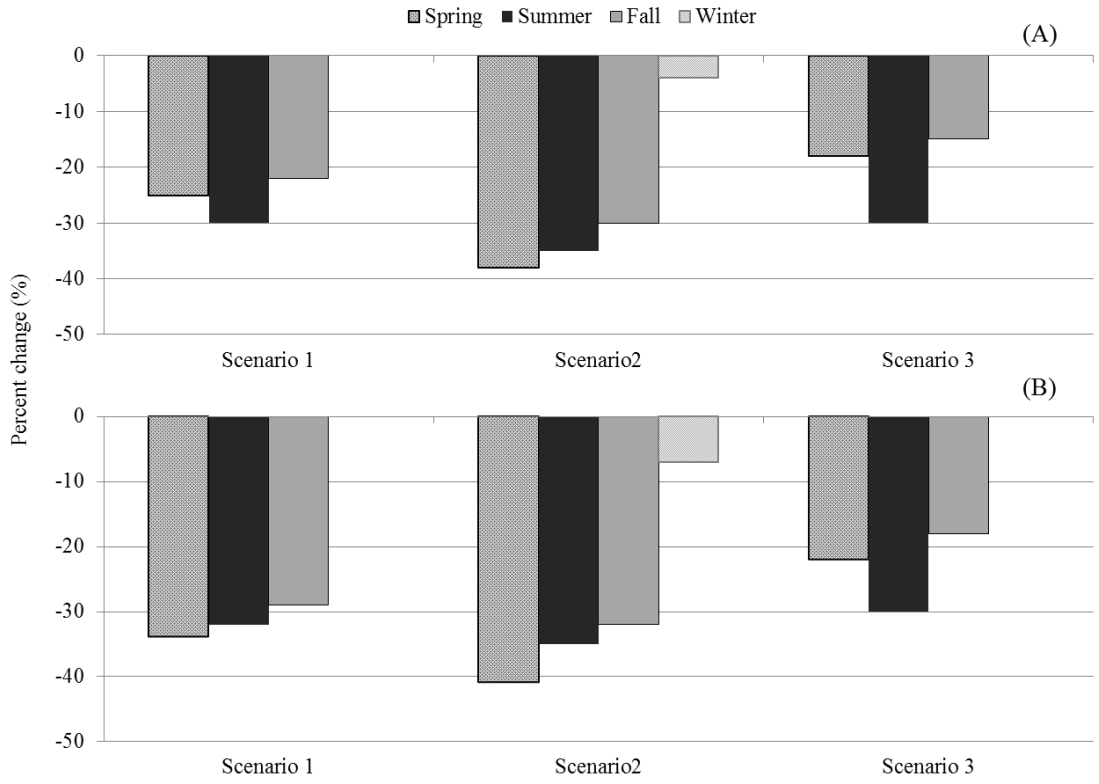

Figure 4.6: Percent change in the ratio of simulated snow to monthly total precipitation relative to 2010-2011 for all three scenarios in the 2050 (A) and 2080 (B) periods.

The greatest difference in simulated *Q* between all future climate scenarios and the historical (2010 to 2011) period was during the spring, with consistently earlier onset of peak *Q* (Table 4.2). The greatest change in overall magnitude of *Q* occurred in

Scenario 2 for both the 2050 and 2080 periods, particularly during June (i.e., peak flows). The largest shifts in peak *Q* were also estimated for 2010, which had lower historical *Q*. In all three scenarios, small reductions in late season *Q* were predicted for both the 2050 and 2080 periods (Figs. 4.7a and 4.7c).

Simulated changes in baseflow generally shifted towards earlier in the spring, with lower baseflow in summer, fall, and winter. In all scenarios the change in peak baseflow did not shift as substantially as the change in peak *Q* in 2010. However, in 2011 a more consistent shift towards an earlier peak baseflow was predicted. The greatest change in baseflow magnitude was predicted to occur in Scenario 2 for both the 2050 and 2080 periods, where baseflow declined in both early and late seasons relative to historical (Figs. 4.7b and 4.7d).

Table 4.2: The 2010 and 2011 date of peak *Q*, and the date of peak *Q* for all three scenarios in the 2050 and 2080 periods.

	Date of peak discharge	
	2010	**2011**
Historical	Jun-06	Jun-06
1 (2050)	May-18	May-27
2 (2050)	May-19	May-25
3 (2050)	Jun-03	Jun-03
1 (2080)	May-19	May-25
2 (2080)	May-18	May-24
3 (2080)	May-19	Jun-03

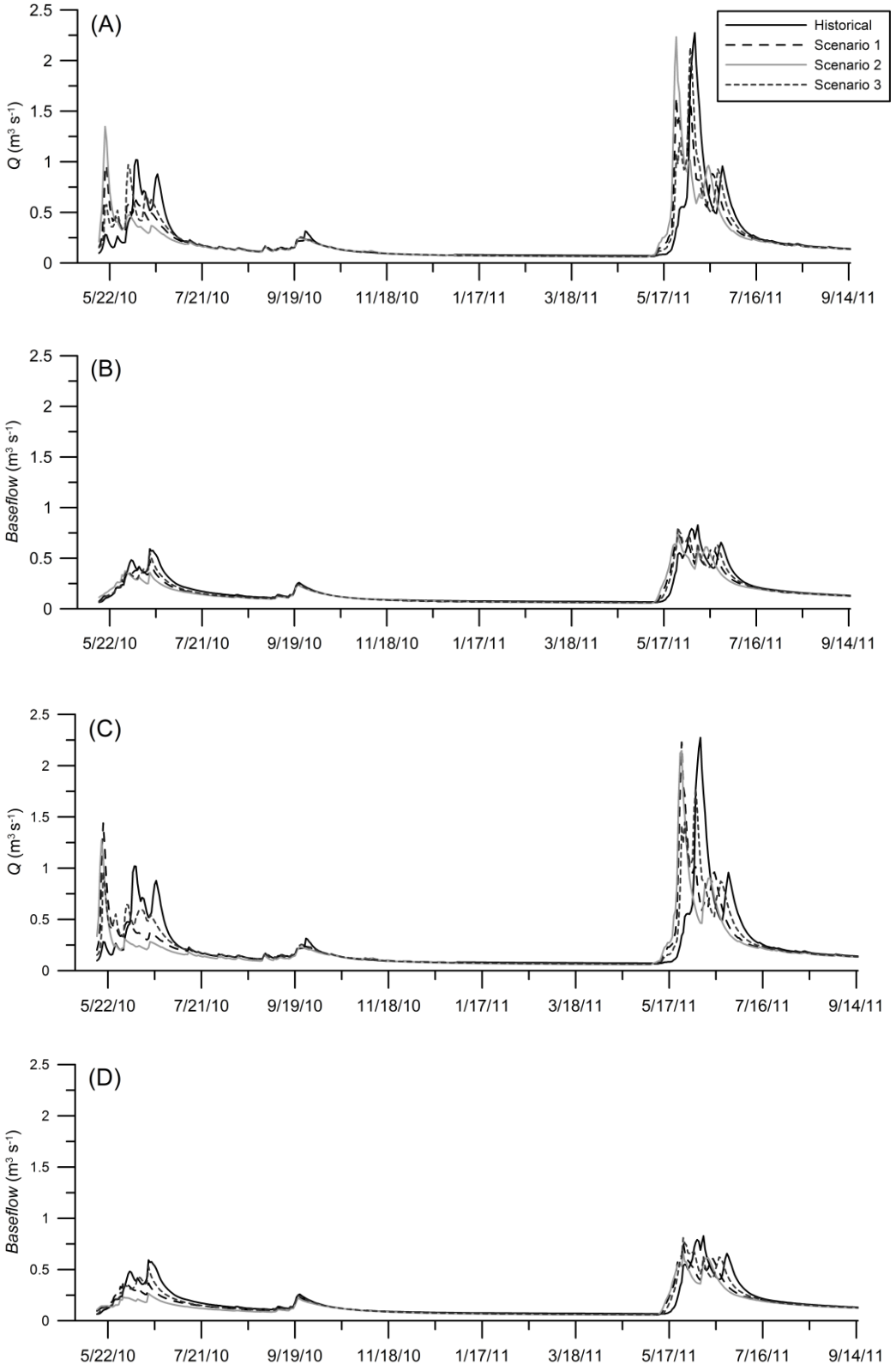

Figure 4.7: Simulated mean daily *Q* (A, C) and baseflow (B, D) for 2010 and 2011, and for all three scenarios in the 2050 and 2080 periods, respectively.

Simulated T_s differences coincided with differences in Q for all three scenarios, with variable seasonal responses and greatest absolute change in mean daily T_s relative to historical predicted for the spring and early summer in the 2050 and 2080 periods. Overall, the low Q year (2010) had a higher magnitude T_s response relative to the higher Q year (2011). Scenario 2 had the greatest response with a negative change in simulated mean daily T_s for early spring (maximum of -1.45°C) and a positive change in mean daily T_s for late-spring and early-summer (maximum of 1.25°C). The simulated late summer mean daily T_s change was well within the range of modelling error and dominantly positive. The fall-winter change in mean daily T_s was also within the range of modelling error and was negative for all scenarios (Figs. 4.8a and 4.8b).

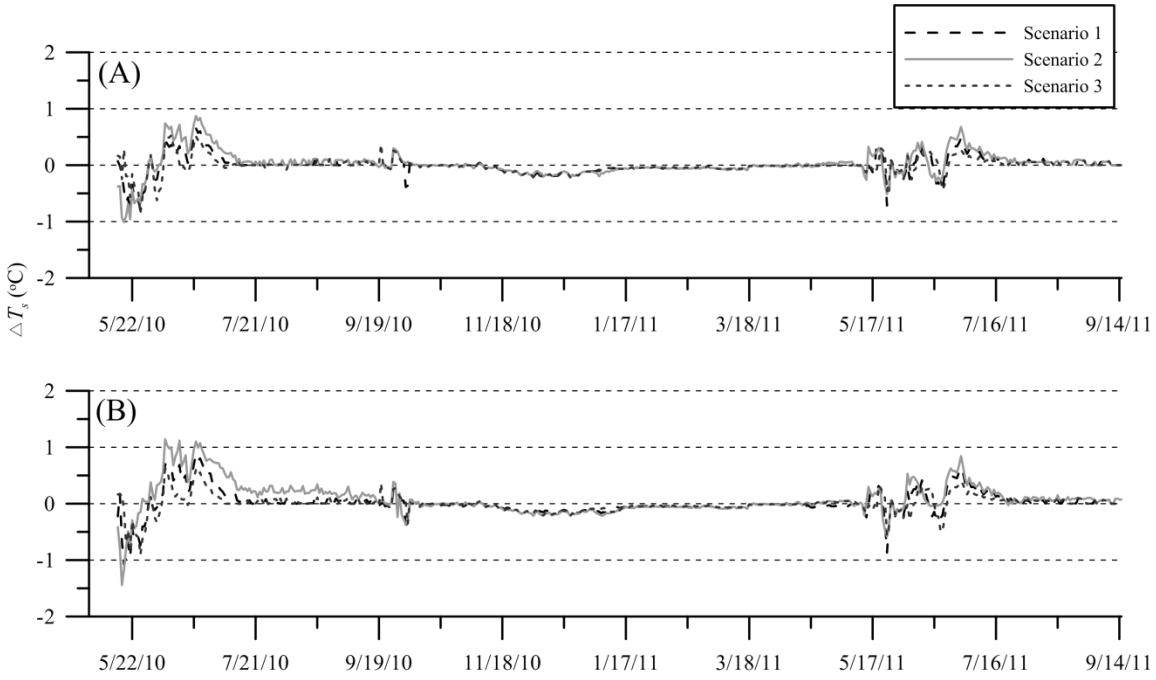

Figure 4.8: Simulated change in mean daily T_s relative to 2010-2011 for all three scenarios for the 2050 (A) and 2080 (B) periods.

Simulated percent change in mean daily T_s was highest for the winter in all three scenarios and both future time periods. The only positive percent change in mean daily T_s was predicted to occur for the summer period, with negative changes predicted for fall, winter and spring. Scenario 2 had the highest magnitude of change in simulated mean daily T_s for all seasons (Fig. 4.9).

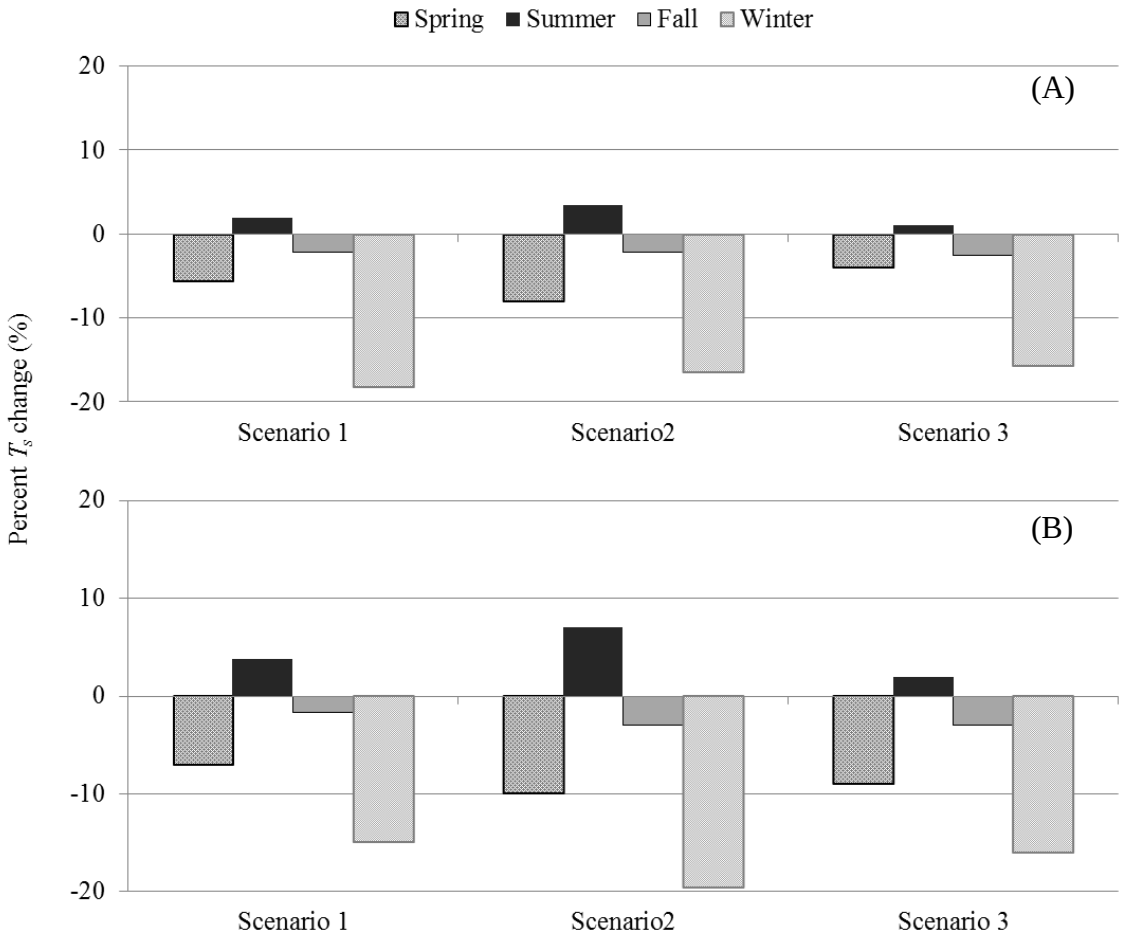

Figure 4.9: Seasonal percent differences in mean daily T_s for all three scenarios in the 2050 (A) and 2080 (B) periods relative to the 2010-2011 study period. For spring and summer comparisons both 2010 and 2011 data were included.

The historical incubation period for WCT was estimated to be 53 days in 2010 and 62 days in 2011. The date of emergence for WCT was predicted to shift earlier in the spring and change by a greater magnitude in 2010 (low Q and high T_s change) relative to 2011 (high Q and low T_s change). The 2010 date of WCT emergence was predicted to occur 18 and 19 days earlier in scenarios 1 and 2, respectively. The 2011 date of WCT emergence was predicted to advance by 11 and 13 days in scenarios 1 and 2, respectively. WCT emergence was predicted to advance by four and five days in Scenario 3 for the 2050 and 2080 periods, respectively (Table 4.3).

Table 4.3: Estimated date of WCT and BT fry emergence for 2010, 2011, and all three scenarios for the 2050 and 2080 periods.

	WCT date of emergence		**BT date of emergence**
	Summer 2010	***Summer 2011***	***Early spring 2011***
Historical	28-Jul	07-Aug	27-Mar
1 (2050)	11-Jul	28-Jul	10-Apr
2 (2050)	10-Jul	26-Jul	10-Apr
3 (2050)	24-Jul	01-Aug	08-Apr
1 (2080)	11-Jul	26-Jul	10-Apr
2 (2080)	10-Jul	25-Jul	11-Apr
3 (2080)	11-Jul	01-Aug	09-Apr

The historical incubation period of BT was estimated to be 194 days and was predicted to shift later in the spring in all three scenarios. Again, the greatest changes in the timing of emergence were predicted in all scenarios for 2010, as this is the year with the greatest predicted T_s change. BT emergence was predicted to occur 15 days later for both the 2050 and 2080 periods in Scenario 1. Scenario 2 was predicted to have the greatest change in BT emergence, occurring 15 days and 16 days later in the 2050 and

2080 periods, respectively. BT emergence was predicted to occur 13 and 14 days later for the 2050 and 2080 periods, respectively in Scenario 3 (Table 4.3).

4.4.4. Inter-catchment comparison

Star and Lynx creeks exhibited very similar temporal T_s patterns, with daily mean T_s reaching approximately 10°C in mid-August and both streams having similar late-season T_s (variable, but >0°C). Early spring T_s was approximately 1°C higher in Star Creek relative to Lynx Creek. T_s increases in Star and Lynx creeks precede increases in Q during the winter period. Q patterns were also similar between Star and Lynx Creeks, with peak Q occurring in both streams on June 8. However, Lynx Creek had higher peak Q and an earlier onset of high Q in the spring. All three creeks had similar T_s patterns in the late fall.

Overall, Lyons East Creek had a substantially different T_s pattern relative to both Star and Lynx Creeks, with a higher maximum (15°C) in August and lower minimum during the winter period (remained stable at 0°C). Lyons East Creek also had higher diurnal and seasonal range in T_s relative to both Lynx and Star creeks. Lyons East Creek had an earlier onset of spring peak Q (May 26) followed by a more rapid decline towards baseflow conditions from mid-summer to winter (Figs. 4.10a and 4.10b).

The differences in Q patterns (earlier onset of spring freshet and lower baseflow) between Lyons East Creek and Lynx and Star creeks were similar to those predicted by future climate scenarios in Star Creek (Fig. 4.7). All three streams had similar T_a patterns, with a slightly lower diurnal T_a range in Star Creek during the winter period (Fig. 4.10c).

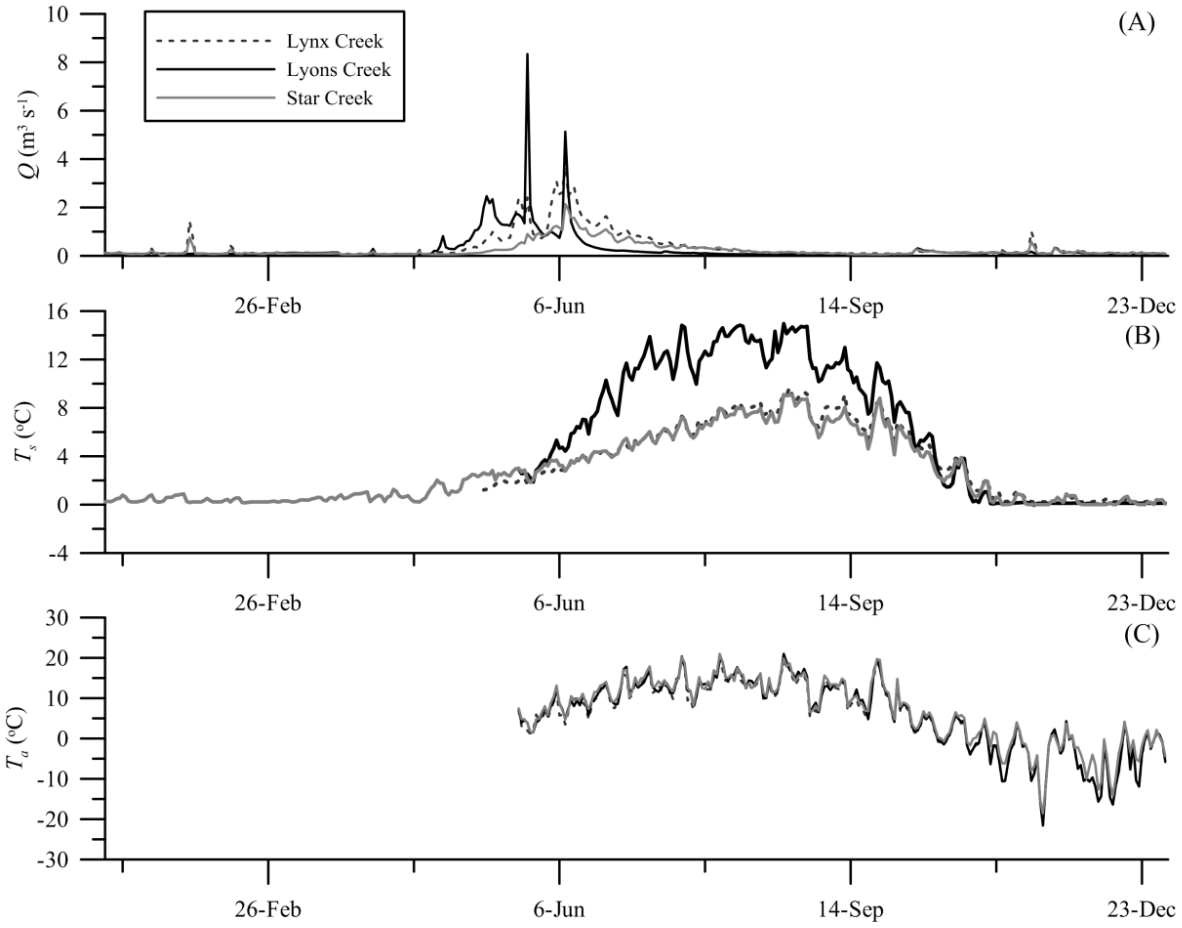

Figure 4.10: Comparison of mean daily Q (A), T_s, (B) and T_a (C) from Star, Lynx, and Lyons East creeks for the period from January 1, 2011 to December 31, 2011.

4.5. **Discussion**

This study provides a mechanistic perspective on T_s response to future climate scenarios, suggesting changes were largely a function of hydrologic shifts in response to earlier onset of spring snowmelt, a trend projected to continue with increased atmospheric warming (Stewart, 2009). This finding is similar to a previous study that demonstrated T_s response to climate change was more related Q reductions than to

increased T_a (Cristea and Burges 2010). We also demonstrate that T_s and subsequent salmonid incubation responses to future climate scenarios are likely to vary with inter-annual hydro-climatological conditions, with 2010 having a greater magnitude of Q and T_s response in all scenarios. This study was limited by assumptions made regarding boundary conditions. However, the inter-catchment comparison between Star, Lynx, and Lyons East creeks supports modelling results by demonstrating that T_s patterns can differ under similar T_a conditions. The inter-catchment comparison presents a conceptual model of stream temperature response to climate change that suggests stream sensitivity to the atmosphere is governed by catchment-scale hydrologic regime.

Many studies suggest increases in future summer T_s and thermal fragmentation in headwater streams during summer months (Isaak *et al*., 2012; Isaak and Rieman, 2013; Jones *et al*. 2013). While the approach used in this study likely produced conservative estimates of summer T_s change, our results support Tague *et al*. (2007). They suggest that groundwater-dominated streams are buffered from summer atmospheric influences. The inter-catchment analysis of T_s and Q conditions also supports Tague *et al*. (2007), demonstrating that Star and Lynx creeks are buffered from atmospheric influences due to high groundwater contribution to total Q. Lyons East Creek had substantially lower groundwater contribution to total Q; therefore, was more susceptible to atmospheric influence.

Results of this study in a continental climate do not suggest an increase in winter flooding demonstrated by other studies (Wegner *et al*. 2011a; Goode *et al*. 2013). It is likely that the cold, dry continental climate of western Alberta is not as susceptible to increased winter flooding events due to the fact that the ratio of snow to total monthly

precipitation is not projected to change substantially during the winter period. This study suggests that even with increased groundwater temperature in scenarios 2 and 3, a peak Q shift towards earlier in the spring, resulting in reduced late-season groundwater contribution to total Q (Huntington and Niswonger, 2012) is likely to increase T_s sensitivity to the atmosphere. These results are supported by the inter-catchment comparison, where under the same T_a conditions Lyons East Creek had colder winter T_s as a function of lower Q relative to Star and Lynx creeks. Therefore, it is reasonable to assume that increased atmospheric sensitivity would likely accelerate in-stream ice formation (Brown *et al*. 2011) and subsequently decrease winter T_s in cold environments.

Decreased winter T_s in critical headwater over-wintering habitat for WCT is of particular concern given that this species is currently restricted in its range. Headwater groundwater-dominated streams provide this over-wintering habitat due to reduced ice formation, tolerable T_s and dissolved oxygen conditions, and relatively stable Q (Jakober *et al*. 1998; Power *et al*. 1999). Decreases in late season Q as a function of earlier onset of spring could; therefore, result in a winter habitat bottle neck for WCT by reducing the carrying capacity of isolated headwater streams.

WCT are likely less sensitive to changes in climate than BT (Wenger et al. 2011b); however, little is known about the potential biological implications of colder spring T_s. Negative trends in spring T_s were observed by Isaak *et al*. (2012) and attributed to cooler T_a during the same period. Early spring T_s and Q differences between Star and Lynx creeks were attributed to higher early-spring Q in Lynx Creek given that T_a was similar between sites.

While our results suggest earlier timing of WCT emergence in response to an earlier onset of peak *Q* and increased CTUs under all scenarios used, it is unlikely that shifts of this magnitude would result in any biologically significant change in young-of-year WCT size. Based on growth rates obtained from Fraley and Shepard (2005), extending the growing period of WCT by 19 days would result in an additional growth of approximately 4 mm for WCT less than four years of age. Others do suggest; however, that an earlier emergence could increase the survivorship of WCT (Coleman and Fausch, 2007), currently limited in their distribution to high elevation portions of catchments, benefiting the species overall. Habitat in high elevation, nutrient poor streams is in fact expected to improve the success of greenback cutthroat (*Oncorhynchus clarki stomias*), with the assumption that populations remain isolated from non-native RT (Cooney *et al*. 2005). This assumption is important, as hybridization between these species is likely to increase in response to higher T_s (Muhlfeld *et al*. 2009; Rasmussen *et al*. 2010).

Thermally stable groundwater-dominated streams provide important BT spawning and incubation habitat by remaining ice-free over the winter period (Baxter and McPhail, 1999; Baxter and Hauer, 2000). Given the habitat selection specificity of these critical life-stages, changes in groundwater-dominated catchments are likely to dramatically affect fall spawning salmonids. Our study suggests that a longer BT incubation period associated with decreased winter *Q* is possible under future climate scenarios. This demonstrates that, independent of reductions in summer habitat (Isaak and Rieman, 2013; Jones *et al*. 2013) and competition with non-native brook trout (*Salvelinus fontinalis*) (Warnock and Rasmussen, 2013), BT populations could be affected by longer incubation periods resulting from decreased *Q* and increased winter ice cover. Therefore, fisheries

management strategies should continue to be implemented in Alberta to help preserve the habitat of native BT populations.

4.6. **Conclusion**

This study provides a year-round perspective on the potential impacts of climate change on native salmonid habitat in the Rocky Mountains of southern Alberta using a process-based T_s modelling approach and inter-catchment comparison of T_s, T_a, and Q. We demonstrate that stream thermal response to climate change is likely to be variable and that fall-spawning salmonids are likely more susceptible. McCullough et al. (2009) demonstrate that sub-lethal effects of altered hydrological and thermal regimes on salmonids are particularly important to consider because integrated population-level impacts are poorly understood. Therefore, we suggest that the perceptual model of T_s response to climate change should focus more on process understanding and representation, as modelling studies have strong potential for guiding management-related decisions.

Chapter 5: Summary and conclusions

This research combined data obtained from a field study conducted over two years with hydrometeorological modelling to assess processes controlling stream temperature in headwater catchments. The approach of combining field and modelling studies was used to help advance our process knowledge while attempting to obtain the "right answers for the right reasons". It is evident that our understanding of factors governing the thermal regime of streams continues to improve based on current literature presented throughout this thesis. Therefore, our representation of processes in models should also improve. A dichotomy remains in stream temperature research where field-based studies are not often used to answer management-related questions and non-process-based models are frequently applied.

This work helped address a research gap with three key objectives, presented as individual chapters in this thesis. In meeting these objectives this study:

1. Defined key atmospheric and hydrologic variables controlling inter-annual variation of stream temperature in a subsurface-dominated catchment using a reach-scale field study;

2. Incorporated reach-scale stream mass and energy balance data into a catchment-scale model; and,

3. Used the newly developed model and field studies to assess how future climate scenarios may affect stream temperature, hydrology, and native salmonid life history in headwater streams.

Chapter 2 addressed the first research question using the two-year field study in Star Creek, which was the most recent study quantifying processes controlling stream temperature on the eastern slopes of the Canadian Rocky Mountains. Stream energy and mass budget data collected in the field study suggest that although net radiation is the

dominant control on stream temperature in small forested catchments, antecedent moisture conditions, controlled by snowmelt contributions to groundwater recharge, can play a large role in determining inter-annual variation in thermal regimes. This work provides insight into how to address the issue of future stream temperature predictions by demonstrating that both atmospheric and hydrologic factors must be considered.

The findings of Chapter 2 are particularly important for headwater streams because changes in the timing and magnitude of snow accumulation and snowmelt runoff are expected to continue in the future. This study demonstrated that decreased snow accumulation, independent of summer precipitation, can result in higher summer stream temperature. Based on these findings, long periods of drought would result in thermal regime shifts in headwater catchments that could fundamentally alter the structure and function of aquatic ecosystems.

Chapter 3 presented the development of a process-based modelling technique for data sparse regions. Results from Chapter 3 demonstrated that key energy and mass balance terms required for process-based stream temperature models can be simulated in mountain catchments using readily available data. In order to achieve this goal, considerable refinements were made in the GENESYS model by including the SCS soil moisture and Muskingum routing routines. The storage-discharge function was also added, providing estimates of baseflow contribution to total stream discharge. Another substantial refinement was the automation of GIS-based downscaling techniques, enabling hydrometeorological output from the GENESYS model to be easily incorporated into the MST model.

The TRU logic in the MST model provides a framework to fully parameterize the stream and riparian environment, and account for processes controlling stream temperature. The technique of coupling the MST model with the GENESYS model in the GIS can be easily applied in mountain catchments with limited data because GENESYS has been shown to reliably simulate hydrometeorological conditions using only air temperature, precipitation inputs, and commonly available catchment physiography data inputs.

Model calibration was required in order to simulate stream temperature at Star Main. However, model energy budget terms compare well with previous studies, providing confidence in the simulation approach. The sensitivity analysis demonstrates that model parameterization is critical and that emphasis should be placed on more field studies to quantify all important variables controlling stream temperature. Results also suggest that no single term in the stream energy budget should be neglected; therefore, models should attempt to quantify all processes controlling stream temperature.

Chapter 4 applied the process-based modelling approach developed in Chapter 3, and although limitations in the approach exist, this work provides important insights into our assumptions of future changes in stream temperature. The results presented in Chapter 4 are biased because boundary stream, streambed, and hyporheic temperature conditions remained constant in the simulation. Regardless of bias, Chapter 4 presents a conceptual framework for stream temperature response to climate change that is supported by field observations. This study supports the assumption that groundwater dominated streams are somewhat buffered from atmospheric influences on stream

temperature and suggests that there is not a direct correlation between air temperature and stream temperature change in all streams.

Winter stream temperature under future climate warming could in fact decrease as a result of earlier spring freshet and late season streamflow conditions - a key finding from Chapter 4 that differs from other studies on the effects of climate change on thermal regimes. Reduced streamflow during winter in the relatively cold-continental climate of the eastern slopes of the Rocky Mountains has a high potential for increasing the spatial and temporal extent of in-stream ice formation because of increased stream sensitivity to the atmosphere. This finding is supported by an inter-catchment comparison between Star, Lynx and Lyons East creeks, where Lyons East Creek encounters freezing conditions in the winter as a result of reduced streamflow. Increased ice formation and colder streams in the winter have important implications for the habitat of native salmonids, which are currently limited in their distribution to these headwater catchments.

The implications of changes in the timing of spring freshet for salmonid life history are not clear, although it does appear that westslope cutthroat trout are less sensitive than bull trout. This finding is primarily based on the assumption that earlier timing of spawning and advanced incubation period for westslope cutthroat trout may improve recruitment. However, more importantly, this study suggests that winter habitat may become more limited, which could dramatically affect isolated pure populations of westslope cutthroat trout. Bull trout are particularly sensitive to changes in hydrological and thermal regimes because of their fall-spawning life history. This study suggests that thermally suitable spawning habitat may be reduced as a function of decreased

streamflow and that the incubation period for bull trout may be more susceptible to ice formation, resulting in decreased egg survival. These findings demonstrate that regional variation in atmospheric, hydrologic, and geomorphic characteristics must be considered when assessing how native salmonid populations may respond to future environmental change.

5.1. **Future research**

This thesis demonstrates that process-based approaches to understanding thermal regimes can provide important insights into knowledge gaps. This work has identified key future research needs:

- There is a necessity for continued investigation into the controls on spatial and temporal variation in stream temperature in headwater streams. This is particularly important given the range of catchment characteristics of headwater regions. Management practices directed at preserving native salmonid populations can be improved by determining catchment-specific thermal responses to environmental change. Therefore, differences in controls on stream temperature between catchments should be clearly defined in order to improve the predictive ability of thermal response to environmental change.
- The role of in-stream ice and snow on spring and winter stream temperature is a key gap in the literature. The effect of ice melt on lake water temperature is better understood and knowledge of ice-melt processes can be gained from literature on lakes. However, it is likely that processes for streams are different, and that long and shortwave radiation, melt water input, conduction, and advection all play a

role in governing stream temperature when snow and ice are present within a stream.

- Additional research should assess spatial and temporal changes in surface-subsurface interactions. As Chapters 2 and 3 identified, there is considerable variation in the interaction between a stream and its surrounding environment. New research using tracer techniques continues to demonstrate the complexity in these interactions. Longer-term tracer and subsurface studies would be highly valuable as these interactions are critical for the maintenance of salmonid habitat in headwater streams.
- Focus should be placed on monitoring stream and bed temperatures simultaneously. Temperature measurement is inexpensive and invaluable as insights into the spatial and temporal changes in processes controlling stream temperature can be most easily gained through monitoring. Monitoring should focus on capturing a range of catchment types, enabling better quantification of expected trends and improved modelling efforts.
- Future studies of the effects of landscape disturbance independent of changes in climate are needed. Stream temperature comparison between Lynx Creek and Star Creek demonstrates that similar thermal regimes can exist between severely burned and unburned catchments. This finding suggests the influence of riparian cover on stream temperature can be outweighed by other factors. Energy and mass balance studies focused on a range of landscape types would help direct management actions and further our understanding of the relative roles of surface and subsurface processes governing stream temperature.

References

AESRD. In prep. The Alberta Westslope Cutthroat Trout Recovery Team. In progress. Alberta Westslope Cutthroat Trout Recovery Plan, 2012-2017. Alberta Environment and Sustainable Resource Development, Alberta Species at Risk Recovery Plan No. 28. Edmonton, AB.

Allen, J.D. 1995. *Stream Ecology: Structure and Function of Running Waters*. Dordrecht: Kluwer Academic Publishers, 388pp.

Arnold, J.G., Allen, P.M., Muttiah, R., and Bernhardt, G. 1995. Automated baseflow separation and analysis techniques. Ground Water. 33: 1010–1018.

Arnold, J.G., and Allen, P.M. 1999. Automated methods for estimating baseflow and ground water recharge from streamflow records. J. Am. Water. Resour. As. 35: 411–424.

Arismendi, I., Johnson, S.L., Dunham, J.B., Haggerty, R., and Hockman-Wert, D. 2012. The paradox of cooling streams in a warming world: Regional climate trends do not parallel variable local trends in stream temperature in the Pacific continental United States. Geophys. Res. Lett. 39: doi:10.1029/2012GL051448.

Arrigoni, A.S., Poole, G.C., Mertes. L.A.K., O'Daniel, S.J., Woessner, W.W., and Thomas, S.A. 2008. Buffered, lagged, or cooled? Disentangling hyporheic influences on temperature cycles in stream channels. Water Res. Res. 44, doi: 10.1029/2007WR006480,2008.

ASRD. 2008. Lidar Digital Elevation Model. Edmonton, AB.

ASRD. 2009. Status of the bull trout (*Salvelinus confluentus*) in Alberta: Update 2009. 61 pp.

ASRD. 2010. Alberta Vegetation Inventory (AVI). Edmonton, AB.

Barnett, T.P., Pierce, D.W., Hidalgo, H.G., Bonfils, C., Santer, B.D., Das, T., Bala, G., Wood, A.W., Nozawa, T., Mirin, A.A., Cayan, D.R., and Dettinger, M.D. 2008. Human-induced changes in the hydrology of the western United States. Science 319: 1080, doi: 10.1126/science.1152538.

Barrow, E., and Yu, G. 2005. Climate Change Scenarios for Alberta - A Report Prepared for the Prairie Adaptation Research Collaborative (PARC) in co-operation with Alberta Environment. Regina, Saskatchewan. 73pp.

Baxter, J.S., and McPhail, J.D. 1999. The influence of redd site selection, groundwater upwelling, and over-winter incubation temperature on survival of bull trout (*Salvelinus confluentus*) from egg to alevin. Can. J. Zool. 77: 1233-1239.

Baxter, C.V., and Hauer, R.F. 2000. Geomorphology, hyporheic exchange, and selection of spawning habitat by bull trout (*Salvelinus confluentus*). Can. J. Fish. Aquat. Sci. 57: 1470-1481.

Baxter, C., Hauer, F.R., and Woessner, W.W. 2003. Measuring subsurface-stream water exchange: New techniques for installing minipiezometers and estimating hydraulic conductivity. T. Am. Fish. Soc. 132: 493-502.

Bayrock, L.A., and Reimchen, T.H.F. 2007. Surficial Geology, Alberta Foothills and Rocky Mountains DIG 2007-0077. Alberta Geological Survey, Edmonton, ArcGIS digital vector data.

BC-MOE. 2012. Water and air baseline monitoring guidance document for mine proponents and operators. Prepared by the Ministry of Environment. 198 pp.

Beacham, T.D., and Murray, C.B. 1990. Temperature, egg size, and development of embryos and alevins of five species of Pacific salmon: A comparative analysis. T. Am. Fish. Soc. 119: 927-945.

Bear, E.A., Mcmahon, T.E., and Zale, A.V. 2007. Comparative thermal requirements of westslope cutthroat trout and rainbow trout: implications for species interactions and development of thermal protection standards. T. Am. Fish. Soc. 136: 1113–1121. doi:10.1577/T06-072.1.

Behnke, R.J. 2002. *Trout and salmon of North America*. The Free Press: Simon & Schuster Inc., New York.

Benyahya, L., Caissie, D., St-Hillarie, A., Ouarda, T.B.M.J., and Bobee, B. 2007. A review of statistical water temperature models. Can. Water. Resour. J. 32: 179-192.

Benyahya, L., Caissie, D., El-Jabi, N., and Mysore, S.G. 2010. Comparison of microclimate vs. remote meteorological data and results applied to a water temperature model (Miramichi River, Canada). J. Hydrol. 380: 247-259.

Beven, K. 2001. *Rainfall runoff modeling: A primer*. Vol 15. John Wiley and Sons., Chichester, England.

Beven, K. 2012. So how much of your error is epistemic? Lessons from Japan and Italy. Hydrol. Procces. doi:10.1002/hyp.9648.

Boyd, M., and Kasper, B. 2003. Analytical methods for dynamic open channel heat and mass transfer: methodology for heat source model version 7.0. 204 pp

Braithwaite, R.J., and Olesen, O.B. 1990. A simple energy-balance model to calculate ice ablation at the margin of the Greenland ice sheet. J. Glaciol. 36: 222-228.

Bristow, R.L., and Campbell, G.S. 1984. On the relationship between incoming solar radiation and daily maximum and minimum temperature. Agr. For. Met. 31: 159-166.

Brown, G.W. 1969. Predicting temperatures of small streams. Water. Res. Res. 3: 68-75.

Brown, G.W., and Krygier, J.T. 1970. Effects of clear-cutting on stream temperature. Water. Res. Res. 6: 1133-1139.

Brown, R.S., and Mackay, W.C. 1995. Fall and winter movements and habitat use by cutthroat trout in the Ram River, Alberta. T. Am. Fish. Soc. 124: 873-885.

Brown, L.E., Hannah, D.M., and Milner, A.M. 2006. Hydroclimatological influences on water column and streambed thermal dynamics in an alpine river system. J. Hydrol. 325: 1-20.

Brown, L.E., and Hannah, D.M. 2007. Alpine stream temperature response to storm events. J. Hydromet. 8: 952-967.

Brown, R. S., and Hubert, W.A. 2011. A primer on winter, ice, and fish: What fisheries biologists should know about winter ice processes and stream-dwelling fish. Fisheries. 36: 8-26.

Buisson, L.L., Blanc, G.G., and Grenoillet, G. 2008. Modelling stream fish species distribution in a river network: the relative effects of temperature versus physical factors. Ecol. Freshwater. Fish. 17: 244-257.

Burles, K., and Boon, S. 2011. Snowmelt energy balance in a burned forest plot, Crowsnest Pass, Alberta, Canada. Hydrol. Process. 25: 3012-3029.

Buffington, J.M., and Tonina, D. 2009. Hyporheic exchange in mountain rivers II: Effects of channel morphology on mechanics, scales, and rates of exchange. Geog. Compass. 3: 1038-1062.

Caissie, D. 2006. The thermal regime of rivers: a review. Freshwater Biol. 51: 1389-1406.

Caissie, D., Mysore, S.G., and El-Jabi, N. 2007. Predicting water temperatures using a deterministic model: Application on Miramichi River catchments (New Brunswick, Canada). J. Hydrol. 336: 303-315.

Chen, D., Carsel, R.F., McCutcheon, S.C., Nutter, W.L. 1998. Stream temperature simulation of forested riparian areas: I. Watershed-scale model development. J. Environ. Eng. 124: 316-328.

Cimmery, V. 2010. SAGA User Guide, updated for SAGA version 2.0.5. 336 pp.

Coleman, M.A., and Fausch, K.D. 2007. Cold summer temperature regimes cause a recruitment bottleneck in age-0 Colorado River cutthroat trout reared in laboratory streams. T. Am. Fish. Soc. 136: 639-654.

Cooney, S.J., Corvich, A.P., Lukacs, P.M., Harig, A.L., and Fausch, K.D. 2005. Modeling global warming scenarios in greenback cutthroat trout (Oncorhynchus clarki stomias) streams: Implications for species recovery. West. N. Am. Naturalist. 65: 371-381.

Constanz, J., and Thomas, C.L. 1997. Stream bed temperature profiles as indicators of percolation characteristics beneath Arroyos in the middle Rio Grande basin, USA. Hydrol. Process. 11: 1621-1634.

COSEWIC. 2009. Canadian wildlife species at risk. 92 pp.

Coulibaly, P., and Burn, D.H. 2004. Wavelet analysis of variability in annual Canadian streamflows. Water Res. Res. 40: W03105, DOI: 10.1029/2003WR002667.2004.

Cox, M.M., Bolte, J.P. 2007. A spatially explicit network-based model for estimating stream temperature distribution. Env. Mod. Soft. 22: 502-514.

Cozzetto, K., McKnight, D., Nylen, T., and Fountain, A. 2006. Experimental investigations into processes controlling stream and hyporheic temperatures, Fryxell Basin, Antarctica. Adv.Wat. Resour. 29: 130-153.

Cristea, N. C., Burges, S. J. 2010. An assessment of the current and future thermal regimes of three streams located in the Wenatchee River basin, Washington State: some implications for regional river basin systems. Climatic Change. 102: 493-520.

Dalla Vicenza, S. 2012. Forest Fire vulnerability in the Northern Rocky Mountains under climate change. University of Lethbridge, MSc Thesis, University of Lethbridge, Alberta. 151 pp.

Daly, C., Halbleib, M., Smith, J.I., Gibson, W.P., Doggett, M.K., Taylor, G.H., Curtis, J., and Pasteris, P.A. 2008. Physiographically-sensitive mapping of climatological temperature and precipitation across the conterminous United States. Int. J. Climatol. 28: 2031-2064.

Dery, S.J., Taylor, P.A., and Xiao, J. 1998. The thermodynamic effects of sublimating, blowing snow in the atmospheric boundary layer. Bound. Lay. Meteorol. 89: 251–283.

Dewalle, D., Henderson, Z., and Rango, A. 2002. Spatial and temporal variations in snowmelt degree-day factors computed from SNOTEL data in the upper Rio Grande basin. Proceedings of the Western Snow Conference. 73-81.

Diabat, M., Haggerty, R., and Wondzell, S.W. 2012. Diurnal timing of warmer air under climate change affects magnitude, timing and duration of stream temperature change. Hydrol. Process. doi: 10.1002/hyp.9533.

Dixon, D. 2011. Catchment-scale controls on snow distribution in a montane catchment. University of Lethbridge, MSc Thesis, University of Lethbridge, Alberta. 184 pp.

Domenico, P.A., and Schwartz, F.W. 1990. Physical and Chemical Hydrogeology. New York, John Wiley and Sons, Inc.

Drinan, D.P. 2010. Thermal adaptation of westslope cutthroat trout *Oncorhynchus clarkii lewisi.* MSc Thesis, Montana State University, Bozeman, Montana. 68pp.

Dunham, J.B., Rosenberger, A.E., Luce, C.H., and Rieman, B.E. 2007. Influences of wildfire and channel reorganization on spatial and temporal variation in stream temperature and the distribution of fish and amphibians. Ecosystems 10: 335-346.

Durance, I., and Ormerod, S.J. 2009. Trends in water quality and discharge confound long-term warming effects on river macroinvertebrates. Freshwater. Ecol. 54: 388-405.

Earman, S., Campbell, A.R., Phillips, F.M., and Newman, B.D. 2006. Isotopic exchange between snow and atmospheric water vapor: Estimation of the snowmelt component of subsurface recharge in the southwestern United States. J. Geophys. Res. 111: doi:10.1029/2005JD006470

Environment Canada. 2012a. National Climate Data and Information Archive, Canadian Climate Normals, 1971-2000 - Coleman, Alberta. Accessed: January 4, 2012. http://www.climate.weatheroffice.ec.gc.ca/climate_normals/index_e.html

Environment Canada. 2012b. National Climate Data and Information Archive, Daily weather data - Coleman, Alberta. Last Updated: January 3, 2012. Accessed: January 4, 2012. http://www.climate.weatheroffice.ec.gc.ca/climate_normals/index_e.html

Evans, E.C., McGregor, G.R., and Petts, G.E. 1998. River energy budgets with special reference to river bed processes. Hydrol. Process. 12: 575-595.

Frazer, G.W., Canham, C.D., and Lertzman, K.P. 1999. *Gap Light Analyzer (GLA) Version 2.0: Imaging software to extract canopy structure and gap light transmission indices from true-colour fisheye photographs, Users Manual and Program Documentation,* Burnaby: Simon Fraser University, and Millbrook: Institute of Ecosystem Studies, 40 pp.

Fraley, J., and Shepard, B.B. 2005. Age, growth, and movements of westslope cutthroat trout, Oncorhynchus clarki lewisii, inhabiting headwaters of a wilderness river. Northwest. Sci. 79: 12-21.

Garner G., Hannah, D.M., Malcom, I.A., and Sadler, J.P. 2012. *Inter-annual variability in spring-summer stream water temperature microclimate and heat exchanges: a comparison of forest and moorland environments*. British Hydrological Society Eleventh National Symposium, Hydrology for a changing world, Dundee. 13 pp

Glassy, J. M., and S. W. Running. 1994: Validating diurnal climatology logic of the MT-CLIM model across a climatic gradient in Oregon. Ecol. Appl. 4, 248–257.

Goode, J. R., Buffington, J.M., Tonina, D., Isaak, D.J., Thurow, R.F., Wenger, S., Nagel, D., Luce, C., Tetzlaff, D., and Soulsby, C. 2013. Potential effects of climate change on streambed scour and risks to salmonid survival in snow-dominated mountain basins. Hydrol. Process. 27: 750-765.

Gordon, N.D., McMahon, T.A., Finlayson, B.L., Gippel, C.J., and Nathan, R.J. 2004. *Stream Hydrology: An Introduction for Ecologists, Second Edition.* Chichester: John Wiley and Sons Ltd, 429 pp.

Gould, W. R. 1987. Features in the early development of bull trout *(Salvelinus confluentus).* Northwest Sci. 61: 264-268.

Groom, J.D., Dent, L., Madsen, L.J., and Fleuret, J. 2011. Response of western Oregon (USA) stream temperatures to contemporary forest management. Forest. Ecol. Manag. 262: 1618-1629.

Guenther, S.M., Gomi, T., and Moore, R.D. 2012. Stream and bed temperature variability in a coastal headwater catchment: influences of surface-subsurface interactions and partial-retention forest harvesting. Hydrol. Process. doi: 10.1002/hyp.9673.

Hannah, D.M., Malcom, I.A., Sousbly, C., and Youngson, A.F. 2004. Heat exchanges and temperatures within a salmon spawning stream in the Cairngorms, Scotland: Seasonal and sub-seasonal dynamics. River Res. App. 20: 635-652.

Hannah, D.M., Malcom, I.A., Sousbly, C., and Youngson, A.F. 2008. A comparison of forest and moorland stream microclimate heat exchanges and thermal dynamics. Hydrol. Process. 22: 919-940.

Hatch, C.E., Fisher, A.T., Ruehl, C.R., Stemler, G. 2010. Spatial and temporal variations in streambed hydraulic conductivity quantified with time-series thermal methos. J. Hydrol. 389: 276-288.

Hawkins, C.P., Kershner, J.L., Bisso, P.A., Bryant, M.D., Decker, L.M., Gregory, S.V., McGullough, D.A., Overton, C.K., Reeves, G.H., Steedman, R.J., and Young, M.K. 1993. A hierarchical approach to classifying stream habitat features. Fisheries. 18: 3-12.

Hay, L.E., Wilby, R.L., and Leavesley, G.H. 2000. A comparison of delta change and downscaled GCM scenarios for three mountainous basins in the United States. J. Am. Water. Resour. As. 36: 387-397.

Hebert, C., Caissie, D., Mysore, S., El-Jabi, N. 2011. Study of stream temperature dynamics and corresponding heat fluxes within Miramichi River catchments (New Brunswick, Canada). Hydrol. Process. 25: 2439-2455.

Herb, W.R., Stefan, H.G. 2011. Modified equilibrium temperature models for cold-water streams. Water Res. Res. 47: doi: 10.1029/2010WR009586,2011.

Hedstrom, N.R., Pomeroy, J.W. 1998. Measurements and modelling of snow interception in the boreal forest. Hydrol. Process. 12: 1611–1625.

Huntington, J.L., and Niswonger, R.G. 2012. Role of surface-water and groundwater interactions on projected summertime streamflow in snow dominated regions: An integrated modeling approach. Water. Res. Res. 48: W11524 doi: 10.1029/2012WR012319.2012.

Hurkett, B., Blackburn,J., and Council, T. 2011. Abundance and distribution of migratory bull trout in the upper Oldman River drainage, 2007 - 2010. Technical Report, T-2011-002, produced by the Alberta Conservation Association, Lethbridge, Alberta, Canada. 34 pp + App.

Isaak, D.J., Luce, C.H., Rieman, B.E., Nagel, D.E., Peterson, E.E., Horan, D.L., Parkes, S., and Chandler, G.L. 2010. Effects of climate change and wildfire on stream temperatures and salmonid thermal habitat in a mountain river network. Ecol. Appl. 20: 1350-1371.

Isaak, D.J., Wollrab, S., Horan, D., and Chandler, G. 2011. Climate change effects on stream and river temperatures across the northwest U.S. from 1980-2009 and implications for salmonid fishes. Climatic Change: doi: 10.1007/s10584-011-0326-z.

Isaak, D.J., Muhlfeld, C.C., Todd, A.S., Al-Chochachy, R., Roberts, J., Kershner, J.L., Fausch, K.D., and Hostetler, S.W. 2012. The past as prelude to the future for understanding 21st-century climate effects on Rocky Mountain trout. Fisheries. 37(12): 542-556.

Isaak, D.J., and Rieman, B.R. 2013. Stream isotherm shifts from climate change and implications for distribution of ecotothermic organisms. Glob. Change Biol. 19: 742-751.

Jakober, M.J., McMahon, T.E., Thurow, R.F., and Clancy, C.G. 1998. Role of stream ice on fall and winter movements and habitat use by bull trout and cutthroat trout in Montana headwater streams. T. Am. Fish. Soc. 127: 223-235.

Johnson, S.L., and Jones, J.A. Stream temperature response to forest harvest and debris flows in western Cascades, Oregon. 2000. Can. J. Fish. Aquat. Sci. 57: 30-39.

Johnson, S.L. 2003. Stream temperature: scaling of observations and issues for modelling. Hydrol. Process. 17: 497-499.

Johnson, S.L. 2004. Factors influencing stream temperatures in small streams: substrate effects and a shading experiment. Can. J. Fish. Aquat. Sci. 61: 913-923.

Jones, L.A., Muhlfeld, C.C., Marshall, L.A., McGlynn, B. L., and Kershner, J. L. 2013. Estimating thermal regimes of bull trout and assessing the potential effects of climate warming on critical habitats. River. Res. Applic. doi: 10.1002/rra.

Kasahara, T., and Wondzell, S.M. 2003. Geomorphic controls on hyporheic exchange flow in mountain streams. Water Res. Res. 38: doi: 10.1029/2002WR001386,2003.

Kirchner, J.W. 2006. Getting the right answers for the right reasons: linking measurements, analyses, and models to advance the science of hydrology. Water Res. Res. 42: doi: 10.1029/2005WR004362,2006.

Kienzle, S.W. 2008. Anew temperature based method to separate rain and snow. Hydrol. Process. 22: 5067–5085.

Kienzle, S.W. 2010. Effects of area under-estimations of sloped mountain terrain on simulated hydrological behaviour: a case study using the ACRU model. Hydrol. Process. DOI: 10.1002/hyp.7886.

Klute, A. 1986. *Method of Soil Analysis*. Soil Science Society of America Inc. Madison, Wisconsin.

Krause, S., Blume, T., and Cassidy, N.J. 2012. Investigating patterns and controls of groundwater up-welling in a lowland river by combining fibre-optic distributed temperature sensing with observations of vertical hydraulic gradients. Hydrol. Earth. Syst. Sci. 16: 1775-1792.

Lapp, S., Byrne, J.M., Kienzle, S.W., and Townshend, I. 2005. Climate warming impacts on snowpack accumulation in an alpine watershed: a GIS based modeling approach. Int. J. Climatol. 25: 521-526.

Larson, R.P., Byrne, J.M., Johnson, D.J., Kienzle, S.W., and Letts, M.G. 2011. Modelling climate change impacts on spring runoff for the Rocky Mountains of Montana and Alberta 11: Runoff change projections using future scenarios. Can. J. Wat. Resour. As. 36: 35-52.

Lautz, L.K. 2012. Observing temporal patterns of vertical flux through streambed sediments using time-series analysis of temperature records. J. Hydrol. 464-465: 199-215.

Leach, J.A., and Moore, R.D. 2010. Above-stream microclimate and stream surface energy exchanges in a wildfire-disturbed riparian zone. Hydrol. Process. 24(7): 2369-2381.

Leach, J.A., and Moore, R.D. 2011. Stream temperature dynamics in two hydrogeomorphically distinct reaches. Hydrol. Process. 25(5): 679-690.

Link, T.E., and Marks, D. 1999. Point simulation of seasonal snowcover dynamics beneath boreal forest canopies. J. Geophys. Res. 104(D22), 27: 841-827, 857.

Liston, G.E., and Hall, D.K. 1995. An energy-balance model of lake-ice evolution. J. Glaciol. 41: 373-382.

MacDonald, R.J., Byrne, J.M., and Kienzle, S.W. 2009. A physically based daily hydrometeorological model for complex mountain terrain. J. Hydrometeorol. 10: 1430- 1446.

MacDonald, R.J., Byrne, J.M., Kienzle, S.W., and Larson, R.P. 2011. Assessing the potential impacts of climate change on mountain snowpack in the St. Mary River catchment, Montana. J. Hydrometeorol. 12: 262-273.

MacDonald, R.J., Byrne, J.M., Boon, S., and Kienzle, S.W. 2012. Modelling the potential impacts of climate change on snowpack in the North Saskatchewan River watershed, Alberta. Water. Resour. Manage. 26: 3053-3076.

MacDonald, R.J., Boon, S., Byrne, J.B., and Silins, U. 2013. A comparison of surface and subsurface controls on summer temperature in a headwater stream. Hydrol. Process. DOI: 10.1002/hyp.9756.

Magruder, I.A., Woessner, W.W., and Running, S.W. 2009. Ecohydrologic process modeling of mountain block groundwater recharge. Groundwater. 47: 774-785.

Mantua, N., Tohver, I., and Hamlet, A. 2010. Climate change impacts on streamflow extremes and summertime stream temperature and their possible consequences for freshwater salmon habitat in Washington State. Climatic. Change. 102:187-223.

McCullough, D.A., Bartholow, J.M., Jager, H.I., Beschta, R.L., Cheslak, E.F., Deas, M.L., Ebersole, J.L., Foott, S., Johnson, S.L., Souchon, K.R., Tiffan, K. F., and Wurtsbaugh, W.A. 2009. Research in thermal biology: Burning questions for coldwater stream fishes. Rev. Fish. Sci. 17: 90-115.

McGuire, K.J., McDonnell, J.J., Weiler, M., Kendall, C., McGlynn, B.L., Welker, J.M., and Seibert, J. 2005. The role of topography on catchment-scale water residence time. Wat. Resour. Res. 41: W05002, doi:10.1029/2004WR003657.

McPhail, J.D., and Baxter, J.S. 1996. A review of bull trout (Salvelinus confluentus) life-history and habitat use in relation to compensation and improvement opportunities. Fisheries Management Report No. 104. 39pp

Meisner, J.D., Rosenfeld, J.S., and Regier, H.A. 1988. The role of groundwater in the impact of climate warming on stream salmonines. Fisheries 13: 2–8.

Meyer, J.L., Sale, M. J., Mulholland, P.J., and Poff, N.L. 1999. Impacts of climate on aquatic ecosystem functioning and health. J. Am. Water. Resour. As. 35: 1373-1386.

Moore, R.D., Sutherland, P., Gomi, T., and Dhakal, A. 2005. Thermal regime of a headwater stream within a clear-cut, coastal British Columbia, Canada. Hydrol. Process. 19: 2591-2608.

Moore, R.D. 2005. Introduction to salt dilution gauging for streamflow measurement part III: Slug injection using salt in solution. Streamline Catchment Management Bulletin 8:1-6.

Mohseni, O., and Stefan, H.G. 1999. Stream temperature/air temperature relationship: a physical interpretation. J. Hydrol. 218: 128-141.

Mohseni, O., Stefan, H.G., and Eaton J.G. 2003. Global warming and potential changes in fish habitat in US streams. Climatic Change 59: 389-409.

Montgomery, D.R., and Buffington, J.M. 1997. Channel-reach morphology in mountain drainage basins. Geol. Soc. Am. Bull. 109: 596-611.

Morrison, J., Quick, M.C., and Foreman, M.G.G. 2002. Climate change in the Fraser River catchment : flow and temperature projections. J. Hydrol. 263: 230-244.

Mote, P.W., Hamlet, A.F., Clark, M.P., and Lettenmaier, D.P. 2005. Declining mountain snowpack in western North America. B. Am. Meteorol. Soc. 86: 39-49.

Muhlfeld, C.C., McMahon, T.E., Boyer, M.C., and Cresswell, R.E. 2009. Local habitat, watershed, and biotic factors influencing the spreah of hybridization between native westslope cutthroat trout and introduced rainbow trout. T. Am. Fish. Soc. 138: 1036-1051.

Nash, J.E., and Sutcliffe, J.V. 1970. River flow forecasting through conceptual models part 1 – A discussion of principles. J. Hydrol. 10: 282-290.

Neilson, B.T., Stevens, D.K., Chapra, S.C., and Bandaragoda, C. 2009. Data collection methodology for dynamic temperature model testing and corroboration. Hydrol. Process. 23: 2902-2914.

Norton, G.W., Bradford, A. 2009. Comparison of two stream temperature models and evaluation of potential management alternatives for the Speed River, Southern Ontario. J. Environ. Manag. 90: 866-878.

Oke, T.R. 1987. *Boundary Layer Climates*. Routledge: London, New York.435 pp.

Parton, W.J., and Logan, J.A. 1981. A model for diurnal variation in soil and air temperature. Agr. Meteorol. 23: 205-216.

Paul, A.J., and Post, J.R. 2001. Spatial distribution of native and non-native salmonids in streams of the eastern slopes of the Canadian Rocky Mountains. T. Am. Fish. Soc. 130: 417-430.

Payn, R.A., Gooseff, M.N., McGlynn, B.L., Bencala, K.E., and Wondzell, S.W. 2009. Channel water balance and exchange with subsurface flow along a mountain headwater stream in Montana, United States. Wat. Resour. Res. 45: W11427,DOI:10.1029/2008WR007644.

Pederson, G.T., Graumlich, L.J., Fagre, D.B., Kipfer, T., and Muhlfeld, C.C. 2010. A century of climate and ecosystem change in Western Montana: what do temperature trends portend? Climatic Change. 98: 133-154.

Poole, G.C., and Berman, C.H. 2001. An ecological perspective on in-stream temperature: Natural heat dynamics and mechanisms of human-caused thermal degradation. Environ. Manage. 27: 787-802.

Power, G., Brown, R.S., and Imhof, J.G. 1999. Goundwater and fish- insights from northern North America. Hydrol. Process.13 : 401-422.

Prata, A.J. 1996. A new long-wave formula for estimating downward clear-sky radiation at the surface. Q. J. Roy. Meteor. Soc. 122, 1127-1151.

Quick, M.C., and Pipes, A. 1977. UBC Watershed Model. Hydrol. Sci. Bul. 306: 215–233.

Rasmussen, J.B., Robinson, M.D., and Heath, D.D. 2010. Ecological consequences of hybridization between native westslope cutthroat (*Oncorhynchus clarkia lewisi*) and introduced rainbow (*Oncorhynchus mykiss*) trout: effects on life history and habitat use. Can. J. Fish. Aquat. Sci. 67: 357-370.

Rieman, B.E., Isaak, D., Adams, S., Horan, D., Nagel, D., Luce, C., and Myers, D. 2007. Anticipated climate warming effects on bull trout habitats and populations across the interior Columbia River basin. T. Am. Fish. Soc. 136: 1552-1562.

Sauchyn, D.J., and Bonsal, B. 2013. Climate Change and North American Great Plains' Drought, in Encyclopedia of Environmetrics, A.-H. El-Shaarawi and W. Piegorsch (eds), John Wiley & Sons Ltd: Chichester, UK. DOI: 10.1002/9780470057339.vnn123. Published online 1/15/2013.

Saxton, K.E., and Rawls, W.J. 2006. Soil water characteristic estimates by texture and organic matter for hydrologic solutions. Soil. Sci. Soc. Am. J. 70: 1569-1578.

Schindler, D.W., and Donahue, W.F. 2006. An impeding water crisis in Canada's western prairie provinces. Proc. Nat. Accad. Sci. 103(19): 7210-7216.

Shanley, J.B., and Chalmers, A. 1999. The effect of frozen soil on snowmelt runoff at Sleepers River, Vermont. Hydrol. Process. 13(12-13), 1843-1857.

Sheppard, D. 1996. Modelling hydrometeorology in the upper Oldman River basin. University of Lethbridge, MSc Thesis, University of Lethbridge, Alberta. 212 pp.

Sidle, R.C. 2006. Field observations and process understanding in hydrology: essential components in scaling. Hydrol. Process. 20, 1439-1445.

Silins, U., Bladon, K., Stone, M., Emelko, M., Boon, S., Williams, C., Wagner, M., and Howery, J. 2009. *Southern Rockies Catchment Project: Impact of natural disturbance by wildfire on hydrology, water quality, and aquatic ecology of Rocky Mountain Catchments Phase 1 (2004-2008)*, Southern Rockies Catchment Project, Edmonton, 89 pp.

Sophocleous, M. 2002. Interactions between groundwater and surface water: the state of the science. Hydrogeol. J. 10: 52-67.

Stewart, I.T. 2009. Changes in snowpack and snowmelt runoff for key mountain regions. Hydrol. Process. 23: 78-94.

Stickler, M., and Alfredsen, K.T. 2009. Anchor ice formation in streams: a field study. Hydrol. Process. 23: 2307-2315.

St-Hillaire, A., Morin, G., El-Jabi, N., and Caissie, D. 2000. Water temperature modelling in a small forested stream: implication of forest canopy and soil temperature. Can. J. Civil. Eng. 27, 1095-1108.

St. Jacques, M.J., Sauchyn, D.J., and Zhao, Y. 2010. Northern Rocky Mountain streamflow records: Global warming trends, human impacts or natural variability? Geophys. Res. Lett. 37: L06407, DOI: 10.1029/2009GL042045.

Story, A., Moore, R.D., and MacDonald, J.S. 2003. Stream temperatures in two shaded reaches below cutblocks and logging roads: downstream cooling linked to subsurface hydrology. Can. J. Forest. Res. 33: 1383-1396.

Tague, C., Farrell, M., Grant, G., Lewis, S., and Rey, S. 2007. Hydrogeologic controls on summer stream temperatures in the McKenzie River basin, Oregon. Hydrol. Process. 32: 3288-3300.

Theurer, F.B., Voos, K.A., and Miller, W.J. 1984. Instream water temperature model. Instream flow information paper 16. U.S. Fish. Wildl. Serv. FWS/OBS-85/15.

Tung, C.P., Lee, T.Y., and Yang, Y.C. 2006. Modelling climate-change impacts on stream temperature of Formosan landlocked salmon habitat. Hydrol. Process. 20: 1629-1649.

USDA, SCS., 1985. National Engineering Handbook, Supplement A, Section 4. US Department of Agriculture, Washington DC, Ch. 10.

Valiantzas, J.D. 2006. Simplified versions for the Penman evaporation equation using routine weather data. J. Hydrol. 331, 690–702.

Von Hoyningen-Huene J. 1983. Die Interzeption des Niederschlages in landwirtschaftlichen Pflanzenbesta¨nden. Dtsch. Verb. Wasserwirtsch. Kulturbau 57: 1–66.

Wang, T., Hamann, A., Spittlehouse, D., and Murdock, T. N. 2012. ClimateWNA - High-Resolution Spatial Climate Data for Western North America. J. Appl. Meteorol. Clim. 61: 16-29.

Ward, J.V. 1994. Ecology of alpine streams. Freshwater Biol. 32: 277-294.

Warnock, W. G., and Rasmussen, J.B. 2013. Abiotic and biotic factors associated with brook trout invasiveness into bull trout streams of the Canadian Rockies. Can. J. Fish. Aquat. Sci. 70: 905-914.

Webb, B.W., Hannah, D.M., Moore, R.D., Brown, L.E., and Nobilis, F. 2008. Recent advances in stream and river temperature research. Hydrol. Process. 22: 902-918.

Webb, B.W. 1996. Trends in stream and river temperature. Hydrol.Process. 10: 205-226.

Webb, B.W., and Zhang, Y. 1997. Spatial and seasonal variability in the components of the river heat budget. Hydrol. Process.11: 79–101.

Wenger, S.J., Isaak, D.J., Luce, C.H., Neville, H.M., Fausch, K.D., Dunham, J.B., Dauwalter, D.C., Young, M.K., Elsner, M.M., Rieman, B.E., Hamlet, A.F., and Williams, J.E. 2011a. Flow regime, temperature, and biotic interactions drive differential declines of trout species under climate change. P. Natl. Acad. Sci. 108: 14175-14180.

Wenger, S.J., Isaak, D.J., Dunham, J.B., Fausch, K.D., Luce, C.H., Neville, H.M., Rieman, B.E., Young, M.K., Nagel, D.E., Horan, D.L., and Chandler, G.L. 2011b. Role of climate and invasive species in structuring trout distributions in the interior Columbia River Basin, USA. Ca. J. Fish. Aquat. Sci. 68: 988-1008.

Williams, G.P. 1969. Water temperature during the melting of lake ice. Water. Res. Res. 5: 1134-1138.

Woessner, W.W. 2000. Stream and fluvial plain ground water interactions: Rescaling hydrogeologic thought. Ground Water 38(3): 423-429.

Wondzell, S.M. 2011. The role of the hyporheic zone across stream networks. Hydrol. Process. 25: 3525-3532.

Wondzell, S.M. 2012. Hyporheic zones in mountain streams: Physical processes and ecosystem functions. Stream Notes. Rocky Mountain Research Station, January-April 2012.

Wyman, R.R. 1995. Modeling snowpack accumulation and depletion. Mountain Hydrology: Peaks and Valleys in Research and Applications, B. T. Guy and J. Barnard, Eds., Canadian Water Resources Association, 23–30.

Yoo, J.H. 2012. Composite Loss Rate Model Combining Four Losses of Precipitation in a Watershed for Engineering Hydrology. J. Hydrol. Eng. 17: 405-413.

Zhang, X., Harvey, K.D., Hogg, W.D., and Yuzyk, T.R. 2001. Trends in Canadian streamflow. Water. Res. Res. 37: 987-998.